https://ntrs.nasa.gov/search.jsp?R=19740023679 2020-03-23T03:47:50+00:00Z

05

"Made available under NASA sponsorship
In the interest of early and wide dis-
semination of Earth Resources Survey
Program information without liability
for any use made thereof."

E7.4-10711
CR-139544

SEA-SURFACE CIRCULATION, SEDIMENT TRANSPORT, AND MARINE MAMMAL DISTRIBUTION, ALASKA CONTINENTAL SHELF

(E74-10711) SEA-SURFACE CIRCULATION, SEDIMENT TRANSPORT, AND MARINE MAMMAL DISTRIBUTION, ALASKA CONTINENTAL SHELF Final Report, Jul. 1972 - (Alaska Univ., Fairbanks.) 84 p HC $7.25 CSCL 08C

N74-31792

Unclas
G3/13 00711

G. D. Sharma, F. F. Wright, J. J. Burns, D. C. Burbank

Color
Original photography may be purchased from:
EROS Data Center
10th and Dakota Avenue
Sioux Falls, SD 57198

Prepared for:

NATIONAL AERONAUTICS AND SPACE ADMINISTRATION
Goddard Space Flight Center
Greenbelt, Maryland 20771

February 5, 1974

1110 H

RECEIVED
AUG 30 1974
SIS/902.6

TECHNICAL REPORT STANDARD TITLE PAGE

1. Report No.	2. Government Accession No.	3. Recipient's Catalog No.

4. Title and Subtitle	5. Report Date
Sea-Surface Circulation, Sediment Transport and Marine Mammal Distribution, Alaska Continental Shelf.	March 13, 1974
	6. Performing Organization Code
7. Author(s) G. D. Sharma, F. F. Wright, J. J. Burns, and D. C. Burbank	8. Performing Organization Report No.
9. Performing Organization Name and Address	10. Work Unit No.
Institute of Marine Science University of Alaska Fairbanks, Alaska 99701	11. Contract or Grant No. NAS5-21833 Task 7
	13. Type of Report and Period Covered Type III - Final Report July 1972 - January 1974
12. Sponsoring Agency Name and Address NATIONAL AERONAUTICS AND SPACE ADMINISTRATION Goddard Space Flight Center Greenbelt, Maryland 20771	14. Sponsoring Agency Code

15. Supplementary Notes

ERTS-1 Project, GSFC No. 110-7
Principal Investigator: G. D. Sharma, GSFC ID No. UN 683

16. Abstract

The area investigated covers most of the Alaskan shelf and the objectives of the study are: 1) to characterize coastal waters, 2) to delineate general surface water circulation, 3) to define sediment flux and pathways of sediment transport, 4) to observe formation of sea-ice and its movement in relation to the marine mammal distribution, and 5) to compile an environmental "Atlas" of Alaskan waters.

On the Alaskan shelf, where large remote and relatively inaccessible areas are difficult to investigate by direct observations and classical oceanographic techniques are often impossible, ERTS-1 imagery provided synoptic data for a number of sea water parameters and sea-ice characteristics. The distribution also identified various water masses and their movements.

In view of rapid changes and development in Alaska, information concerning coastal environment is urgently needed to form policies which would provide wise use and long term protection of the coastal zones and shelf. ERTS imagery can provide such information expeditiously at low cost.

17. Key Words (Selected by Author(s))	18. Distribution Statement
ERTS Remote Sensing Alaskan Shelf Environment Sediment Transport Ecology	

19. Security Classif. (of this report)	20. Security Classif. (of this page)	21. No. of Pages	22. Price*
Unclassified	Unclassified		

PRECEDING PAGE BLANK NOT FILMED

PREFACE

The Alaskan shelf waters are among the most productive waters of the world oceans and are actively exploited by various nations. The coastal zone of Alaska is in an era of rapid economic change and development. The impact of oil development and production on the coastal zone will be substantial. Information therefore is needed to make rational decisions to implement effectively the Coastal Zone Management Act, the Ocean Dumping Act, fishery management and mineral resource recovery. ERTS imagery can provide much of the information on a large scale at nominal cost.

An understanding both of sediment-transport mechanics, and of the dynamics of the sediment-transporting medium is essential for elucidating the physical and biological characteristics of a particular environment. These phenomena can be effectively studied from ERTS imagery. The objectives of the investigation are 1) to characterize coastal waters, 2) to delineate general surface water circulation, 3) to define sediment flux and pathways of sediment-transport, 4) to observe formation of sea ice and its movement in relation to marine mammal distribution, and 5) to compile an environmental "Atlas" of Alaskan waters.

The analyses of limited imagery from the eastern Chukchi Sea, Bering Sea, Cook Inlet and Gulf of Alaska identified various sediment sources and the movement and deposition of these sediments. The formation and orientation of nearshore plumes indicated formation of various near shore water masses and near surface water circulation.

Variations in reflectance were used for identifying various ice types in the Chukchi and Bering Sea. The direction and rates of sea-ice movement were also determined in the vicinity of the Bering Strait.

Further ERTS imagery is needed to cover the entire shelf of Alaska and repeated seasonal imagery is required to assert the sediment distribution and general surface water circulation. It is hoped that imagery will be made available to complete the project undertaken.

LIST OF ILLUSTRATIONS

PRECEDING PAGE BLANK NOT FILMED

LIST OF ILLUSTRATIONS (cont'd)

LIST OF ILLUSTRATIONS (cont'd)

LIST OF ILLUSTRATIONS (cont'd)

INTRODUCTION

The distribution and movement of sediments in nearshore regions is important from several standpoints. Deposition of suspended sediments affects channels, harbors and biologically productive wetlands or seafloor. In some cases they may be considered a pollutant because of their detrimental effects on certain organisms and because they can carry absorbed metallic and organic compounds that are toxic. In view of the ecological changes related to sediment movements, the dynamics of sediments is an essential part of the *Environmental Quality Program* as well as an important requisite for the *Sea Bed Assessment Program.*

Along the Alaskan coastline, where large remote and relatively inaccessible areas are under study and direct observations by classical techniques are often impossible, ERTS imagery provides synoptic data for a number of sea water parameters. Distinct water masses interfacing in nearshore waters are clearly discernable in ERTS-1 imagery. The gray shades evident in the coastal water masses exhibit a strong correlation with the suspended load and sunlight penetration, serving as a tracer for sediment source and movement. Thus the distribution of the suspended load as seen on ERTS-1 imagery can be used as a tool for investigating physical oceanographic problems. Because sediments are retained in suspension over a period of days, concentrations of suspended matter can be used as tags on water masses by which their movement can be traced.

Sediment plumes along the Alaskan coast are formed from sediment input carried by jet flow of water from river mouths and tidal inlets. The entire coastline is indented with intercoastal bays, lagoons, fiords and inlets with waters less saline than open marine waters. The plumes from these sources form surface layers similar to those from rivers. Coastal currents carry these plumes to that their distal ends are oriented with the current direction.

During summer, river flow attains an equilibrium with the prevailing water movement such that the river plume approaches a steady-state form. The plume is usually very heavy near the mouth and becomes lighter with distance as the sediments disperse and settle out. The distal end generally aligns itself with the predominant current and drifts passively with it. The sediment plumes from tidal inlets, on the other hand, do not attain a steady-state form due to their pulsing nature. A sediment plume formed in a coastal inlet is detached at the end of each ebb tide. Soon after its detachment, the plume is deformed such that its sharply defined updrift edge becomes oriented obliquely offshore in the direction of drift while the nearshore end is left behind. Most plumes observed were oriented either parallel or oblique to the shoreline. Bands of turbid water, however, were observed several hundred kilometers offshore. These bands are presumably driven by Ekman transport or by the inertia of the flow system during calm weather conditions.

The movement of sea ice, to a limited extent, can also be used for the study of general water movements and sea mammal ecology. Considerable information concerning various types of ice floes and pack ice and their concentrations, ice belts, brash ice, rotten ice, shorefast ice, leads, fractures, cracks, puddles, thaw holes and flood ice can be obtained from ERTS imagery. Successive overlapping imagery over 24 hour periods or more provides quantitative information on the ice movement which can be related to general water flow or wind drift.

Major currents on the shallow shelf, therefore, can be delineated from surface water characteristics as manifested by sediment plumes and sea ice movements, both of which can be exploited by remote sensing. A time series study, however, is needed to determine certain aspects of these surface expressions and related water movements. With the advent of ERTS-1 an extensive program for the study of surface water movement on the Alaskan shelf was initiated and is described here.

METHODOLOGY

Suspended Load Distribution

A) Ground truth data

1) Filter preparation and weighing

Millipore type HAWP 047 00 (0.45 μ pore size) filters were prewashed for 15 minutes in distilled water at 50°C, followed by washing for an additional 15 minutes in distilled water at room temperature. During this washing process the average weight lost by each filter was between 300-800 micrograms (mostly detergent). Additional washing produced no significant additional weight loss. After washing, the filters were placed in individual petri dishes and air dried.

The filters were weighed with a Mettler S-6 microbalance. A large desiccation chamber was attached to the

balance and both the balance and chamber were sealed such that the filters were kept in a constant state of desiccation during the weighing process. The chamber and balance were desiccated using 'Drierite' (amphydrous $CaSO_4$). Prior to weighing, the filters were desiccated overnight although it was determined that the filters reached their maximum state of desiccation within two to three hours. To eliminate electrostatic effects during weighing, the filters were passed over a polonium source prior to placement on the balance pan. This was found to be the most satisfactory procedure since placement of the polonium source over the pan was found to affect the balance movement and to give slightly erratic values. Standard weights and control filters were used to check and compensate for any weight variations caused by changes in balance temperature and the degree of desiccation of either the balance or the filters. After weighing, the filters were placed in individually numbered petri dishes.

2) Sample collection and filtering

Surface suspended loads were normally collected using a plastic bucket thrown over the side of the ship. Sampling was conducted forward of the ship's various discharge ports to eliminate any contamination. Suspended loads at depth were sampled by either Niskin or Nansen bottle casts. All suspended load samples were taken prior to any bottom sampling to prevent resuspension of bottom sediments.

One to four liters of water sample, depending on the concentration of the suspended load, was filtered through a preweighed filter, followed by washing with two 25ml aliquots of distilled water to remove sea salts. The filtering apparatus itself consisted of an array of six plastic Millipore filter holder assemblies connected to the ship's vacuum system.

After washing, the filters were placed back in their respective petri dishes. A drop of $HgC1_2$ solution (averaging 30 micrograms $HgC1_2$/drop) was added to each filter to inhibit possible biological growth while in transit to the laboratory for drying and weighing. The weight of mercuric chloride added was corrected for in the final weight calculations.

Water temperature was read immediately after collection of each sample using a partial immersion thermometer for surface samples and for deep samples taken with Niskin bottles. Reversing thermometers were used for temperature measurements at standard hydrocast stations.

Salinity samples were analyzed onboard ship using a *Bisset-Berman Model 6230* inductive salinometer. After malfunction of the onboard salinometer, salinity samples were stored and analyzed ashore using a *Hytech Model 6220* inductive salinometer.

3) Final weighing of filters

The filtered suspensions were returned to the laboratory and weighed using the same technique as in (1) above. Final weights were computed to give milligrams of suspended load-liter and values were rounded to 0.1mg for contouring the suspended load distribution.

Considering errors contributed by the weighing procedure, variations in the state of dessication during weighing, and salt retention on the filters, the accuracy of the value of the recorded suspended load is considered to be $\pm$ 0.2mg.

B) Processing of ERTS imagery

1) Selection of imagery for analysis

NASA furnished this project with imagery which contained 50% or less cloud cover. The imagery provided by NASA was screened to reject scenes with heavy cloud cover. The selected useable scenes were further subdivided into those which could be color density sliced (see below) and those which could not be adequately density sliced due to atmospheric haze or absence of suspended sediments.

2) General analytical method

The principle analytical tool used was an Interpretation Systems Incorporated 'VP-8 Image Analyzer'. This system electronically density slices the black and white transparencies (placed on a light table beneath a vidicon camera), coding the various gray shades contained in the transparency into as many as eight different colors. The color coded image is displayed on a television screen.

The range of gray shades coded as any particular color and the total range of gray shades contained in the entire color spectrum of the display are all continuously variable such that the normally small range of gray shades found in coastal waters can be density sliced into the full eight colors, each color representing a different range of reflectance value or suspended load concentration. The color coded image displayed on the television screen was photographed using high speed 35mm direct-positive color film. The 35mm color slides obtained were then projected, using a photographic enlarger, onto base maps of the Alaskan coast. The projection of the color slide was aligned such that the color image and the base map coastlines conformed, and the color boundaries were

traced onto the base map to produce the relative suspended load concentrations as shown in the black and white drafted figures.

The focal length of the vidicon camera could be varied sufficiently to allow density slicing of relatively small areas.

3) Isodensity analysis (VP-8)

The positive and negative transparencies furnished by NASA were initially density sliced with the VP-8 to determine their relative utility in the density slicing technique. It was found that, for the scenes tested, the 70mm positive transparency density sliced as good, if not better, than the 9.5 inch positive transparencies, and that the 70mm negative transparency provided, in almost all cases, the best results in all MSS bands. The better utility of the negative transparencies in the density slicing technique is primarily due to the operational limitations of the VP-8 ancillary equipment. Using the positive transparencies the generally darker water areas would not allow sufficient light to reach the vidicon camera while at the same time the lighter shaded land areas would locally oversaturate the vidicon camera. The negative transparencies essentially eliminate both problems. However, in areas of very heavy sedimentation, in which case the shade of the water approached or was even lighter than the surrounding land mass, the positive 70mm transparencies most often density sliced best.

Intercomparison of MSS bands 4-7 for a multitude of images indicated that MSS band 5 (negative 70mm transparency) generally provided the optimum results in the density slicing technique. However, each one of the MSS bands was found to provide optimum results in different situations, depending almost entirely on the concentration of the suspended load. The range of suspended load concentrations over which each MSS band is useable has been estimated on the basis of ground truth obtained in several areas of study, primarily Cook Inlet. These ranges are:

MSS Band	Surface Suspended Load (mg/1)
4	0–20
5	2–60
6	20–1000
7	40–2000+

Notwithstanding the above ranges, MSS band 5 often gave better results than band 4 in areas of very low suspended load concentration. This appeared to be due to atmospheric interference in band 4.

The most significant difficulty experienced in isodensity analysis was that of a variable density within the individual transparencies, which was not related to gray shade variation due to the suspended load or atmospheric interference. The color density slice of the transparencies in which this occurred usually appeared either as approximately vertical bands of color, again originating in the middle and varying equally towards the two sides of the transparency. Most transparencies like these were easily recognized, however, and any imagery which produced doubtful results was not used.

Many transparencies also contained a darker shaded band at the top and bottom of the image, corresponding to the area of overlap (approximately 10% at both top and bottom) of the preceding and following images, rendering about 20% of such images unuseable in the VP-8 density slicing technique.

Attempts to standardize color density slicing such that specific gray shades represented specific ranges o suspended load for all imagery proved futile using the VP-8 system. Approximately twenty clear images (standard transparencies) in areas of known relatively low suspended load concentrations were selected to test the feasibility of standardization of imagery density slicing. For each scene the VP-8 base level was standardized using the gray scale provided on the image to compensate for differences in photographic processing. While maintaining the widths of the individual color bands constant, the base level of the VP-8 was adjusted to give a standard density slice color for the waters selected, and the difference in base level recorded. If the differences in the scene density of the water areas were due only to differences in the overall density (differences due to photographic processing) of the negative, then the relative differences in base level required to color code the water areas of the different scenes the same color should roughly (assuming no significant variation in reflectivity due to sea state or atmospheric interference) show some relation to sun angle. However, the base level differences recorded were highly variable and erratic. In one area overlapping scenes from two successive days showed a difference in corrected base levels almost as great as the total variation in Cook Inlet, equivalent to a suspended load variation of almost 1000 mg/1. No attempt was made to correlate the relative differences to sea state and atmospheric interference.

A fair degree of success was obtained in standardizing the color density slices of successive images from the same satellite pass, particularly in areas of high suspended load concentration. The continuity of the color

density slice contours from scene to scene for successive images was remarkably good for some satellite passes, and good results were obtained by splicing the transparencies of successive images together prior to density slicing.

Although many of the difficulties encountered in the VP-8 density slicing technique, such as variable density within individual transparencies (apparently due to photographic processing), could be circumvented using the digital tape data, the large areas under consideration make the cost and time required for this approach prohibitive.

VP-8 control settings used in color density slicing the various images are, for the most part, arbitrary. The base level and the bandwidth of the total color spectrum were normally adjusted such that the entire range of gray shades contained in the coastal waters of the specific image being analyzed equaled the range of the color spectrum displayed by the VP-8. Individual color bandwidths were normally kept equal to each other (linear slicing), however, the relative bandwidths were at times varied to bring out specific details, such as eddies, in some images. In one instance, an acetate transparency showing the suspended load distribution for a scene for which near synchronous ground truth data had been obtained was overlain on the VP-8 TV screen. After enlarging and orienting the TV screen image to conform with the overlay, the image was density sliced to conform with the suspended load contours of the ground truth data. This procedure gives good results where at least a limited amount of ground truth data is available.

The overall procedure used, from the initial color density slice to the eventual black and white drafted version of the suspended load distribution, inherently produces some areal distortion, primarily in the VP-8 TV screen presentation and in the projection of an equal area image onto the Mercator projection base maps used south of 65°N latitude. North of 65°N latitude equal area projection base maps were used. Maximum distortion experienced in the overall procedure is approximately 5%. The areal coverage of the imagery contained in this report is outlined in Figure 1.

Sea Ice Studies

The ERTS-1 imagery of the ice covered regions indicates that, because of its high reflectance, sea ice can be identified in all the MSS bands. Although ice and clouds may have similar reflectances, ice can be easily distinguished by various parameters such as uniformity of brightness over sea ice, presence of ice floes and leads, and fractures. Clouds generally cast shadows over the ice and can be easily differentiated. On repetitive coverage some ice features remain stable and, even over longer periods between ERTS-1 cycles, some large floes can still be identified.

On the basis of variations in reflectance and the shapes and sizes of the patterns various ice types and types of ice surface features can be identified. Differences in reflectance between the shorter wavelength bands (MSS-4 and MSS-5) and the near-infrared band (MSS-7) have been useful for differentiating ice types.

ERTS-1 imagery provides multispectral data at a resolution previously not available. The identification of sea ice characteristics and movements were studied from the photographic products acquired by the MSS (Multispectral Scanner) system of the ERTS-1 and U.S. Air Force DAPP system. The resolution of the ERTS-1 MSS system permitted identification of elements with moderate contrast and linear dimensions of less than 100 meters. Distortions in the ERTS-1 imagery appeared to be systematic and in general, the root mean square err in position for points on any MSS image ranged from 200 to 450 meters, with no detectable additional error associated with image duplication or enlargement (Colvocoresses and McEven, 1973).

The positioning of ice floes required stationary identifiable points, (generally landmasses) on the imagery. The area of study is close to shore and landmass was identified in all the imagery examined. The most distinct points on land therefore provided the basis for the mapping of ice on the repetitive images and determination of the movement of ice floes from sequential images obtained on successive days. This was done by overlapping 9 x 9 inch positive transparencies (scale 1 :1,000,000) of images acquired on successive days on a light table, followed by plotting of various ice characteristics. Plotting on base maps of the same scale appeared perfect to the naked eye and, it is estimated that at the scale of the transparencies, errors of registration of less than 500 meters would have been easily detectable.

Photographic images obtained from the DAPP system were available in both the visible and infrared bands. The DAPP imagery has a resolution of about 0.3 nautical miles on a scale of approximately 1 :15,000,000. One scene for each of the first ten days of March 1973 was examined. No attempt was made to accurately map specific leads or to track the movement of ice floes visible on these images. Instead, these images were used to provide qualitative information on the overall regional aspects of the problem under study.

The orbit of the ERTS-1 was selected to provide about 10 percent overlap of images acquired on successive

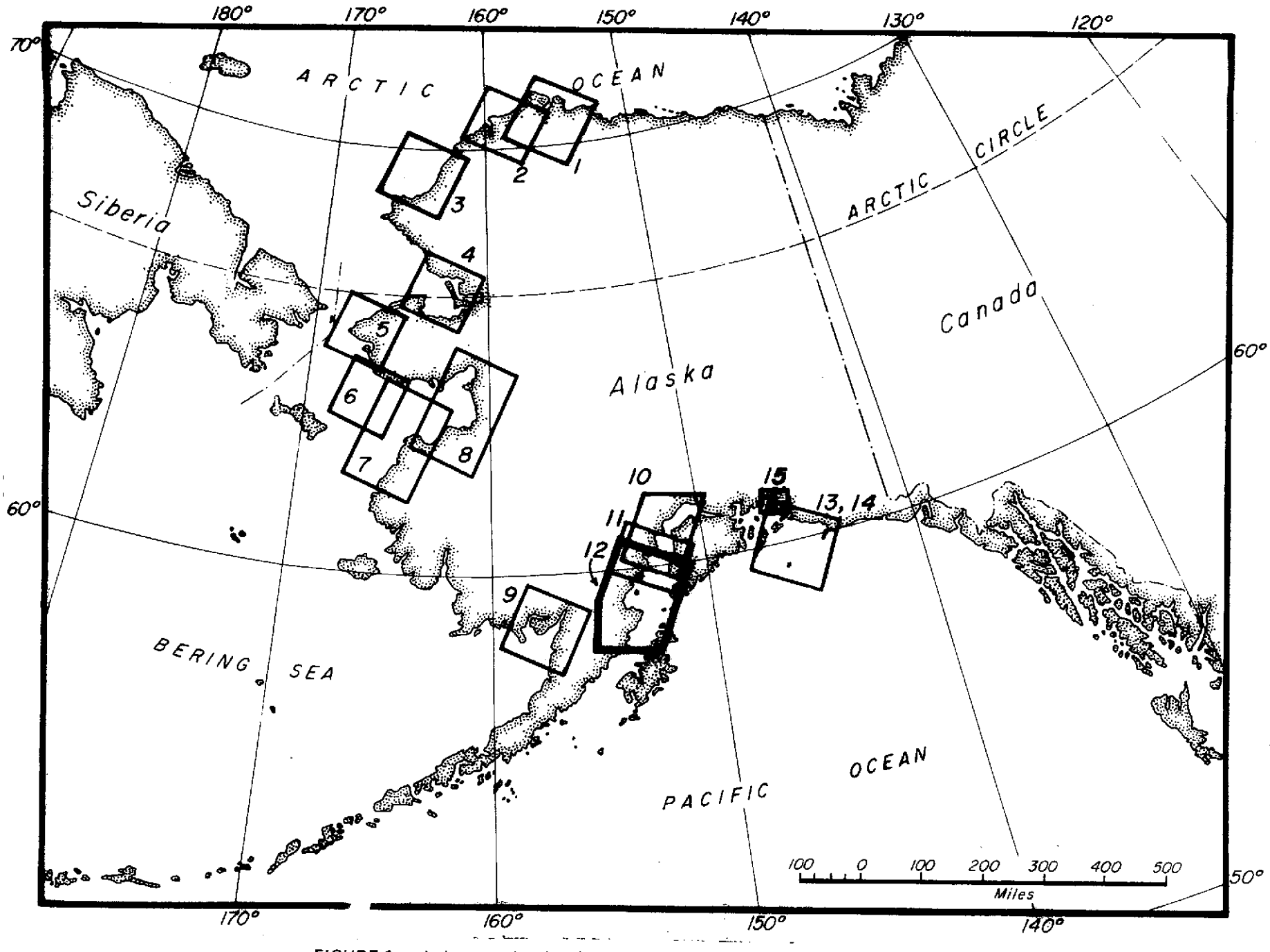

FIGURE 1. Index map showing the study area and locations of ERTS-1 imagery (bounded and numbered) used for density slicing.

days at the equator. This overlap increases at higher latitudes, and reaches about 65 percent at the latitude of the Bering Strait, providing overlapping coverage of a strip about 135 km wide along the orbital path for two successive passes. This overlap significantly facilitates the study of sea ice movement.

RESULTS

Suspended Load Study

Chukchi Sea

A) General

Most of the Chukchi sea floor was exposed to erosion during the Wisconsin sea level recession. During the past 15,000 years, sea level has risen over 100 meters and the marine transgression onto the large platform has formed an extensive shallow shelf. The rapid sea level rise has produced the contemporary sedimentary and oceanographic regimes which are still in relative disequilibrium. The resulting rapid rate of coastal erosion causes a large sediment influx from the young coast and these sediments are distributed by the prevailing currents. The accelerated rate of erosion, shallow shelf and strong currents makes ERTS-1 imagery particularly useful for the study of surface water circulation of the Chukchi Sea.

The waters of the Chukchi Sea are characterized by two dominant water masses and an almost permanent northward moving current in the eastern Chukchi Sea. (Figure 2) The major water masses consist of northward flowing cold saline Bering Sea Water and the warmer, less saline Alaskan Coastal Water which is formed along the Alaskan coast. The magnitude and direction of the major surface and near bottom currents have been described by Fleming and Hegarty, 1966, and Creager and McManus, 1966. Current speeds vary from 5 to 200 cm/sec. The imagery analyzed and described here lies along the Alaskan coast. The warm, less saline Alaskan Coastal Water is predominant water mass in this region. The boundary between the coastal water and the offshore water is well defined in areas of strong currents. This is particularly true during the summer when the temperature and salinity boundaries extend vertically throughout the water column. In the Chukchi Sea, the Alaskan Coastal Water tends to retain the coastal sediment and relatively little sediment migration into offshore water occurs. These sediments, therefore, provide an excellent tracer for the study of coastal water movement and sediment source, and thus the major sediment migration path.

The interaction between marine processes and the coast in high latitudes is uniquely influenced by freezing and thawing effects, the large Coriolis force and resulting Ekman drift, and the persistent strong winds. These factors set up a seasonably variable environment resulting from the changing atmospheric conditions. Opposing strong winds may at times completely stop the prevailing surface currents. The interpretation of ERTS imagery, therefore, calls for the inclusion of the interaction between the two mobile components of the environment, the ocean and the atmosphere, and the stationary land component. Repetitive ERTS imagery shows the ever changing coastal environment dictated by the multitude of combinations of oceanic and atmospheric conditions.

B) Field Work

Suspended load measurements were obtained from sparsely distributed stations in the Chukchi Sea during summer 1973 (R/V Acona cruise, 24-28 July and R/V Alpha Helix cruise, 14 Aug. -6 Sept.). The density of station locations and the consolidation of data obtained during different months provides only a limited basis for interpretation of sediment movement in suspension (Figure 3). It appears that Alaskan coastal waters generally retain the coastal sediments as observed in various ERTS-1 imagery. The configuration of the 3 mg/1 contour extending from northwest of Cape Lisburne to northwest of Cape Dexhneya suggests an anticlockwise gyre. A similar surface water circulation in this region has been proposed by McManus, *et al.*, 1969.

The somewhat higher sediment concentration ($>$ 2mg/1) in waters northwest of Point Barrow is primarily biogenics, possibly contributed by high productivity near the edge of the sea ice.

C) Point Barrow and Icy Cape

The coastal zone east of Point Barrow (Figure 4, right) is drained by the Mead and Ikpikpuk Rivers which are major rivers with significant drainage areas. Sediment input along the coast is also contributed by numerous minor rivers, streams, ponds and lakes. The major outlets for these sediments are Dease and Smith Inlets. Warmer and less saline water discharged from these rivers carries significant quantities of sediment into the nearshore zone where it is deposited to build coastal deltas.

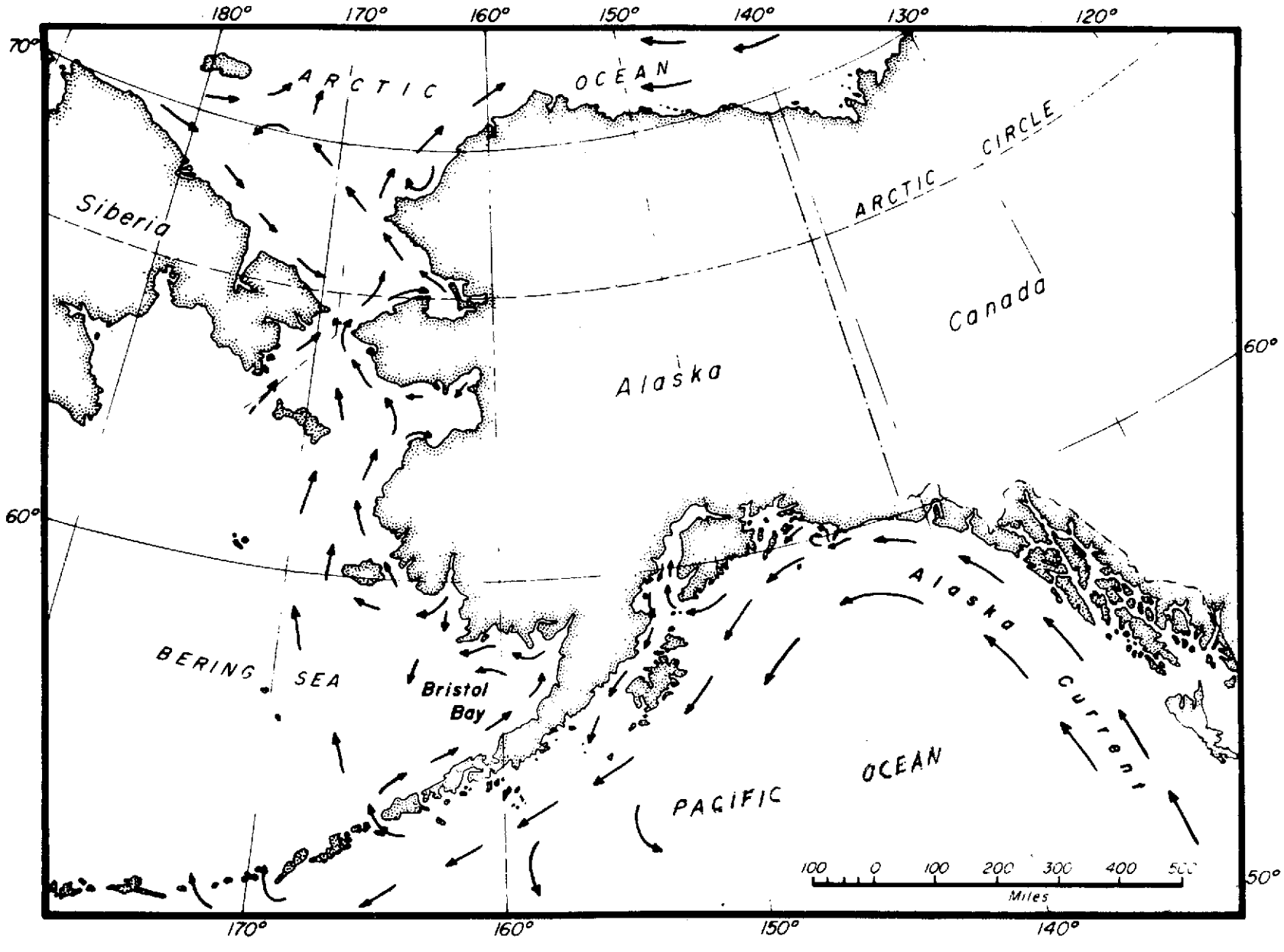

FIGURE 2. Surface currents in Alaskan coastal and adjacent waters.

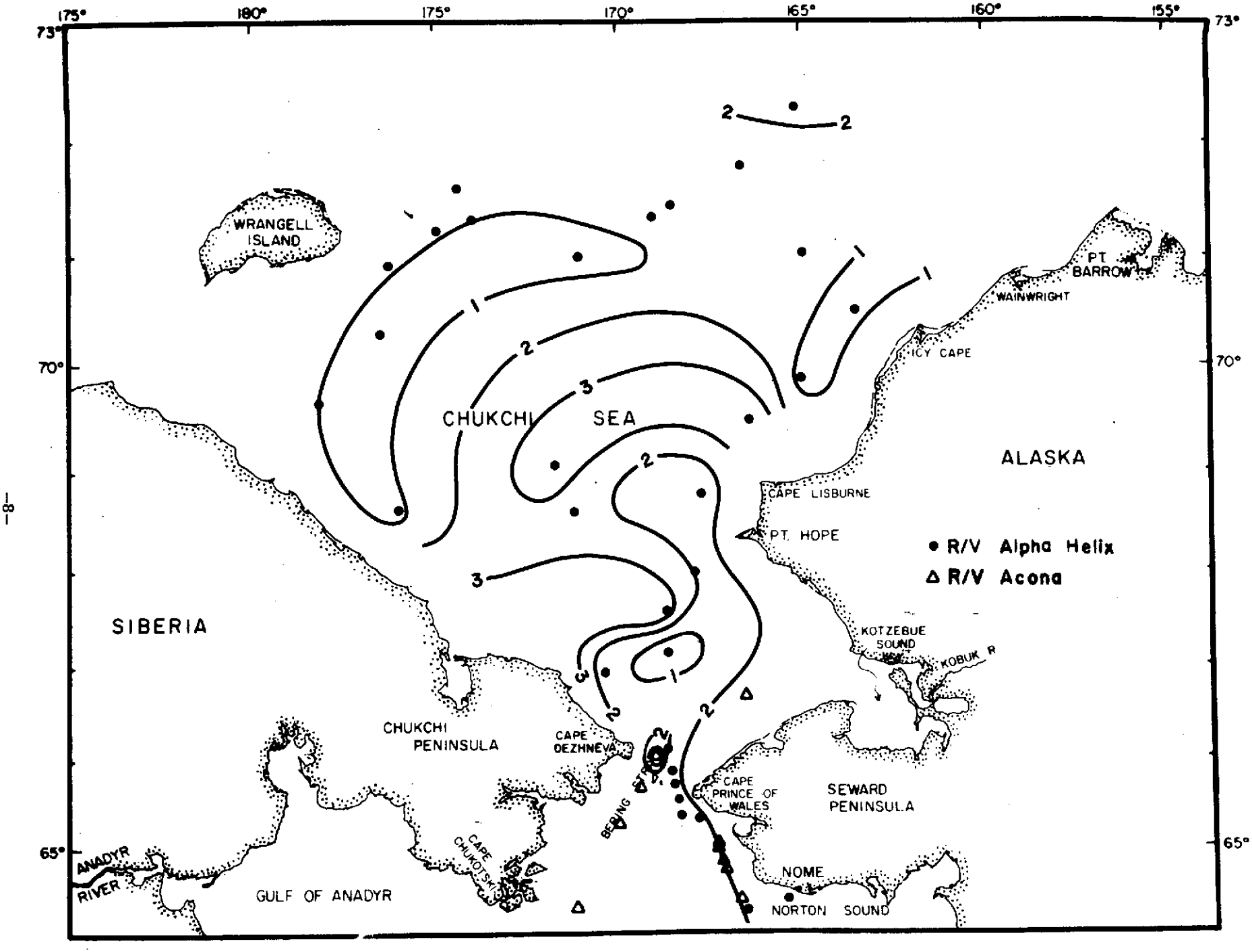

FIGURE 3. Surface suspended load distribution (mg/1) in the Chukchi Sea during 24-28 July 1973 (RV/ACONA) and 14 Aug. -6 Sept. 1973 (RV/ ALPHA HELIX).

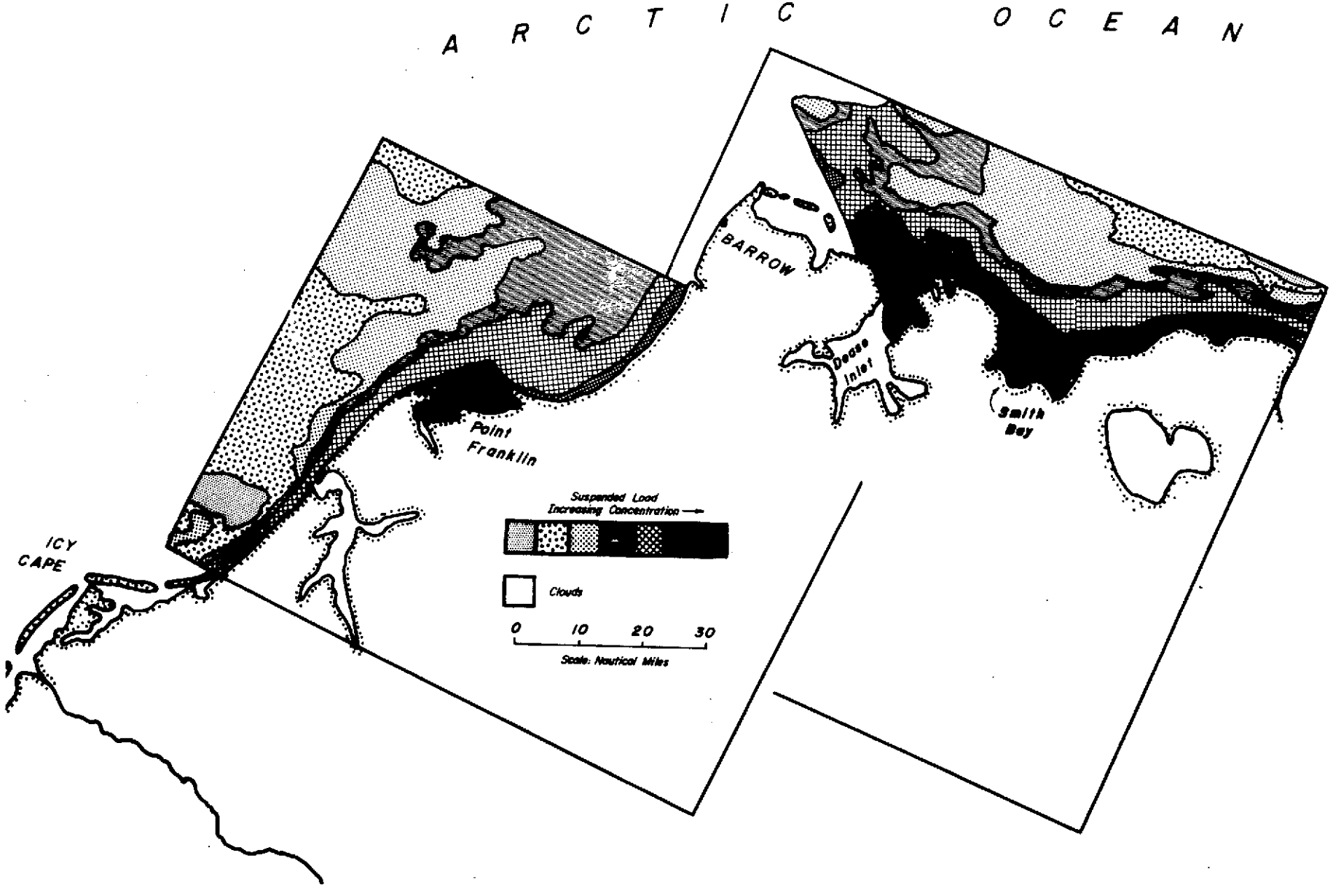

FIGURE 4. Relative suspended load distribution in the vicinity of Barrow on 21 Sep 1972 (right) and Point Franklin on 5 Sep 1972 (left) based on color density slices of image I.D.'s 1060-21510-5 and 1044-2202404, respectively. Refer to areas 1 and 2 of Figure 1.

The ERTS-1 image I.D. 1060-21510-5 obtained on 21 September 1972 was color density sliced to obtain the relative suspended load distribution as shown in Figure 4 (right). Clearly the source for sediment lies along the coast, in particular Dease and Smith Inlets. The contours of relative suspended load concentration parallel the coast, suggesting sediment movement perpendicular to the coast carried by surface water flow or through diffusion. Most sediments, however, are retained close to the shore where they form numerous small northwest-southeast oriented, highly arched barriers separated by broad, shallow tidal passes.

Point Barrow is the convergent point for two major water masses and current systems. The offshore sediment distribution northeast of Point Barrow suggests a westward drift of water originating in the Beaufort Sea. The distribution of suspended sediment in this region becomes quite confused because of the mixing of Bering Strait waters transported by the northeastward moving offshore current along the eastern Chukchi Sea coast.

Southwest of Point Barrow the color density slice of ERTS-1 image I.D. 1044-22024-4 shows a high concentration of sediment in suspension in the vicinity of Point Franklin (Figure 4, left). The thin parallel bands formed close to the shore indicate movement of sediment along the coast with minimal diffusion into offshore waters. This is perhaps due to lack of mixing between Alaskan Coastal Water and offshore water in this region. It should be noted here that, due to the density slicing technique, the relative suspended load concentrations shown in any one image cannot be quantitatively compared to concentrations in other images. Thus the heaviest sediment concentrations in the image east of Barrow (Figure 4) does not represent the same concentration as the region of heaviest sediment concentration in the image west of Barrow.

The nearshore surface currents in this region are predominantly controlled by the northerly and westerly onshore winds. The northerly winds carry sediments southwest along the coast and build the cape at Point Franklin. The westerly winds on the other hand transport sediments northeastward and once again deposit sediments at Point Franklin. Most sediments are retained in the Alaskan Coastal Water and the offshore diffusion of sediments in this region is minimal. Northeast of Point Franklin an eddy is formed which disperses the sediments over a wider area.

D) Cape Lisburne

Similar conditions for sediment transport prevail farther south along the eastern Chukchi Sea Coast. ERTS-1 image I.D. 1047-22201-5 (Figure 5) obtained on 8 September 1972, through color density slicing, revealed a significant sediment concentration near Cape Lisburne and also northeastwards along the coast. The prevailing offshore current and seasonal wind drift appear to control the movement of sediments in this region. The major offshore current emerges from Kotzebue Sound, moves along the southern shore of Point Hope and turns northeast to Cape Lisburne. The coastal sediments, however, are generally moved towards the cape depending upon the wind direction. This particular imagery suggests northeasterly wind carrying sediment towards Cape Lisburne.

E) Kotzebue Sound Region

Partly clouded ERTS-1 image I.D. 1385-21580-4, obtained on 12 August 1973, was color density sliced and is shown in Figure 6. The major source for sediments in Kotzebue Sound apparently lies in the mouth of Noatak River. Most sediments are deposited at the mouth, forming an impressive delta. Sediments in lesser quantities, however, are carried northwards. High sediment concentrations and extensive building of barrier islands also can be seen near the southern shores of the entrance to Kotzebue Sound. These sediments are carried by the Bering Strait currents which flow northwards into the Chukchi Sea and dominate the entire coast between Bering Strait and Cape Espenburg. The northward moving waters appear to bifurcate near Cape Espenburg where part of the sediment carrying waters turn into Kotzebue Sound due to Coriolis effect while the rest of the water moves northeastwards.

Kotzebue Sound therefore serves as a sediment trap and is rapidly being filled by sediment contributed not only from its own drainage but also by sediments brought from the Bering Sea and the northwestern shores of the Seward Peninsula. Only part of the sediments contributed by the Noatak River are carried northward, transported by Alaskan Coastal waters moving close to the shore.

F) Bering Strait Region

Clear ERTS-1 imagery I.D. 1351-22102-4 was obtained on 9 July 1973 and color density sliced for suspended sediment distribution (Figure 7). Sediment laden plumes extending northeastwards from Bering Strait were observed. These plumes mostly remain close to the coast, however, sediments carried offshore rapidly diffuse into northward moving Bering Strait waters.

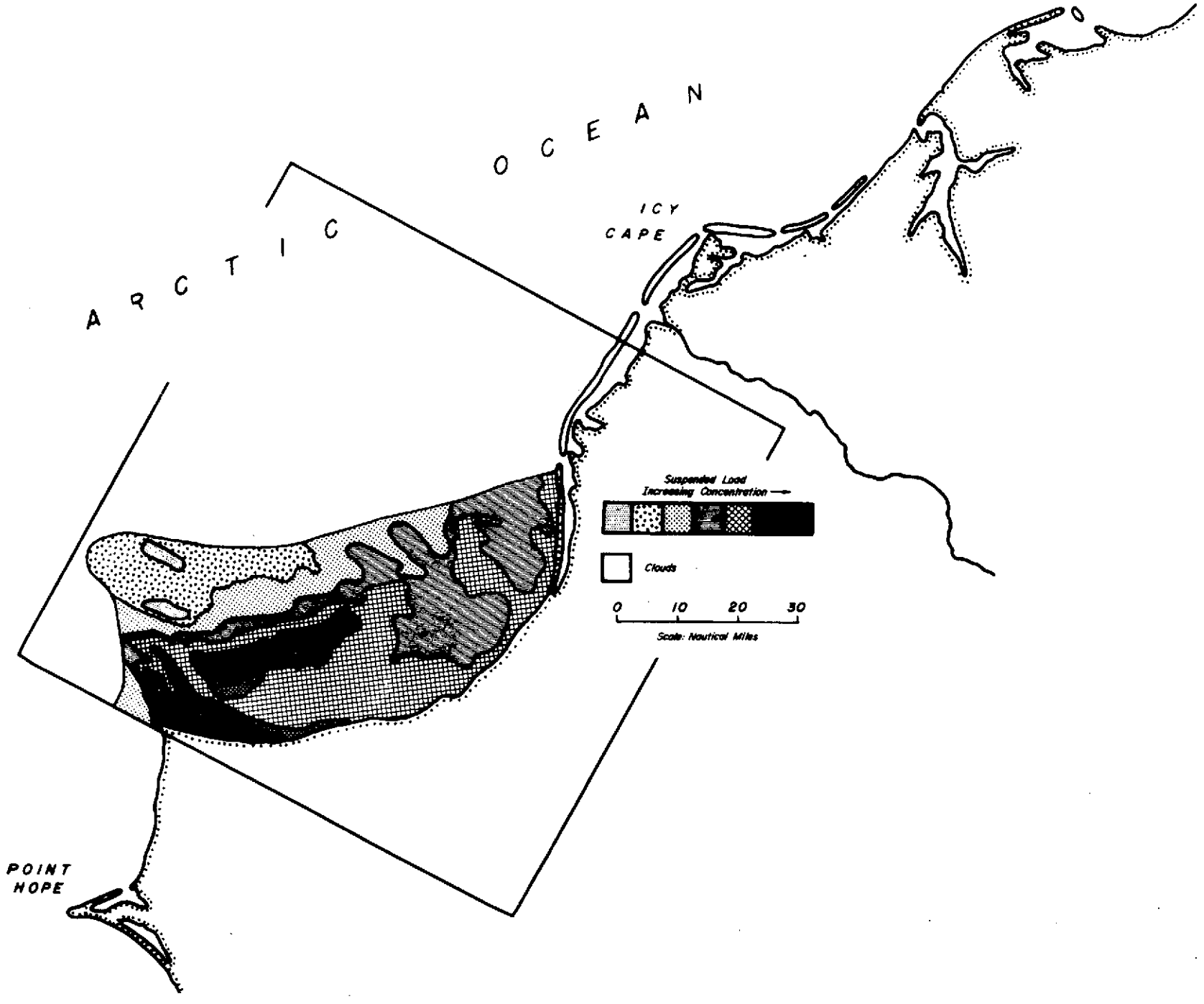

FIGURE 5. Relative suspended load distribution in the vicinity of Cape Lisburne on 8 Sep 1972, based on color density slice of image I.D. 1047-22201-5. Refer to area 3 of Figure 1.

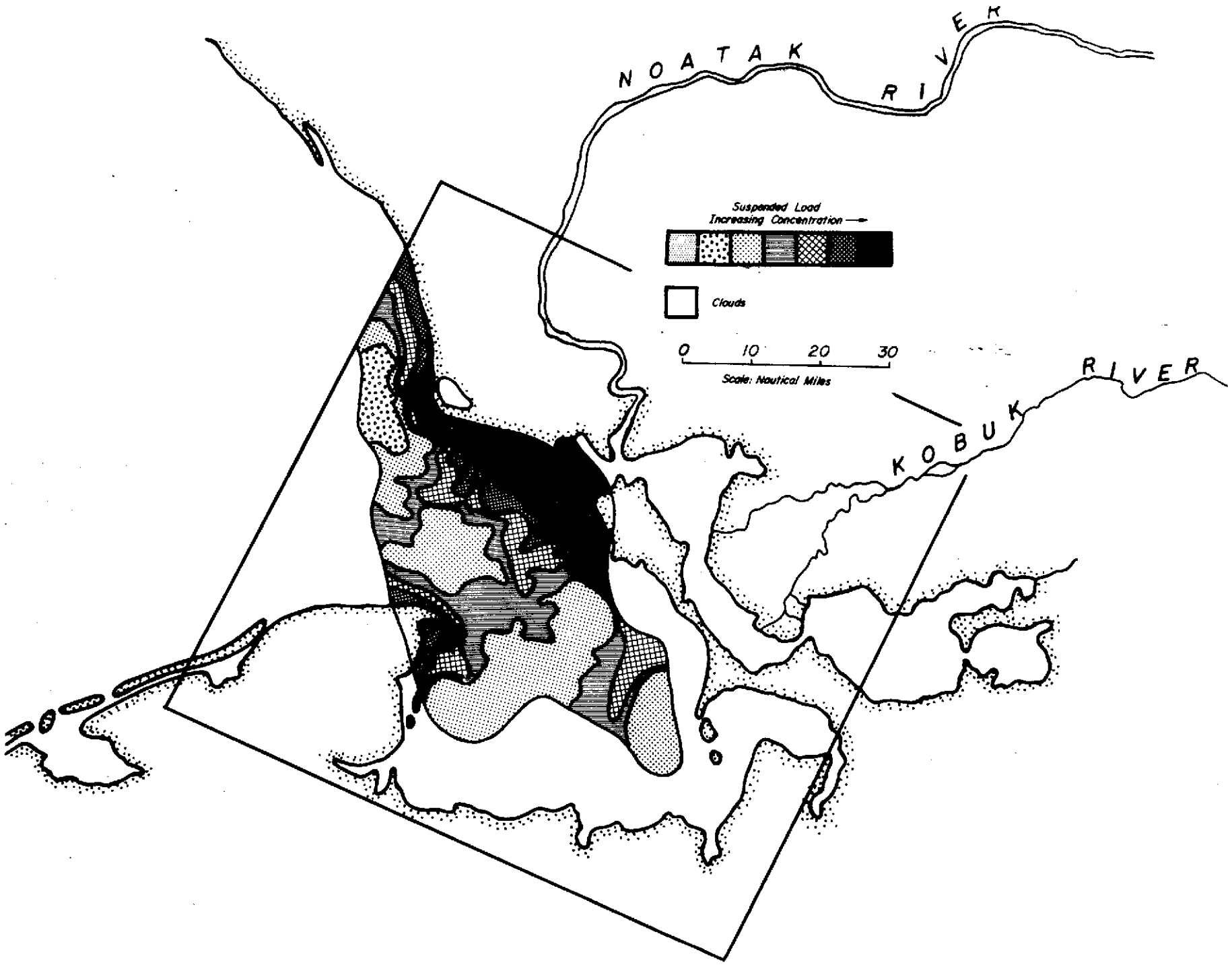

FIGURE 6. Relative suspended load distribution in the vicinity of Kotzebue Sound on 12 Aug 1973, based on color density slice of image I.D. 1385-21580-4. Refer to area 4 of Figure 1.

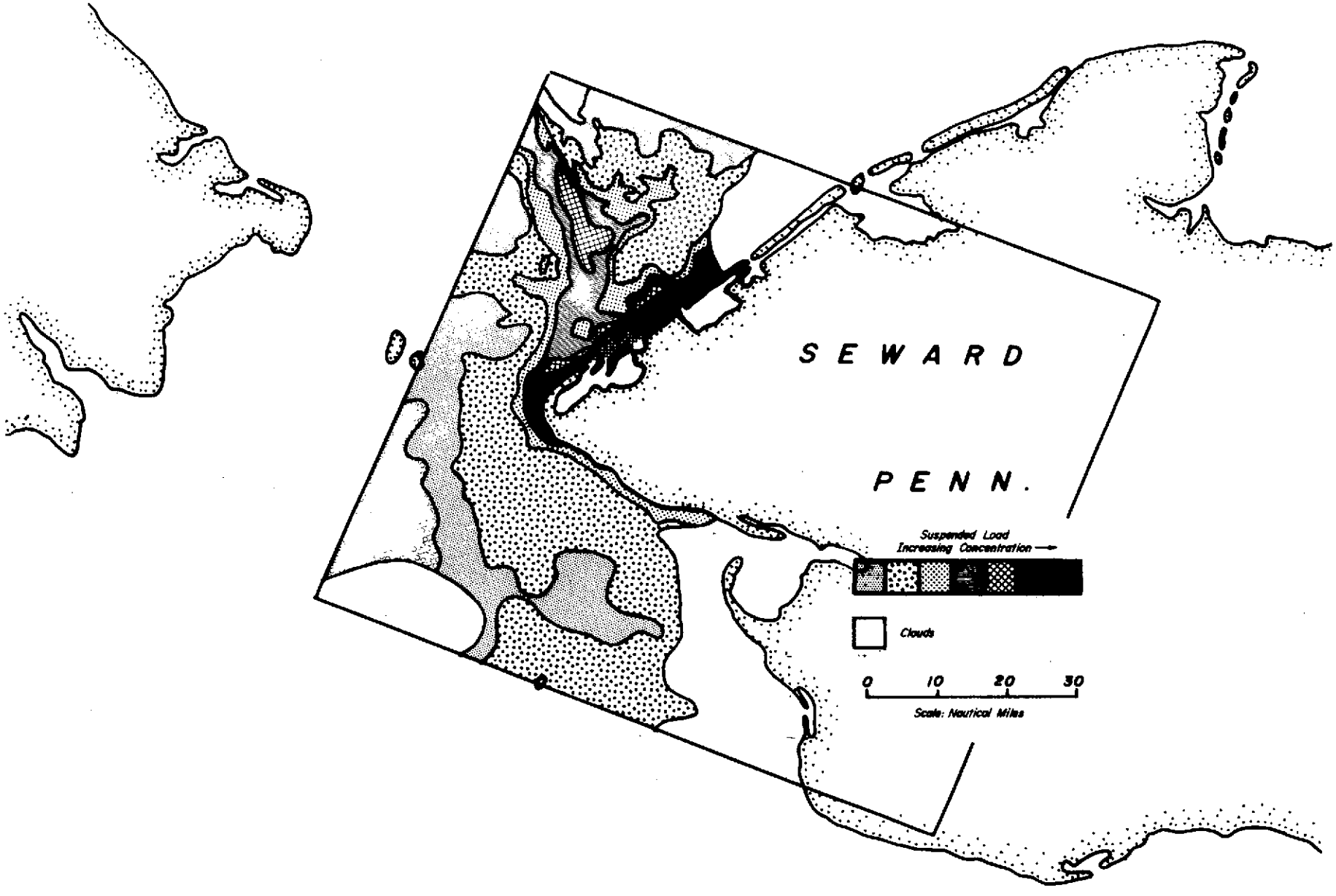

FIGURE 7. Relative suspended load distribution in the vicinity of the Bering Strait on 9 Jul 1973, based on color density slice of image I.D. 1351-22102-4. Refer to area 5 of Figure 1.

Surface current measurements during summers in the Bering Strait and along the flank of Cape Prince of Wales Shoal, were found to average between 7 to 75 cm/sec. (Fleming and Hegarty, 1966; Creager and McManus, 1966). These northward moving currents are the primary media for sediment transport in this region. The coastal sediments are brought into an extensive system of lagoons and long offshore barrier islands. The sediments are moved from these lagoons either by fresh water input or by water gradients caused by atmospheric pressure systems. Tides are low in the northern latitudes and their effect minimal. The movement of sediments along the shore is possibly due to minimal mixing between Alaskan Coastal Waters and colder, more saline Bering Strait Water.

Bering Sea

A) General

The general climate of the Bering Sea is controlled by solar radiation and general global atmospheric circulation. The atmospheric circulation to an extent also controls the rate and extent of water exchanges between the Bering Sea, Arctic Ocean, and Pacific Ocean, and the climatic conditions in the Bering Sea during an annual cycle are thus affected by the Arctic and Honolulu maxima. During winter the Honolulu maximum occupies a southeastern position and in summer it becomes more vigorous and moves to a northeastern position. The summer shifting of the Honolulu maximum (anticyclone) to the west and northwest leads to an intense location of cyclonic circulation and an increase in the frequency of south winds. The winter shifting of the Honolulu anticyclone to the east results in a simultaneous advance of the Arctic anticyclone to the south, thus intensification of frequency of north winds.

The Bering Sea is frequently ravaged by storms because it lies in the path of extratropical cyclonic and anticyclonic storms. These storms destroy water structures on the shallow shelf which in turn causes mixing and movement of various water masses.

B) Field work

An extensive reconnaissance survey in the eastern Bering Sea was conducted during the summer of 1973. During May - June measurements of suspended sediment load were conducted aboard the R/V Oshoru Maru in the southeastern and southcentral Bering Sea (Figures 8-11). A north-south track covering the entire Bering Sea from Unimak Pass to the Seward Peninsula was completed during July aboard R/V Acona. Salinity, temperature, and suspended load data were also collected from the Norton Sound and Bristol Bay regions and are shown in Figures 12-14.

The shallow eastern Bering Sea shelf is characterized by pronounced seasonal layering of water masses. In summer the shelf has a well defined thermocline and halocline reaching to depths of 20 meters. The temperature of the surface layer may rise to 8 to 13^{o}C while the bottom layer remains at 0 to -1.5^{o}C. Salinity increases with depth and locally the Yukon, Kuskokwim and Kvichak rivers reduce the salinity of the surface waters.

Three water masses are formed in the Bering Sea: Alaskan Coastal Water, Northern St. Lawrence water and Basin water. Along the coast and the shelf, Alaskan Coastal Water is the dominant water mass. This water mass is characterized by relatively warmer temperatures (8-13^{o}C) and salinities below 32$^{o}/_{oo}$.

C) Northeastern Bering Sea (Norton Sound and Yukon River delta)

The northeastern Bering Sea has a complex water circulation which is primarily driven by the meteorlogical conditions prevailing in this region. During the ice free summer period the warm fresh water input to Norton Sound builds up a strong pycnocline at a depth ranging from 5-15 meters in the water column; the maximum water depths in Norton Sound are about 25 meters. The large region of Norton Sound thus develops a two-layered system which is similar to estuarine flow. Under these conditions the fresh water in the surface layer continually moves westward and ultimately passes through the Bering Strait. The Yukon River input (fresh water and sediments) is mostly caught up in the northward moving current which originates near Unimak Pass (Figure 2) and flows north through the Strait of St. Lawrence and to the Chukchi Sea through the Bering Strait. Part of the Yukon River outflow, however, is diverted to the east (into Norton Sound) due to the Coriolis effect and is clearly seen in Figures 15A, 15B and 16. ERTS-1 composite image I.D. 1384-21530 and -21533-5 (Figure 15) shows the sediment distribution at the mouth of the Yukon River on 11 August 1973. The plume shows a limited movement of sediments to the south of the river mouth, however, the major sediment transport direction is to the north and northwest towards the Bering Strait, as indicated by the enlarged bands (caused by

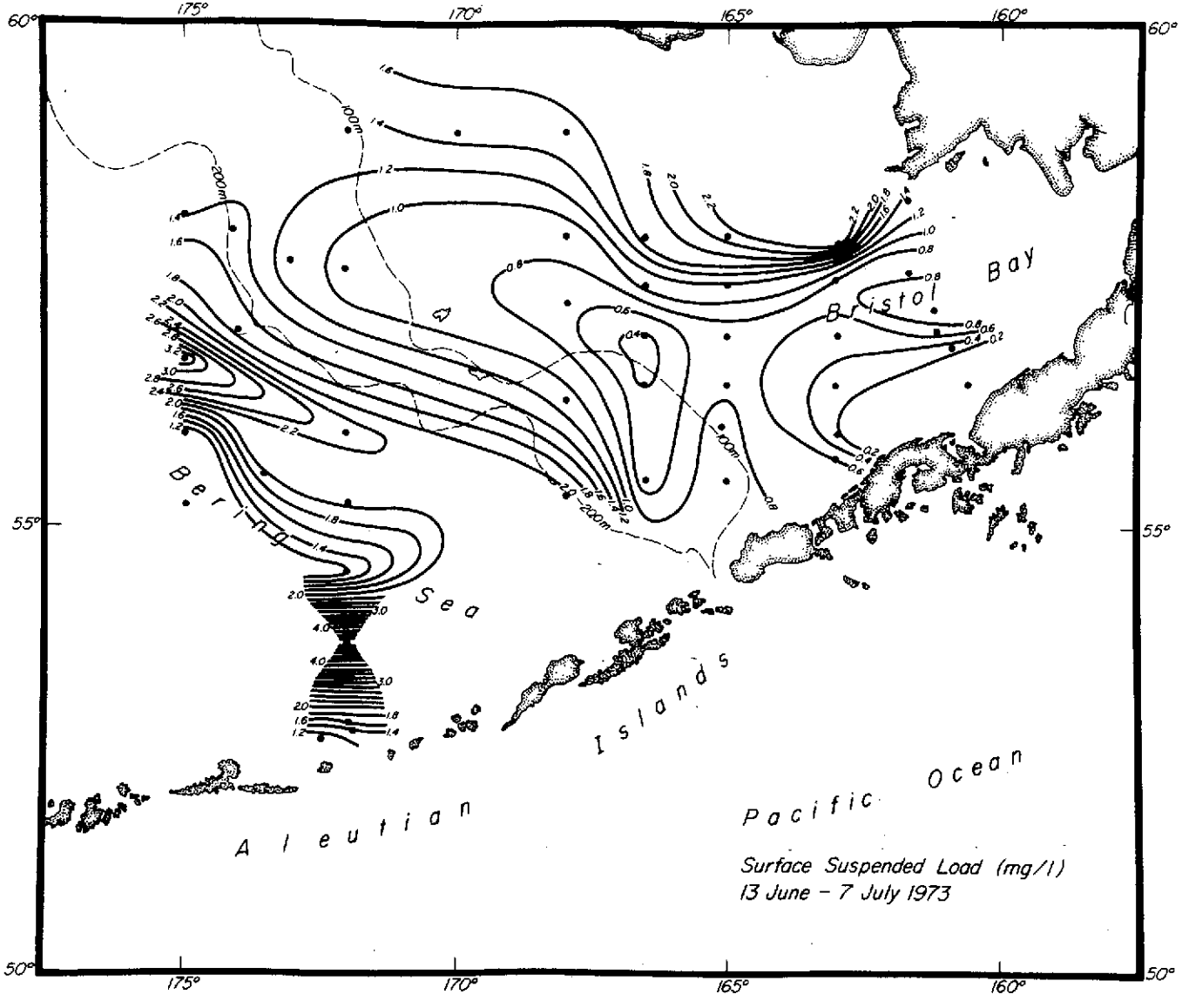

FIGURE 8. Surface suspended load distribution (mg/1) in the southeastern Bering Sea, 13 Jun-7 Jul 1973.

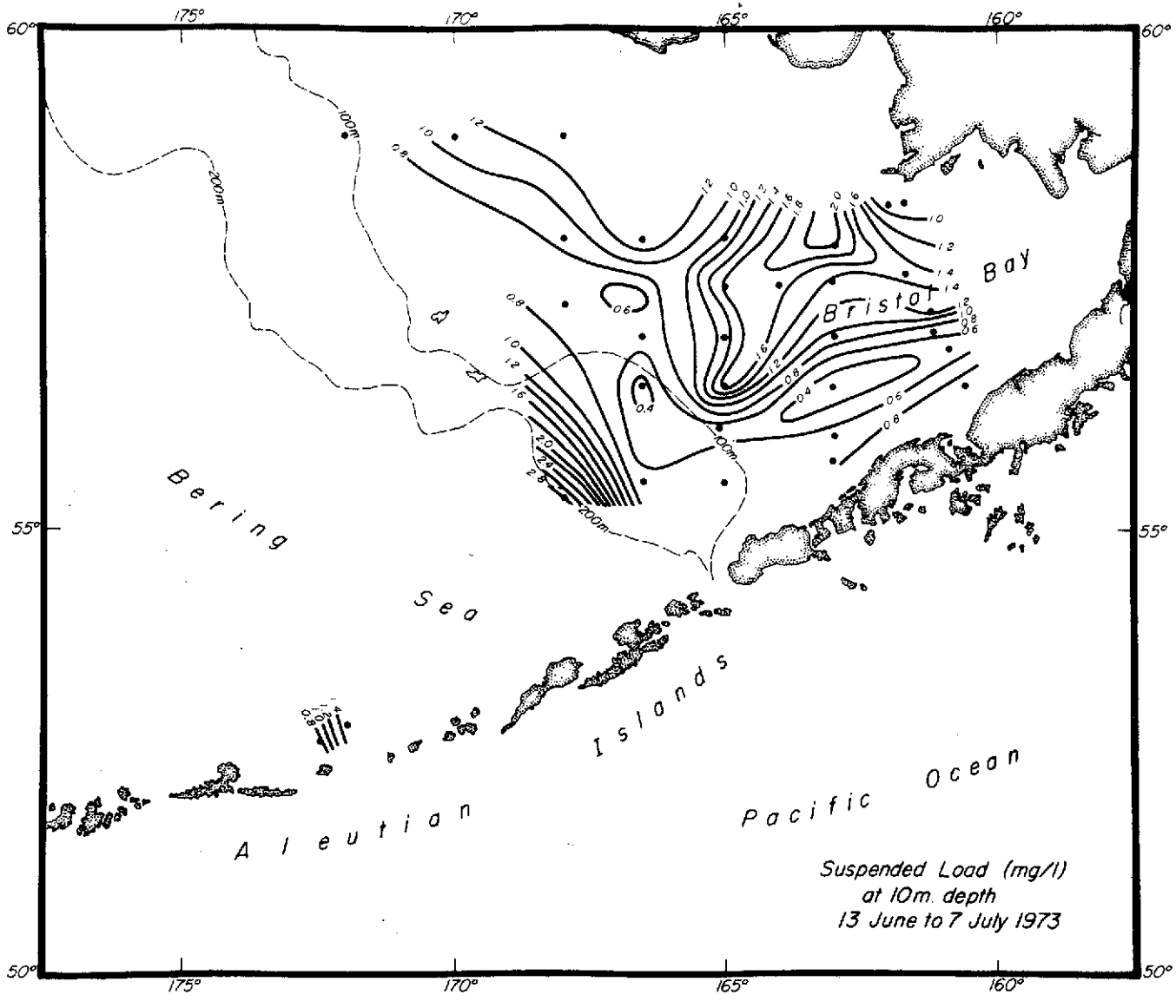

FIGURE 9. Suspended load distribution (mg/1) at 10 meters depth in the southeastern Bering Sea, 13 Jun - 7 Jul 1973.

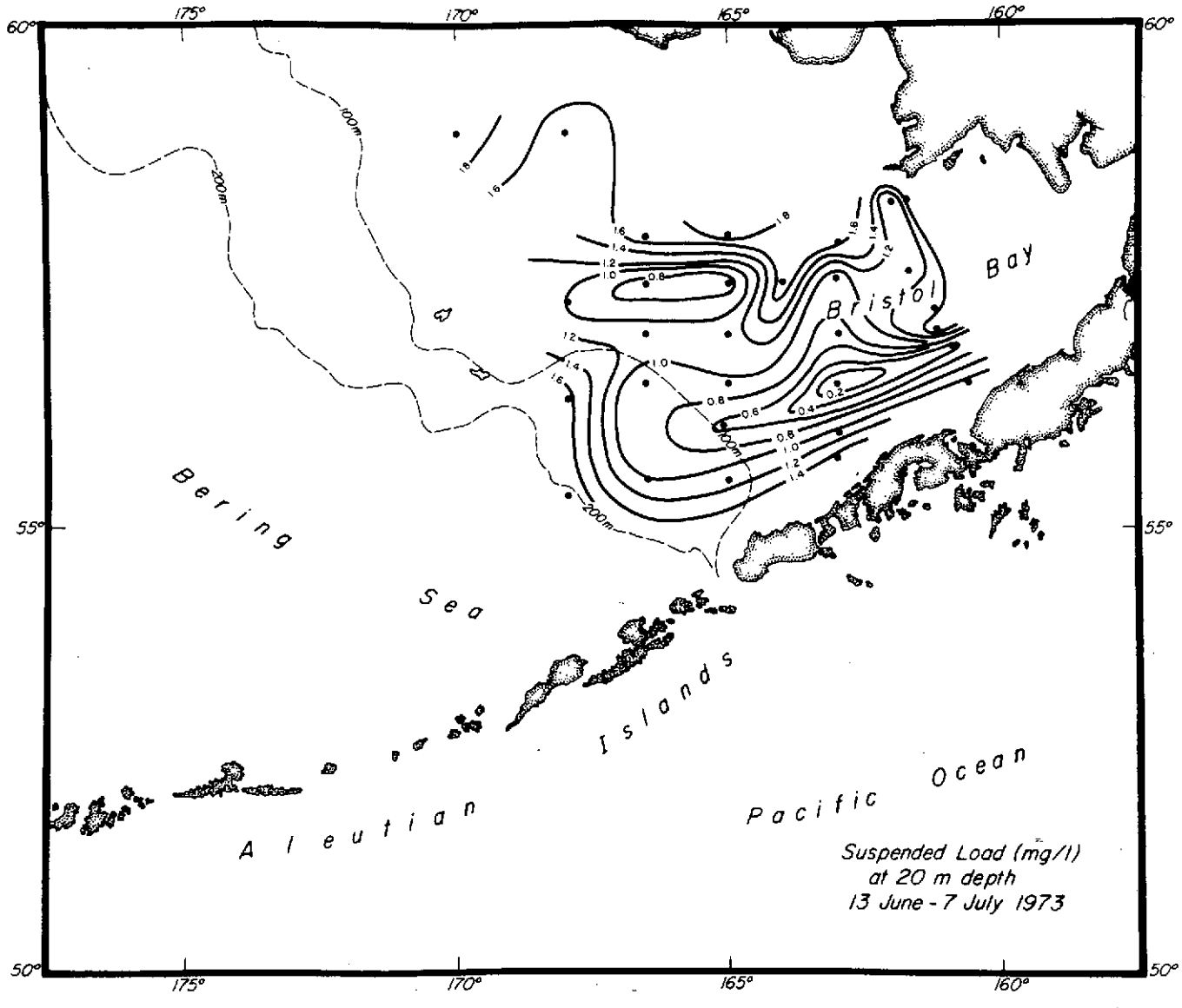

FIGURE 10. Suspended load distribution (mg/1) at 20 meters depth in the southeastern Bering Sea, 13 Jun - 7 Jul 1973.

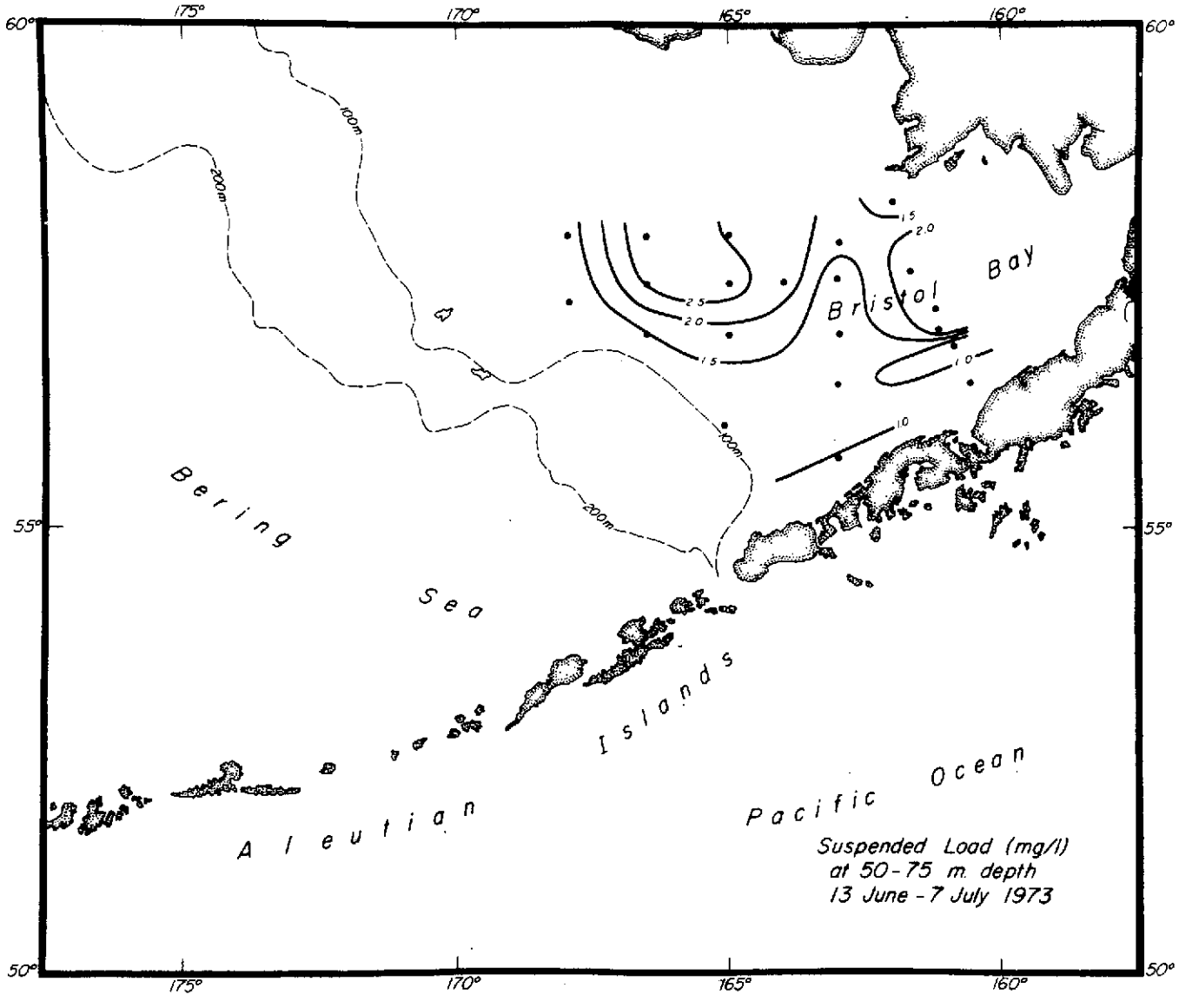

FIGURE 11. Suspended load distribution (mg/1) at 50 - 75 meters depth in the southeastern Bering Sea, 13 Jun - 7 Jul 1973.

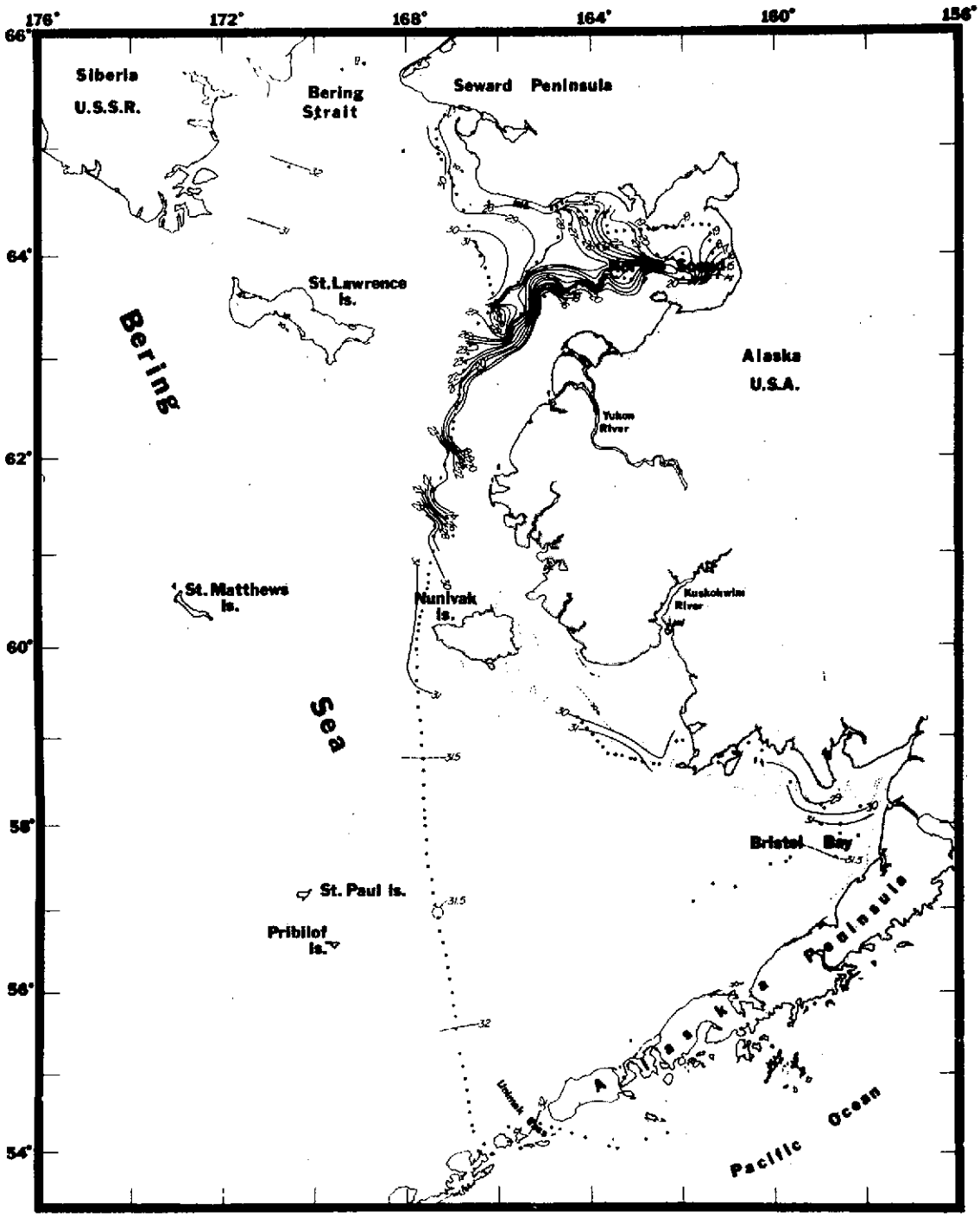

FIGURE 12. Surface salinity ($^{o}/_{oo}$) in the eastern Bering Sea; 11 July - 11 August 1973.

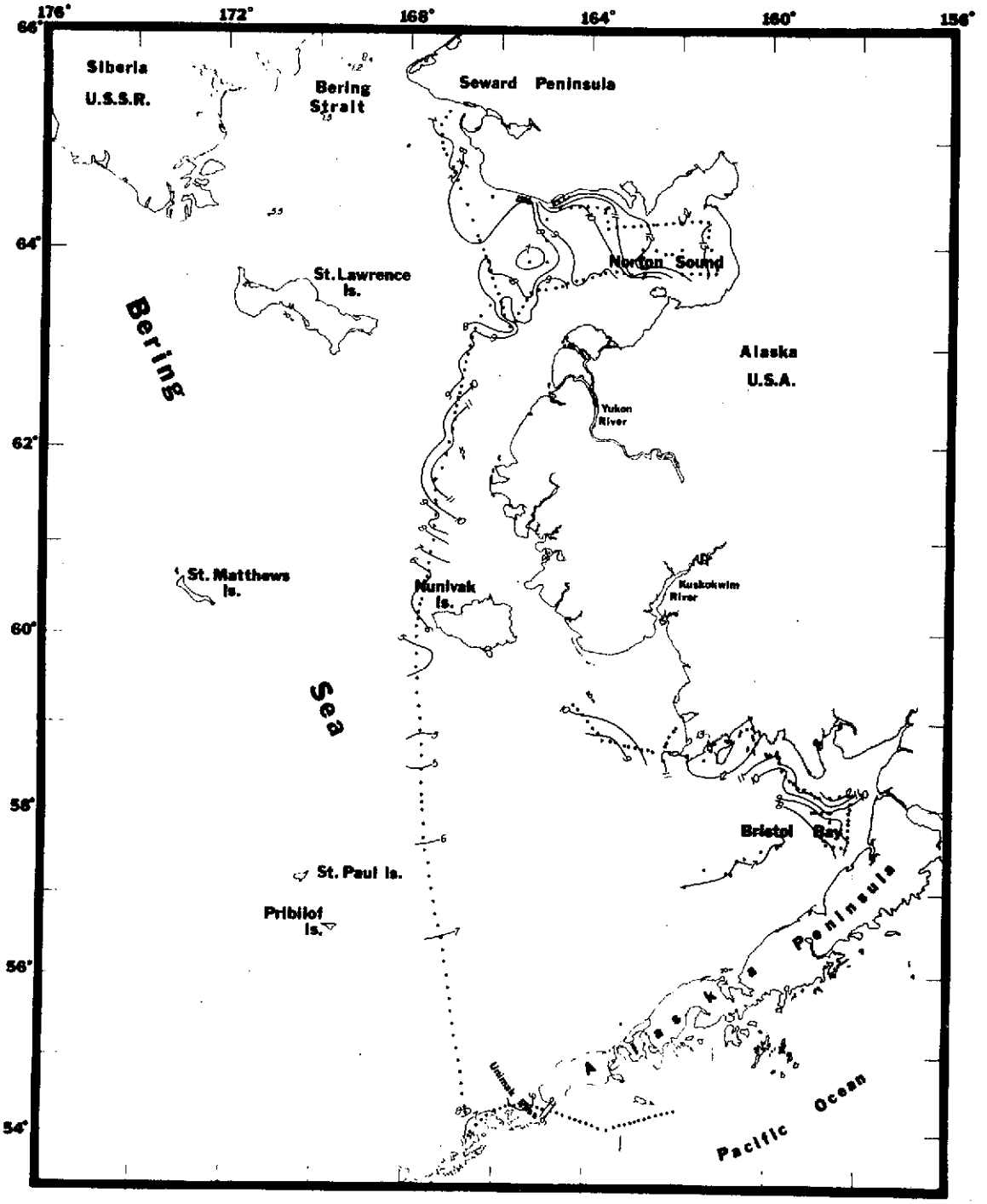

FIGURE 13. Surface temperature (^{o}C.) in the eastern Bering Sea; 11 July - 11 August 1973.

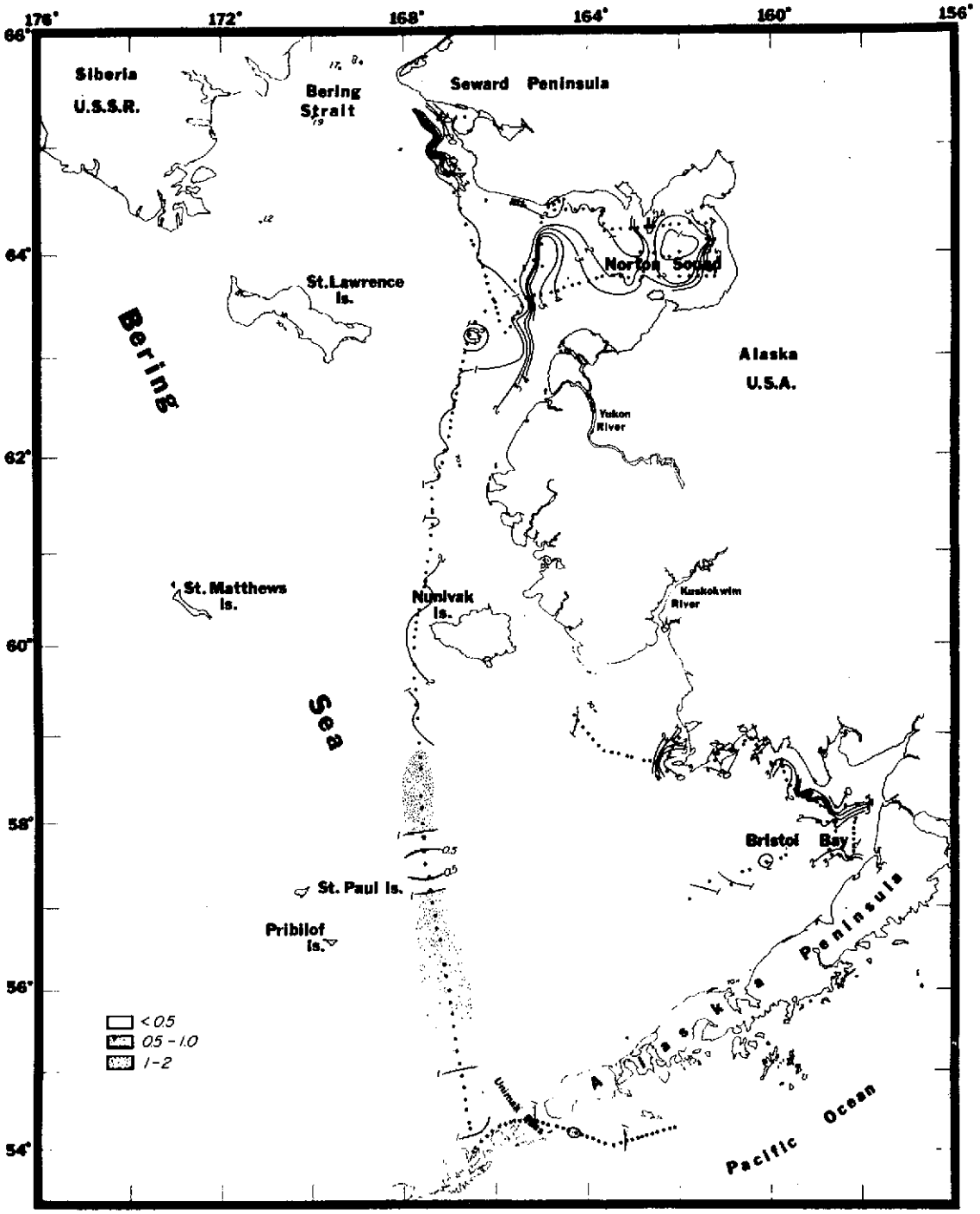

FIGURE 14. Surface suspended load distribution (mg/1) in the eastern Bering Sea; 11 July - 11 August 1973.

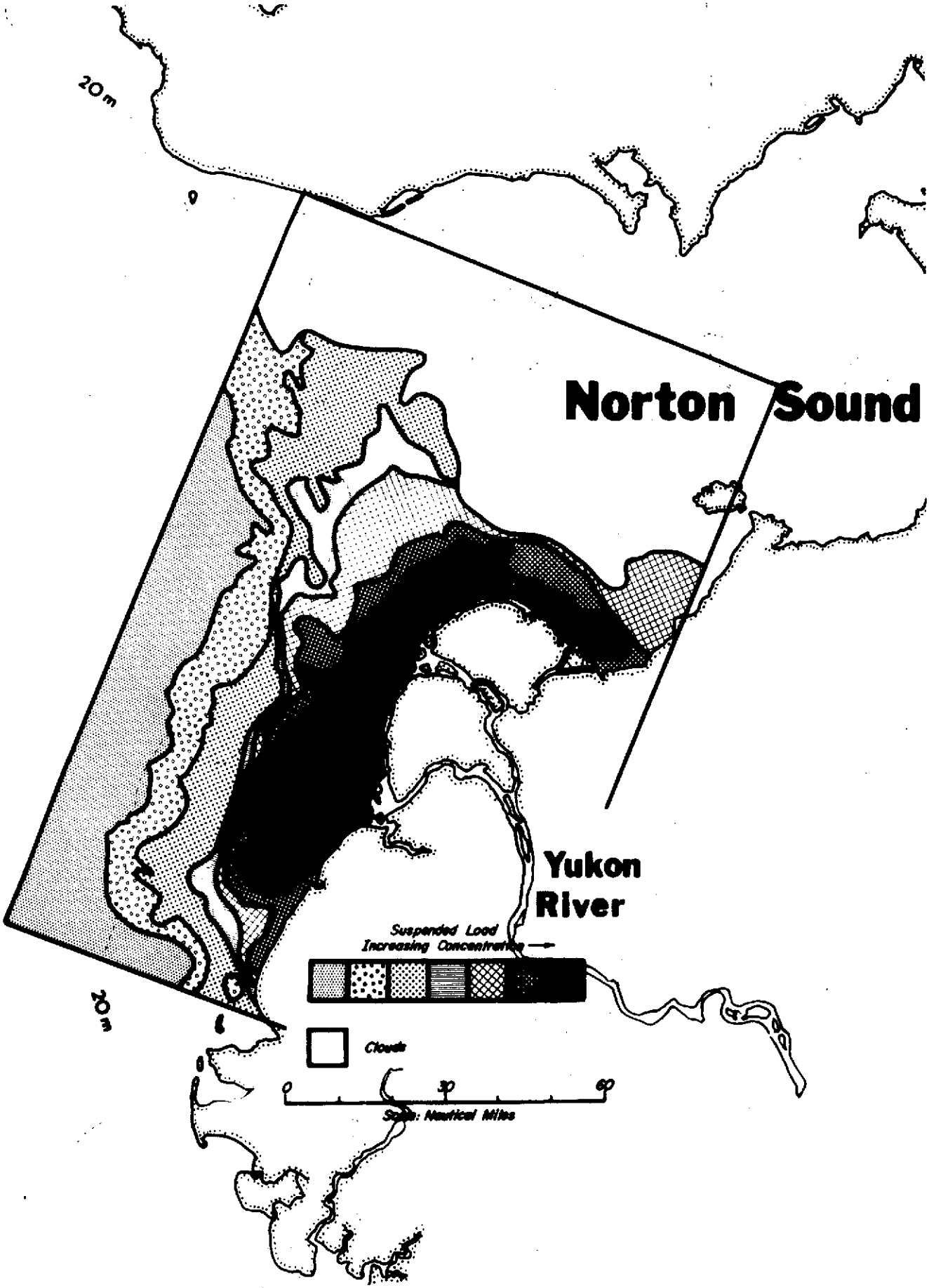

FIGURE 15A. Relative suspended load distribution in the vicinity of the Yukon River on 11 Aug 1973, based on color density slice of image I.D.'s 1384-21530 and -21533-5. Refer to area 7 of Figure 1.

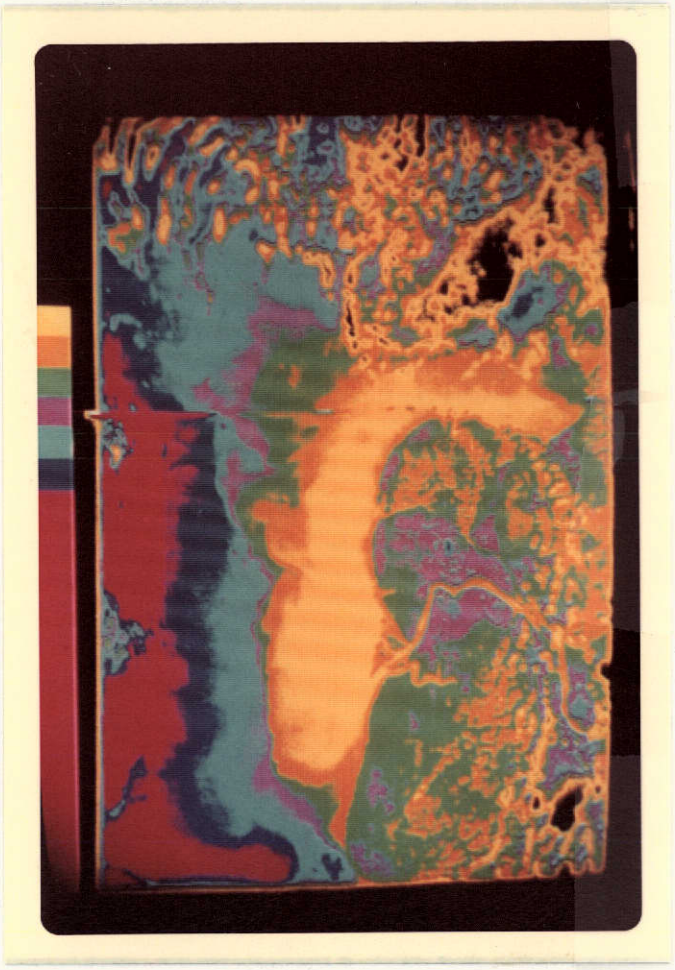

FIGURE 15B. Color density slice of image I.D.'s 1384-21530 and -21533-5, used to prepare Figure 15A. The order of increasing suspended load is from red to yellow in the sequence shown at the left-hand side of the picture.

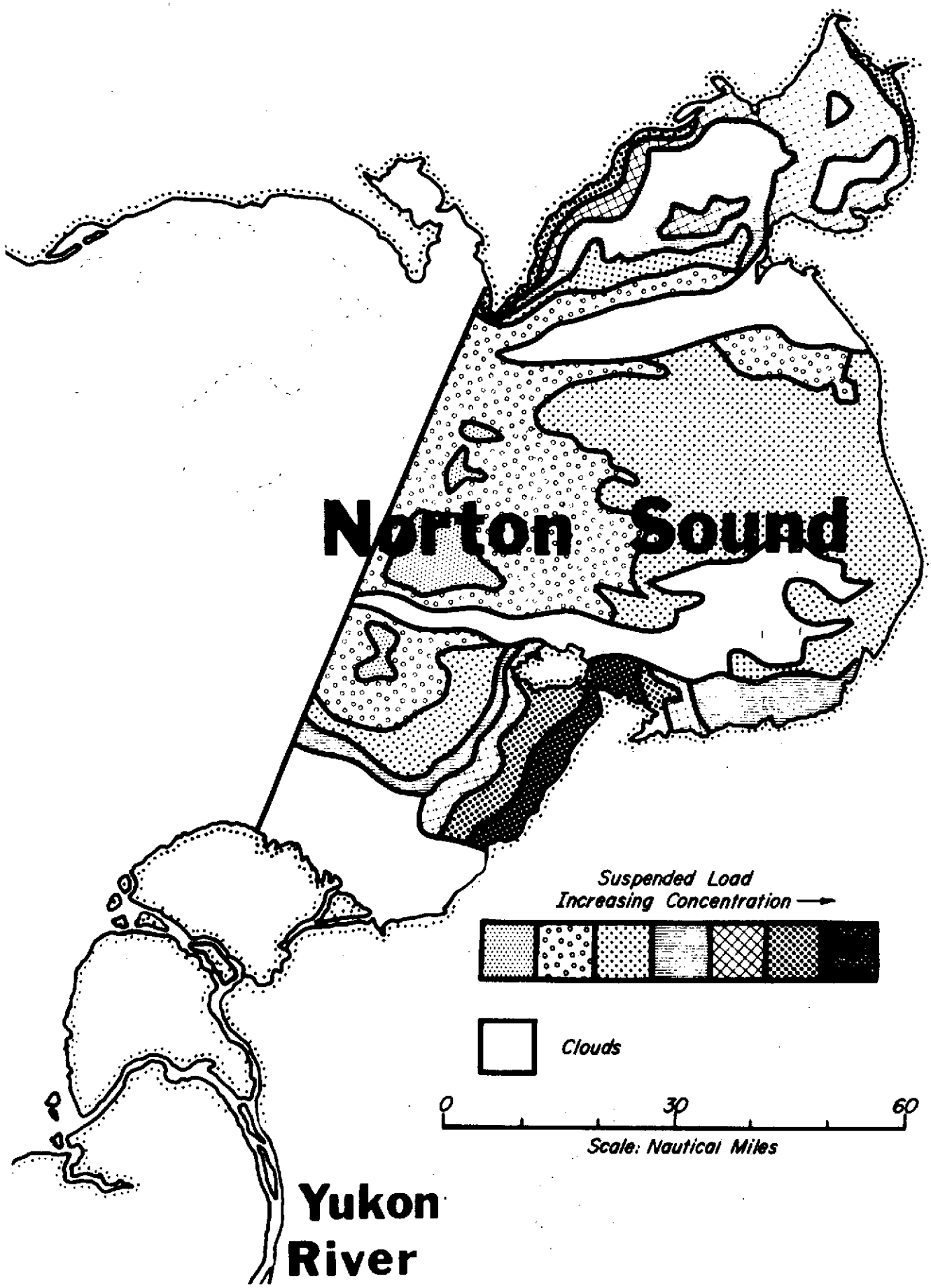

FIGURE 16. Relative suspended load distribution in the vicinity of Norton Sound on 4 Jul 1973, based on color density slice of image I.D.'s 1346-21420 and -21423-6. Refer to area 8 Figure 1.

advective transport of sediment) to the north, and to a lesser extent to the east into Norton Sound. The movement of sediments therefore explains the paucity of Yukon River sediments in Norton Sound. The surface salinity, temperature and suspended load distribution also indicate that Yukon sediments partly move close to shore eastward into Norton Sound and northwestward to the Bering Strait (Figures 12-14).

The partly clouded composite image I.D. 1346-21420 and -21423-6 (Figure 16) obtained on 4 July 1973 and also image I.D. 1062-22044-4 (Figure 17) of 23 September 1972 suggests a similar sediment distribution and water circulation in the northeastern Bering Sea.

The shallow water (average depth 30 meters) structure of the northeastern Bering Sea is affected by frequent and sometimes severe summer storms. The winds associated with these storms alter the circulation by either inducing wind generated surface currents or by mixing the otherwise stratified waters to form a homogenous water mass which flows westward and is subsequently replaced by Bering Sea shelf and Yukon River waters. The latter (storm induced) circulation draws Yukon River sediments eastward along the southern shores of Norton Sound. Some Yukon River sediments near the southern and eastern shores of Norton Sound are retained, as suggested by the textural distribution of the bottom sediments. (Sharma, unpublished data.) Because summer storms generally are accompanied by cloudy weather, ERTS images of the sediment distribution and circulation under these conditions are difficult to obtain.

D) Southeastern Bering Sea – Bristol Bay

The head of Bristol Bay receives drainage of the Kvichak River from the east and the Nushagak River from the north. Both rivers contribute significant amounts of sediments in suspension. Once brought into the open bay these sediments are transported offshore by tidal movement and the anticlockwise gyre encompassing the entire bay. Density sliced ERTS-1 image I.D. 1071-21144-5 (Figure 18) of 2 October 1972 shows the Nushagak River and Bay as a major source for sediment. The sediment influx from Kvichak Bay, however, cannot be seen here due to cloud cover. Although the denser sediment plume remains close to shore it appears that advective sediment transport offshore is primarily brought about by tidal currents. The tides in this region are amplified and tidal variations are approximately 8 meters. Farther offshore the configuration of the various bands of suspended load show the increasing effects of the anticlockwise current which carries sediment to the west.

Cook Inlet

Cook Inlet, (Figure 19) located in southcentral Alaska, is readily accessible and is the industrial and population center for Alaska. Active petroleum exploration and production and the fisheries in this region have provided a firm base for industrialization. With the advent of industrial growth and the rapid increase in population the sewage and industrial waste outfall has also increased. In order to relate the increasing pressure of human activity on the marine environment Cook Inlet was ideally chosen as a test site for the study of ERTS-1 imagery to provide information for better management of the regional development.

The program in this area was initiated in August 1972. A total of five oceanographic cruises were conducted to obtain synchronous ground truth data on suspended sediment load, temperature and salinity of waters throughout Cook Inlet. Water samples from the inlet have also been routinely collected at various oil platforms during ERTS-1 passes on clear days.

In August 1972, research was accomplished using a chartered 26' work boat from the port of Homer. This chartered boat proved excellent for surface water sampling, for its speed of 25-30 knots permitted very rapid coverage of the study area. A series of stations extending from Homer to the bifurcation of the inlet near Anchorage were obtained on 22-23 August 1972 (Figure 20). In September 1972 the University of Alaska's R/V Acona was used to conduct a much more comprehensive study throughout the inlet. The ship time for this cruise was provided by the Institute of Marine Science at no cost to the ERTS 110-7 project. However, because of Acona's speed (approximately 8 knots) stations cover a much longer time span (25-29 September, Figure 21). The ERTS-1 imagery obtained over the Cook Inlet area during both the August and September 1972 cruises was unuseable; the cloud cover over the inlet was over 70% on both occasions. The basic ground truth obtained during these cruises included temperature and salinity profiles over the upper segment of the water column (routinely to a depth of 12 meters, at one meter intervals) and the collection of water samples for suspended load determination. The surface water data from these cruises is shown in Figures 22-27. Subsurface measurements show that the suspended load normally increased with depth in the water column whereas temperature and salinity remained relatively constant throughout the water column.

During the 1973 season, three more cruises were scheduled in Cook Inlet to obtain synchronous ground

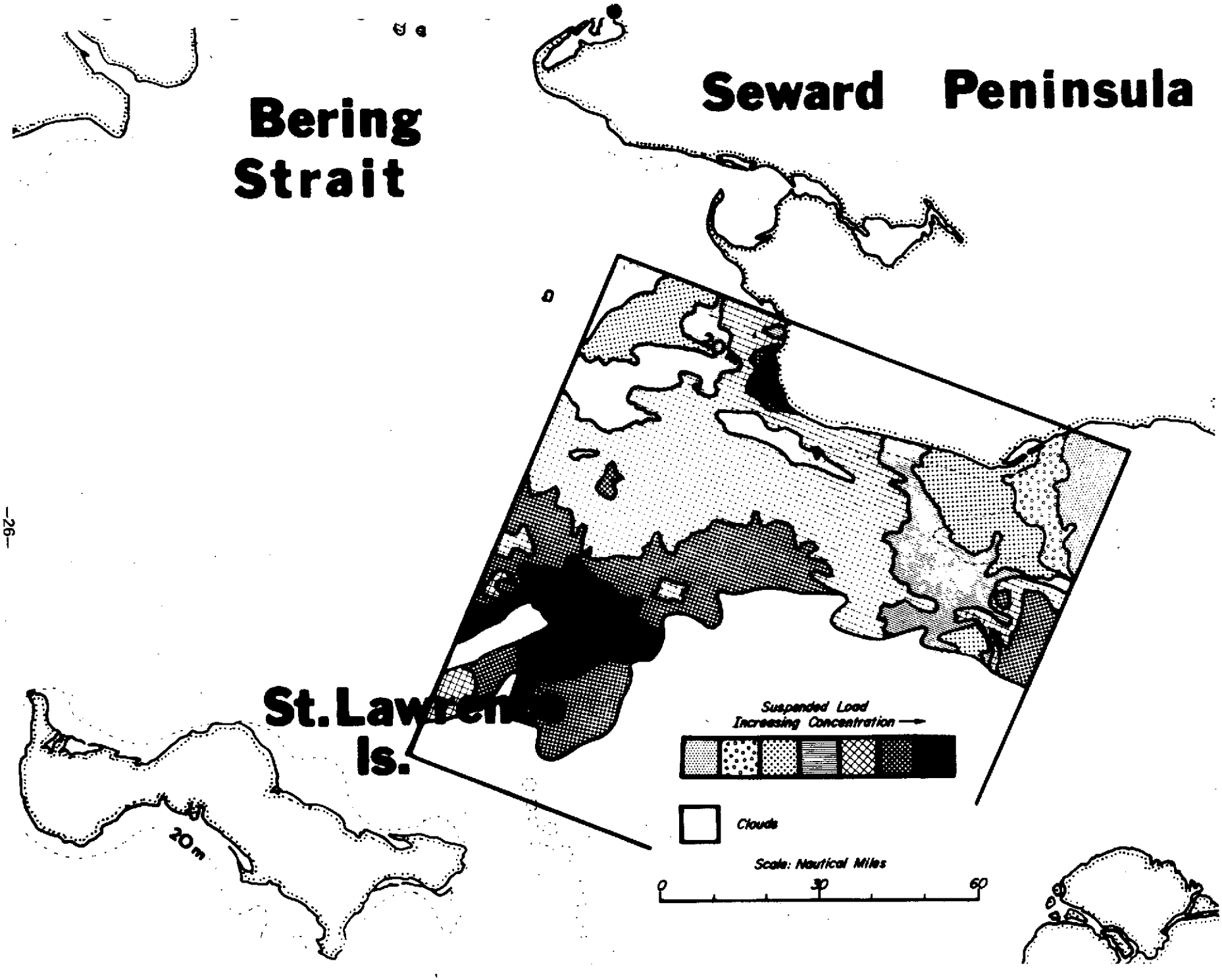

FIGURE 17. Relative suspended load distribution in the vicinity of Nome on 23 Sep 1972, based on color density slice of image I.D. 1062-22044-4. Refer to area 6 of Figure 1.

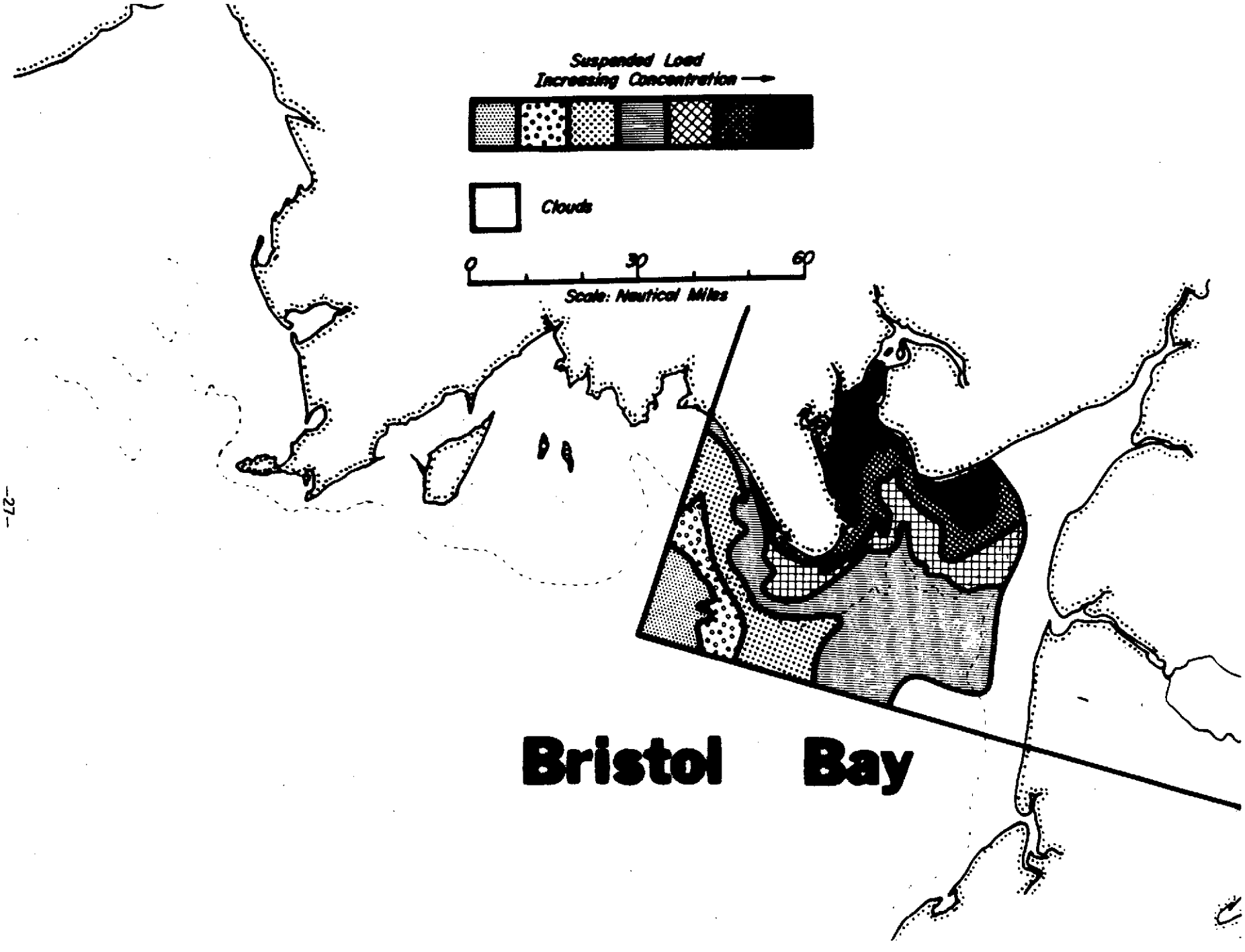

FIGURE 18. Relative suspended load distribution in the vicinity of Nushagak Bay on 2 Oct 1972, based on color density slice of image I.D. 1071-21144-5. Refer to area 0 of Figure 1.

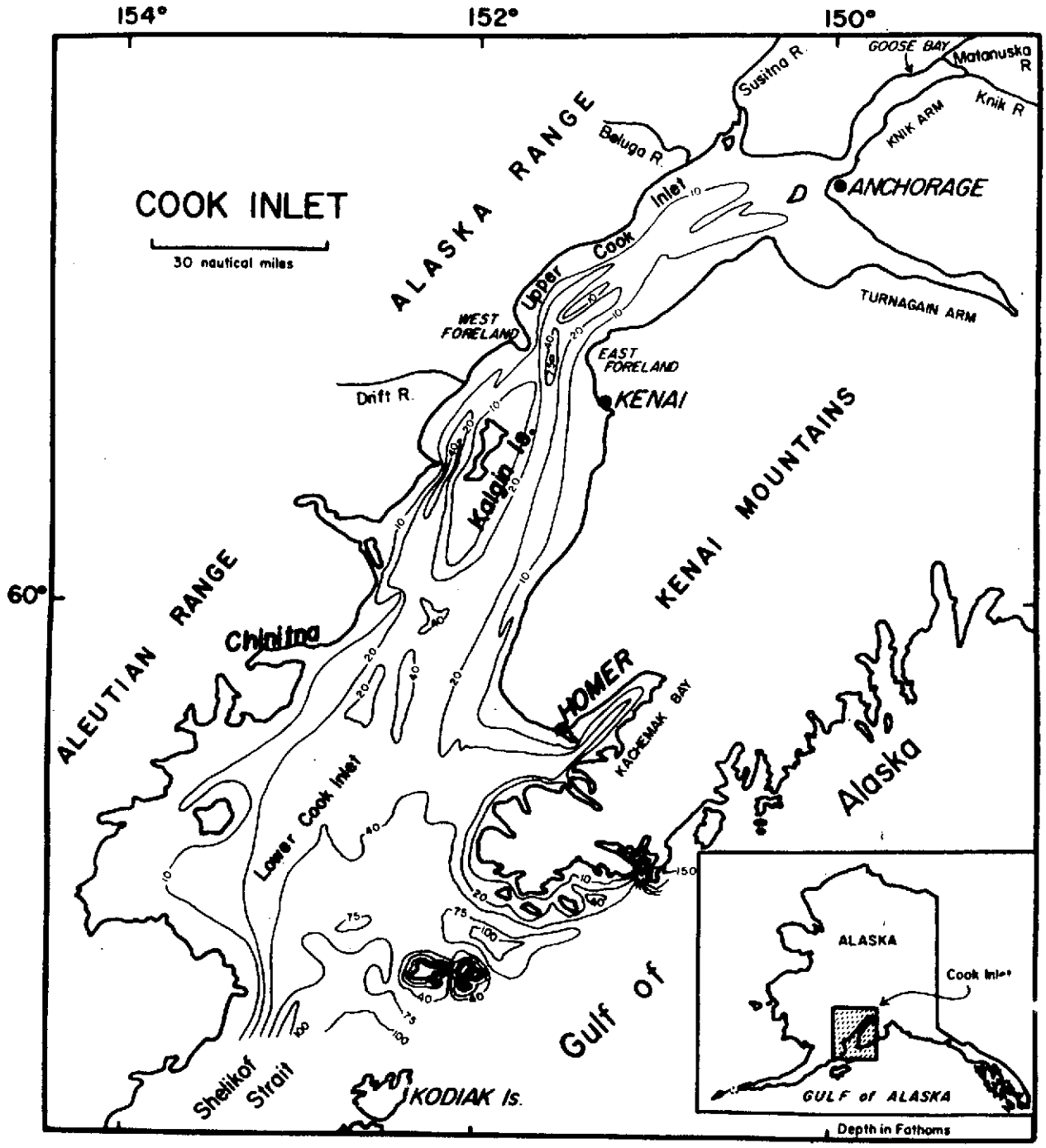

FIGURE 19. Index map of Cook Inlet.

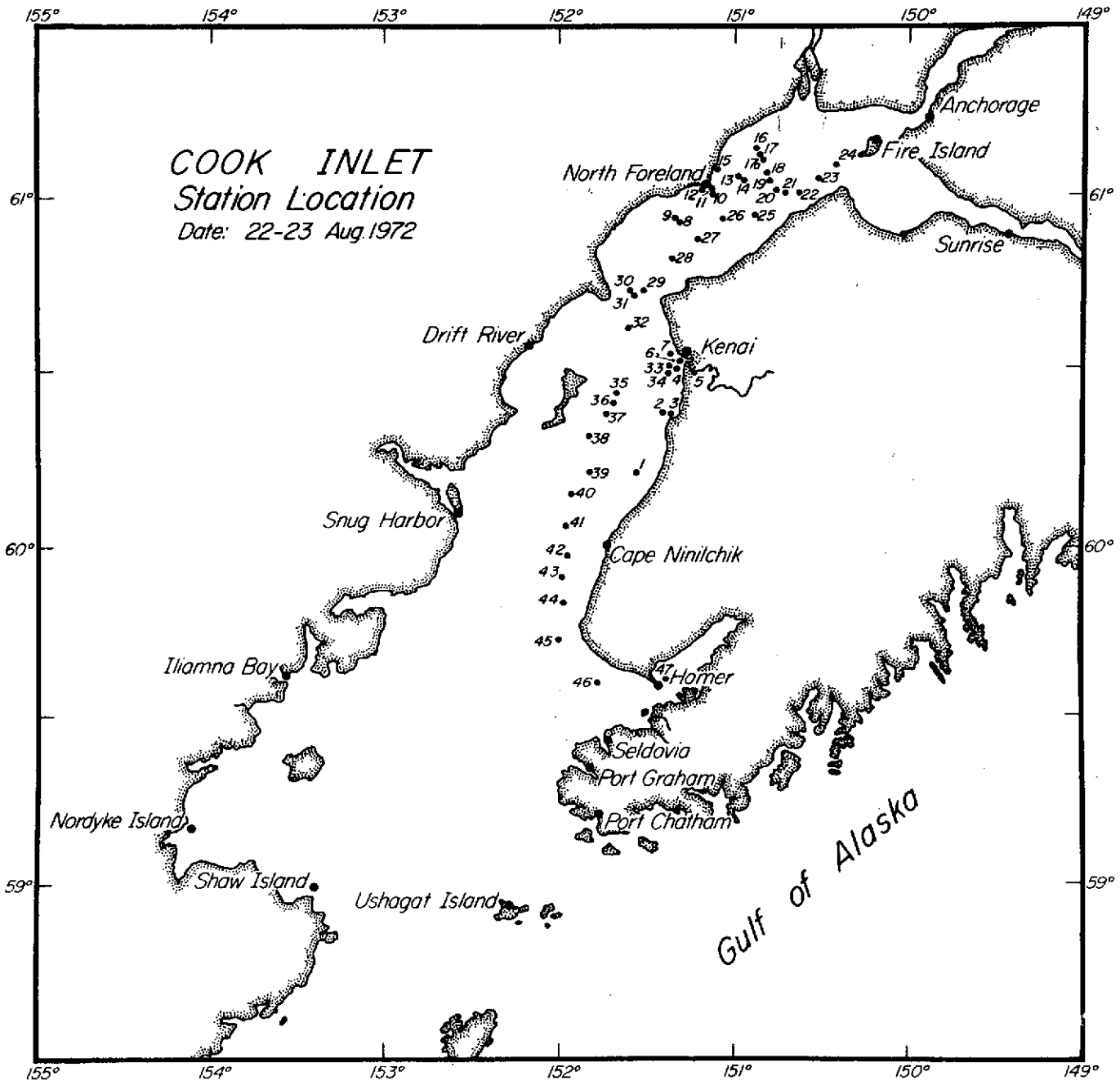

FIGURE 20. Station locations for sampling in Cook Inlet, Alaska; 22-23 August 1972.

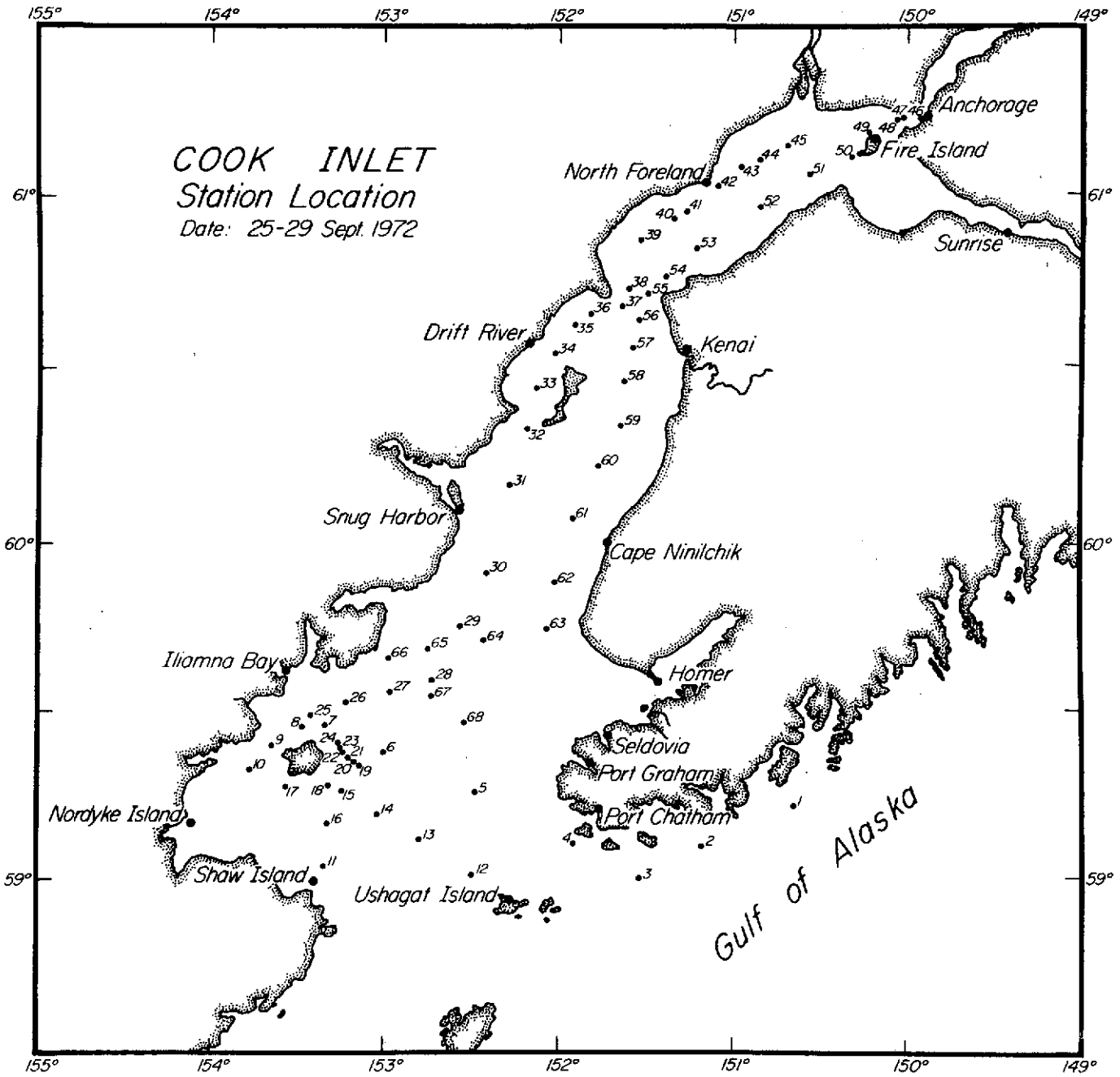

FIGURE 21. Station locations for sampling in Cook Inlet, Alaska; 25-29 September 1972.

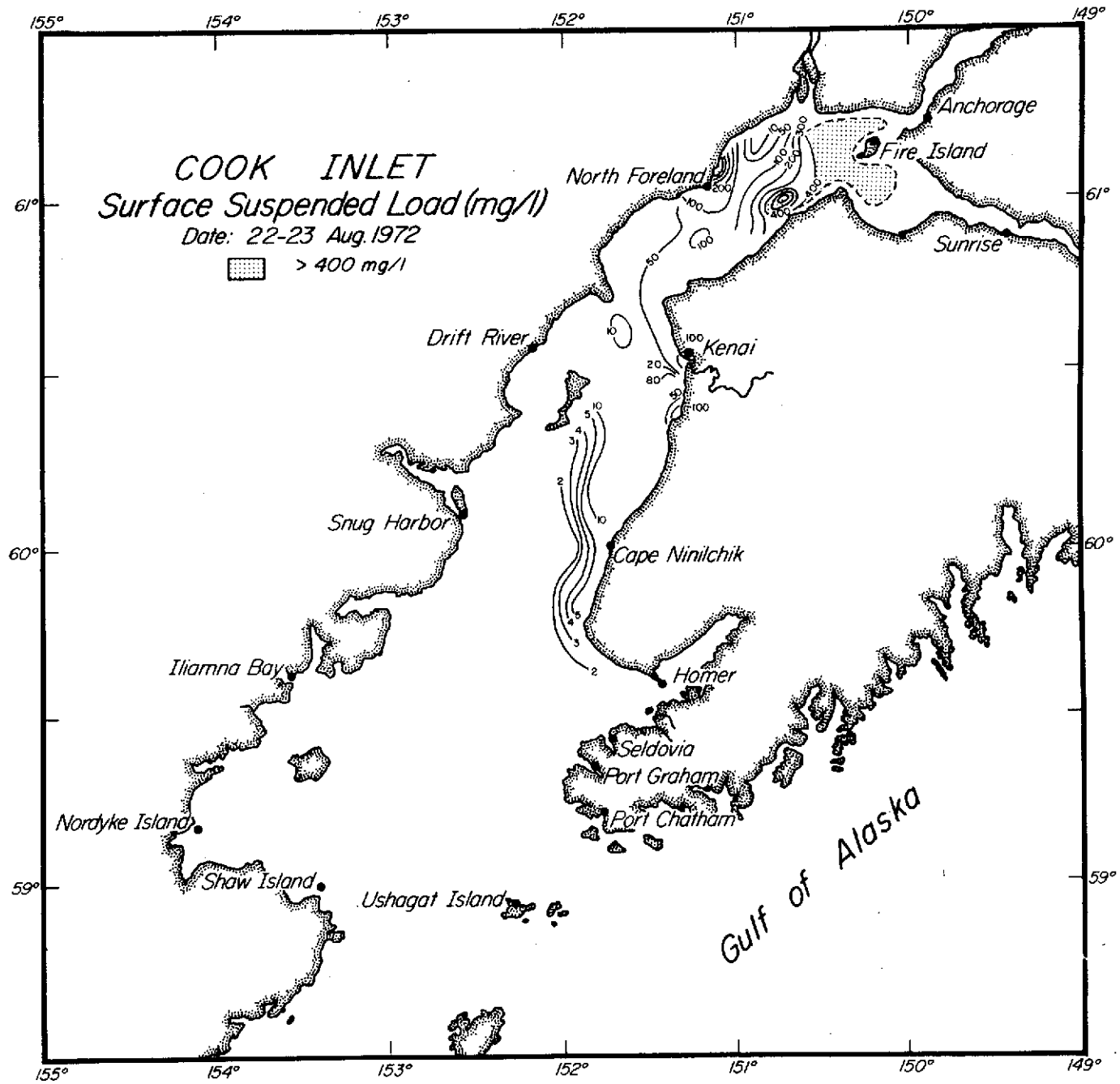

FIGURE 22. Suspended load distribution (mg/1) in surface waters of Cook Inlet, Alaska; 22-23 August 1972.

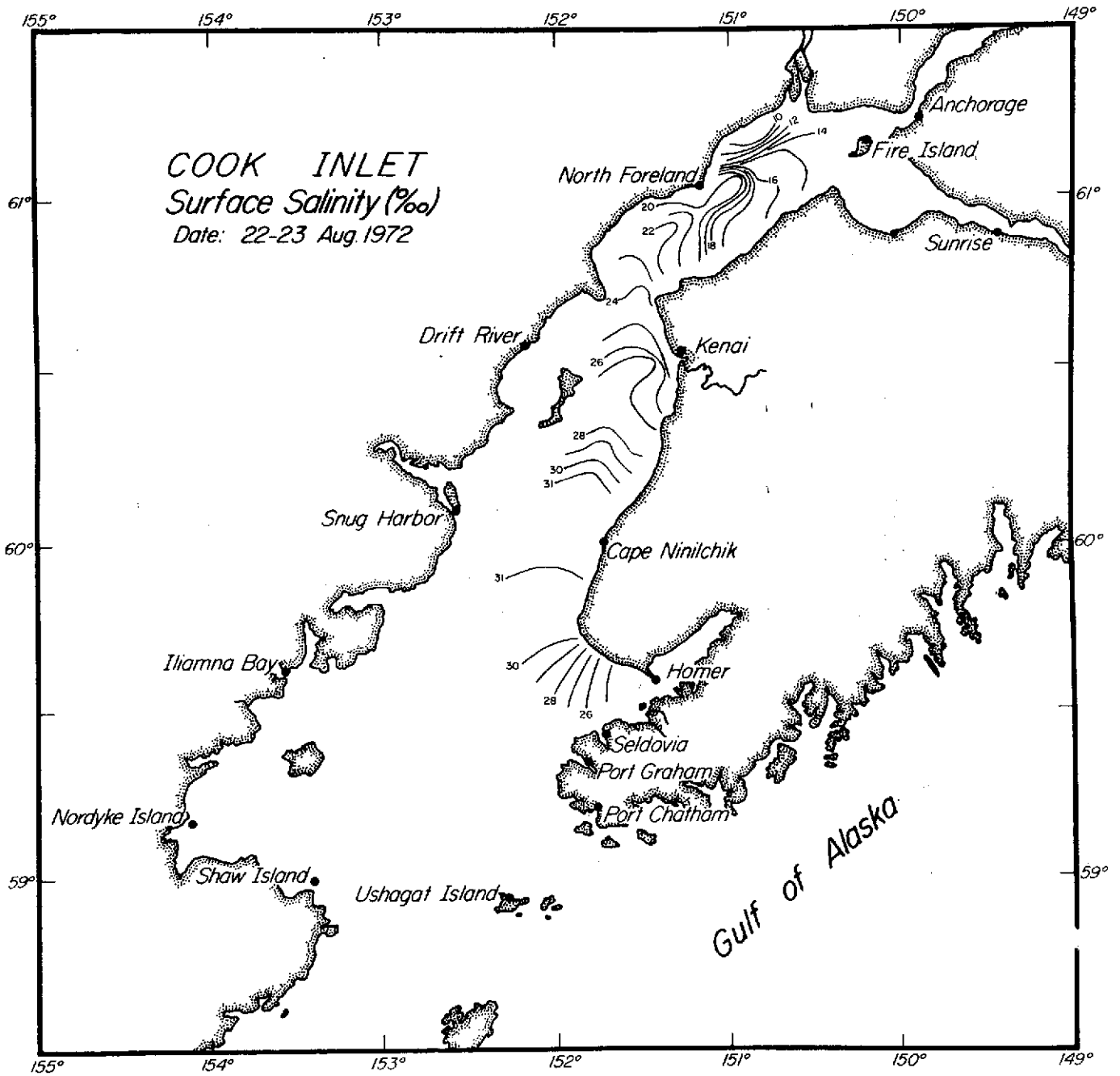

FIGURE 23. Surface water isohalines ($^{o}/_{oo}$) in Cook Inlet, Alaska; 22-23 August 1972.

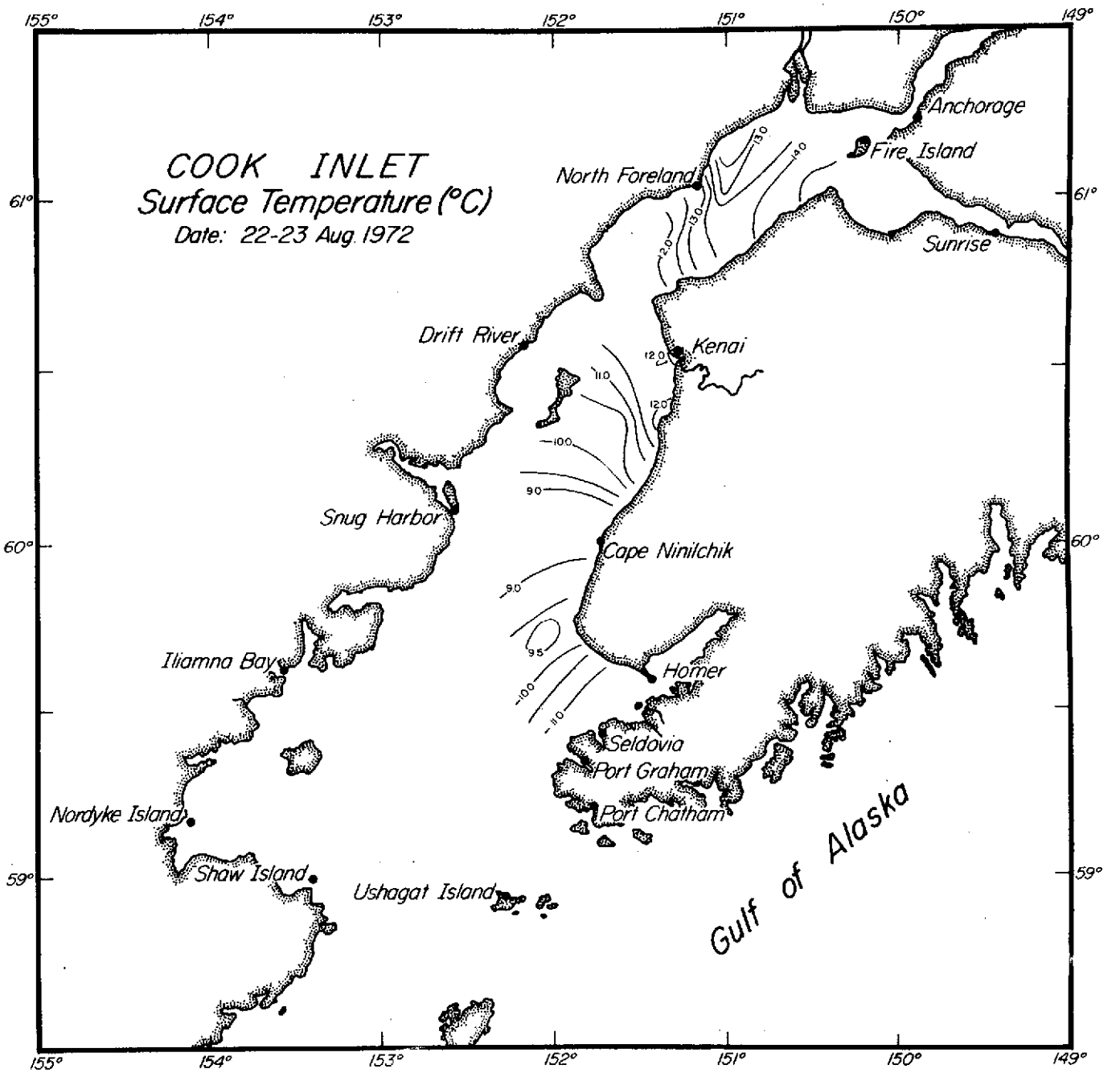

FIGURE 24. Surface water isotherms (°C.) in Cook Inlet, Alaska; 22-23 August 1972.

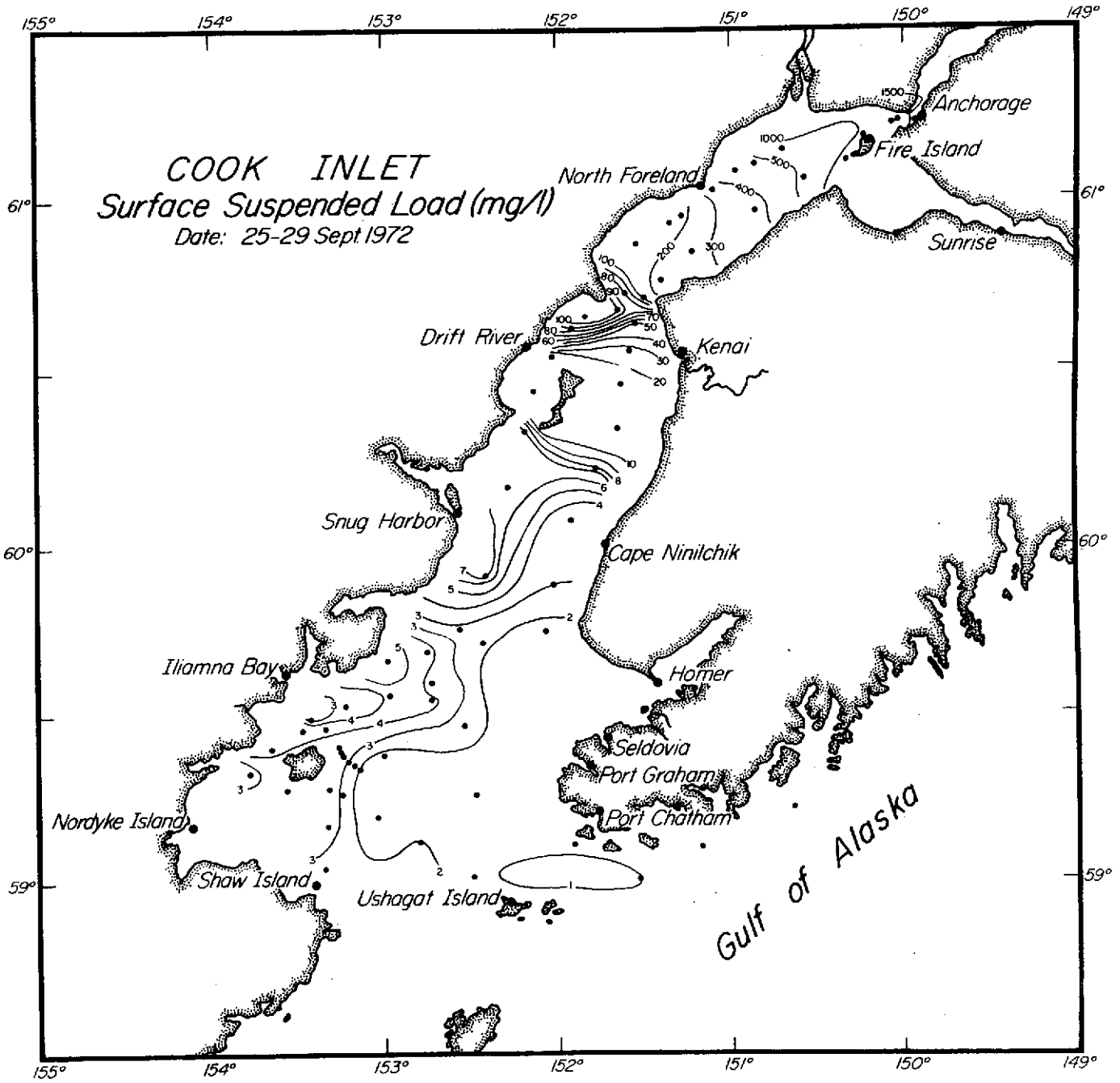

FIGURE 25. Suspended load distribution (mg/1) in surface waters of Cook Inlet, Alaska; 25-29 September 1972.

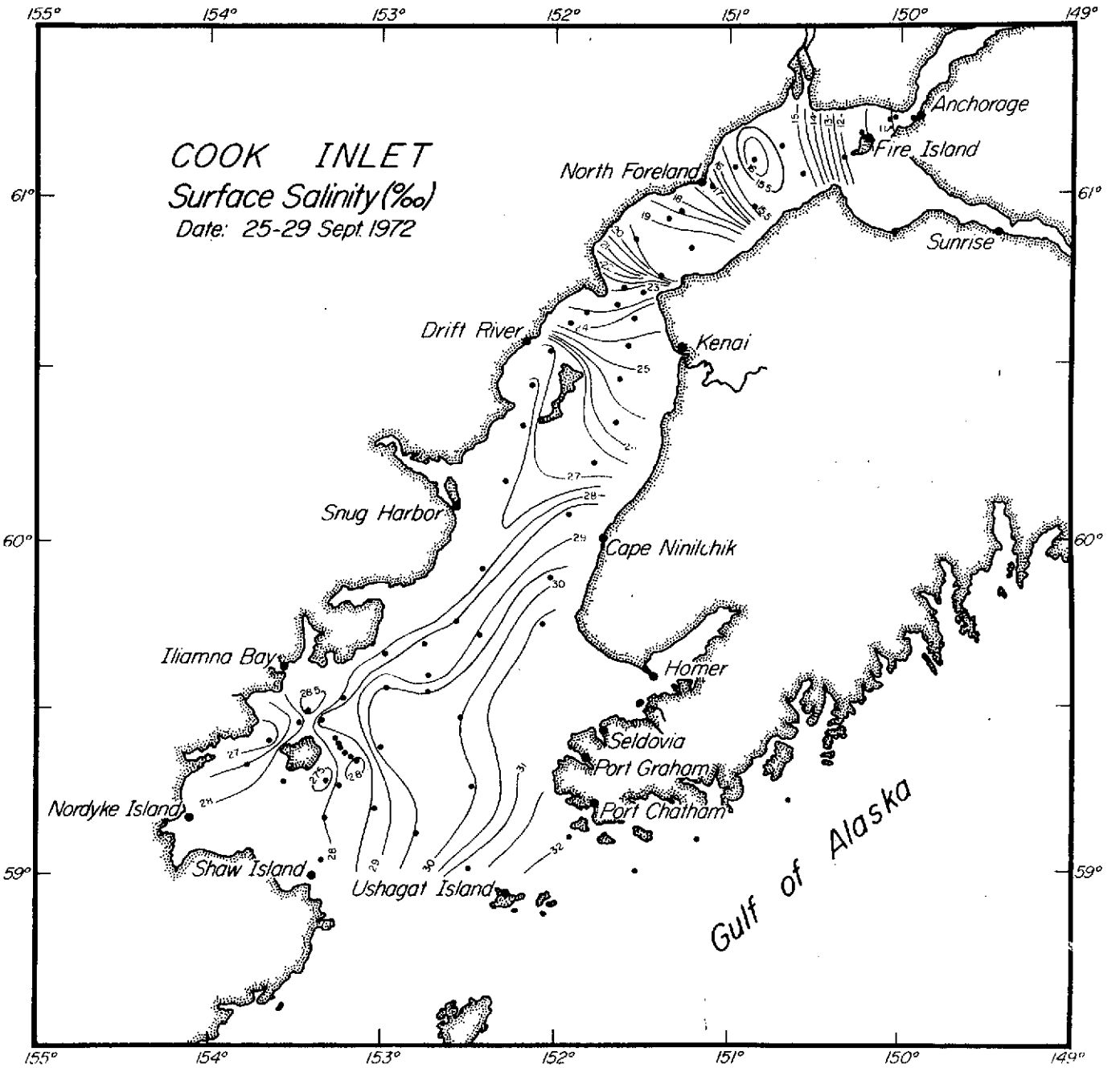

FIGURE 26. Surface water isohalines ($^{o}/_{oo}$) in Cook Inlet, Alaska; 25-29 September 1972.

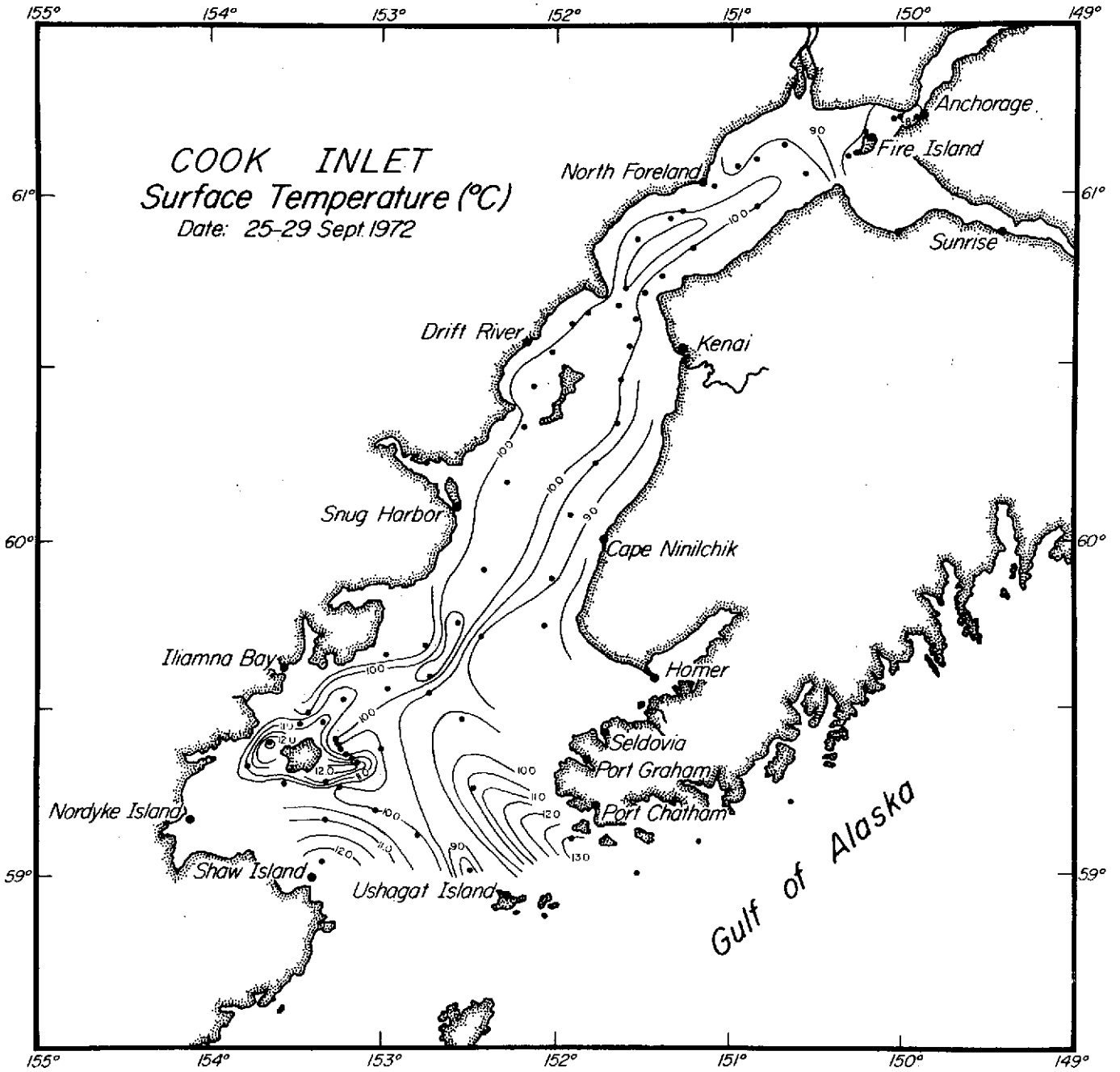

FIGURE 27. Surface water isotherms (°C.) in Cook Inlet, Alaska; 25-29 September 1972.

truth data during ERTS-1 satellite passes. These cruises were conducted during 27 March 1973, 14 April 1973 and 7-8 June 1973. The stations for sampling were arranged to cover an area containing a maximum variation in suspended sediment in a minimum amount of time. Cloudy skies during the first cruise (27 March) did not permit ERTS-1 to obtain imagery of the area, and ice and rough seas impeded ground data acquisition. April 14 was also cloudy, however, clear imagery was obtained the following day, providing useful ground truth correlation which is discussed below. The final cruise of the 1973 season also experienced excessive cloud cover and no useful imagery was obtained. The results of these cruises are shown in Figures 28-35.

The 14 April 1973 cruise consisted of a straight track from Homer to Chinitna Bay on the west side of the inlet and back to Homer. The leg from Homer to Chinitna Bay was conducted during flood tide and is indicated by the open circles and dashed contours in Figures 30-32. The return leg from Chinitna Bay to Homer was conducted during ebb tide and is indicated by the solid circles and contours. The satellite passed overhead while the boat was in Chinitna Bay. During ebb tide the contours of suspended load (Figure 31) are shifted to the east due to intensification of the southward moving wedge of sediment laden water in the western half of the inlet. Temperature contours (Figure 32), however, are shifted in an opposite sense (the intruding sea water on the east side of the inlet is warmer than the outflowing turbid water on the west side of the inlet) and may reflect a complex, possibly three-dimensional circulation in this region of the inlet.

The relatively clear ERTS-1 image for the following day (I.D. 1266-20581, 15 April 1973) is regarded as closely synchronous to the ground truth obtained the previous day since the tidal stage and general meteorological and runoff conditions were approximately the same. The suspended load distribution of 14 April (Figure 31) was overlain on the VP-8 TV screen while density slicing the band 4 image of the clear 15 April scene (Figure 36) and the density slice contours were adjusted to conform roughly with the ebb tide contours (Figure 37). Although it would probably be more correct to position the density slice color boundaries approximately midway between the contours for flood and ebb tide, the critical area near the center of the image is obscured by clouds, leaving only the ebb tide contours within the clear portion of the image. However, more importantly Figure 37 illustrates a technique wherein, given a limited amount of relatively synchronous ground truth data, the distribution of the surface suspneded load over a relatively large area can be contoured reasonably accurately.

Figure 37 also illustrates the upper limits (about 20 mg/1) of suspended load concentration for which band 4 is useable in the density slicing technique. Band 5 must be used to bring out detail in the western part of the inlet.

The hydrographic data obtained from Cook Inlet covers almost the entire spring, summer and fall fresh water runoff seasons. The overall water circulation pattern emerging from the analyses of the data from each cruise appears to be consistent throughout the spring to fall period. Salinity, temperature and suspended sediment concentration in upper Cook Inlet change significantly with the season and reflect variations in fresh water input, however, these parameters remain relatively unchanged near the mouth of Cook Inlet during ice-free seasons. The clear Gulf of Alaska sea water, intruding along the east side of the inlet and extending as far north as Kenai, has been found to consistently carry 1-2 mg/1 of suspended load and has provided a standard for the comparative density slicing of the entire Cook Inlet area. Using the relative variations in concentration, we have been able to delineate the general circulation pattern, the influx of sea and fresh water masses, and the mixing of these water masses within Cook Inlet. Although the general water circulation in Cook Inlet can be easily interpreted from the water parameters measured during the various cruises, the ERTS-1 imagery has brought out previously unknown regional eddies and temporary water currents which exist in various parts of the inlet only for short periods at certain tidal stages.

Water temperature and salinity values for Cook Inlet cover a fairly broad range of values, but are certainly not unusual for high latitude estuaries. The suspended sediment values, however, are of particular interest. They may range to over 1500 mg/1 in the surface waters near the head of the inlet. This suspended material consists largely of mechanically abraded rock debris transported by glacial meltwater streams. It is predominantly finely comminuted quarts, the bulk of which is in the silt size range, but often contains material as coarse as fine sand or as fine as clay particles. The percentage clays in this material is quite variable and mineralogically the clays tend towards illite (Sharma and Burrell, 1970). Such suspended sediments, commonly referred to as "glacial flour", are typical of northern latitudes and produce the highly turbid waters. When these turbid waters enter the inlet they generally persist as discrete layers on or in the water column for a considerable period of time and permit ERTS observation of the detailed circulation in Cook Inlet and other inshore water.

The analysis of the various ERTS-1 images obtained so far shows a striking and clear, although complex, surface circulation. In general, all imagery shows that turbid water introduced by glacial meltwater streams and rivers, mostly towards the head of the inlet, completely dominates the surface for the upper two-thirds of the

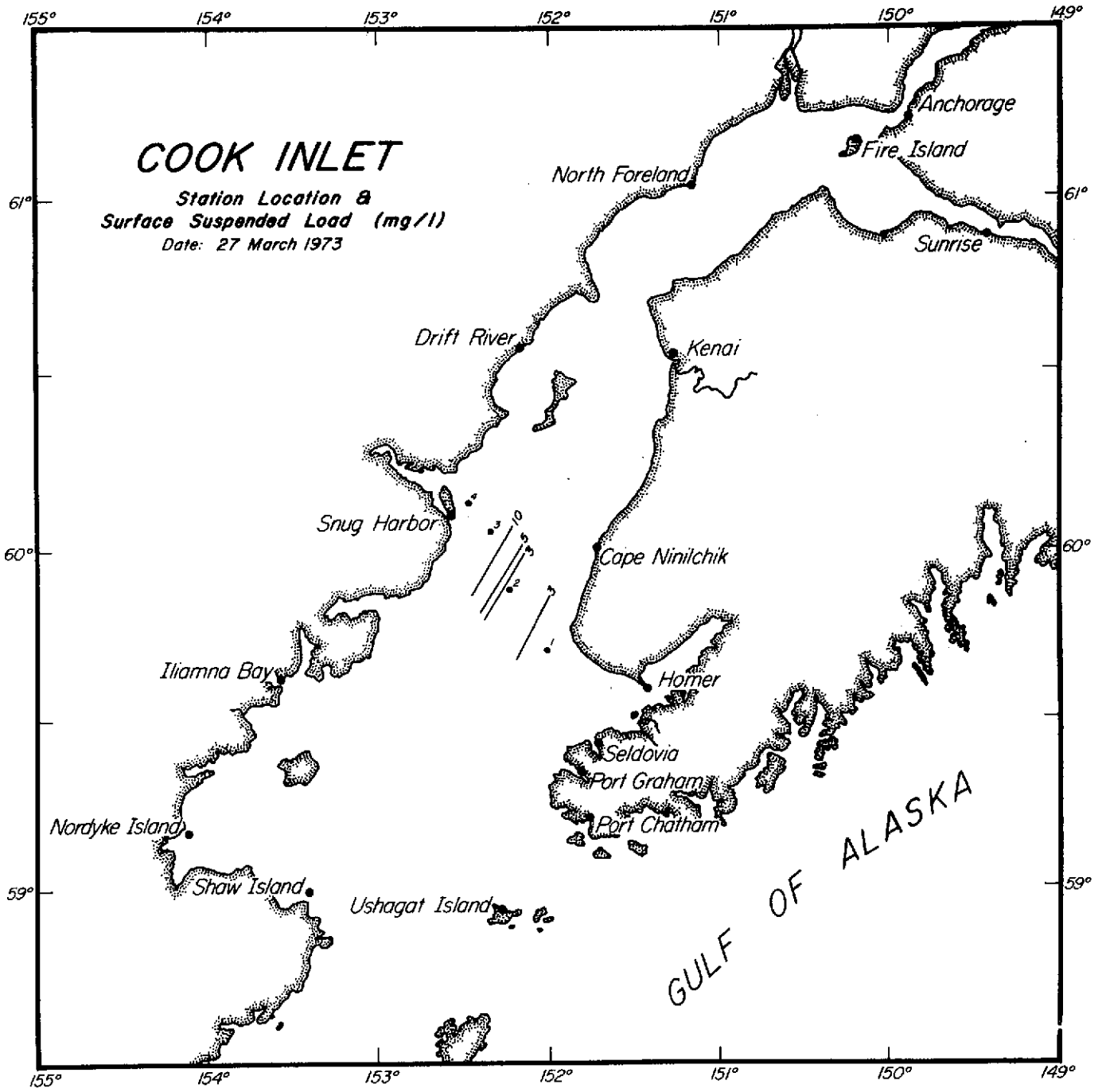

FIGURE 28. Suspended load distribution (mg/1) in surface waters of Cook Inlet, Alaska; 27 March 1973.

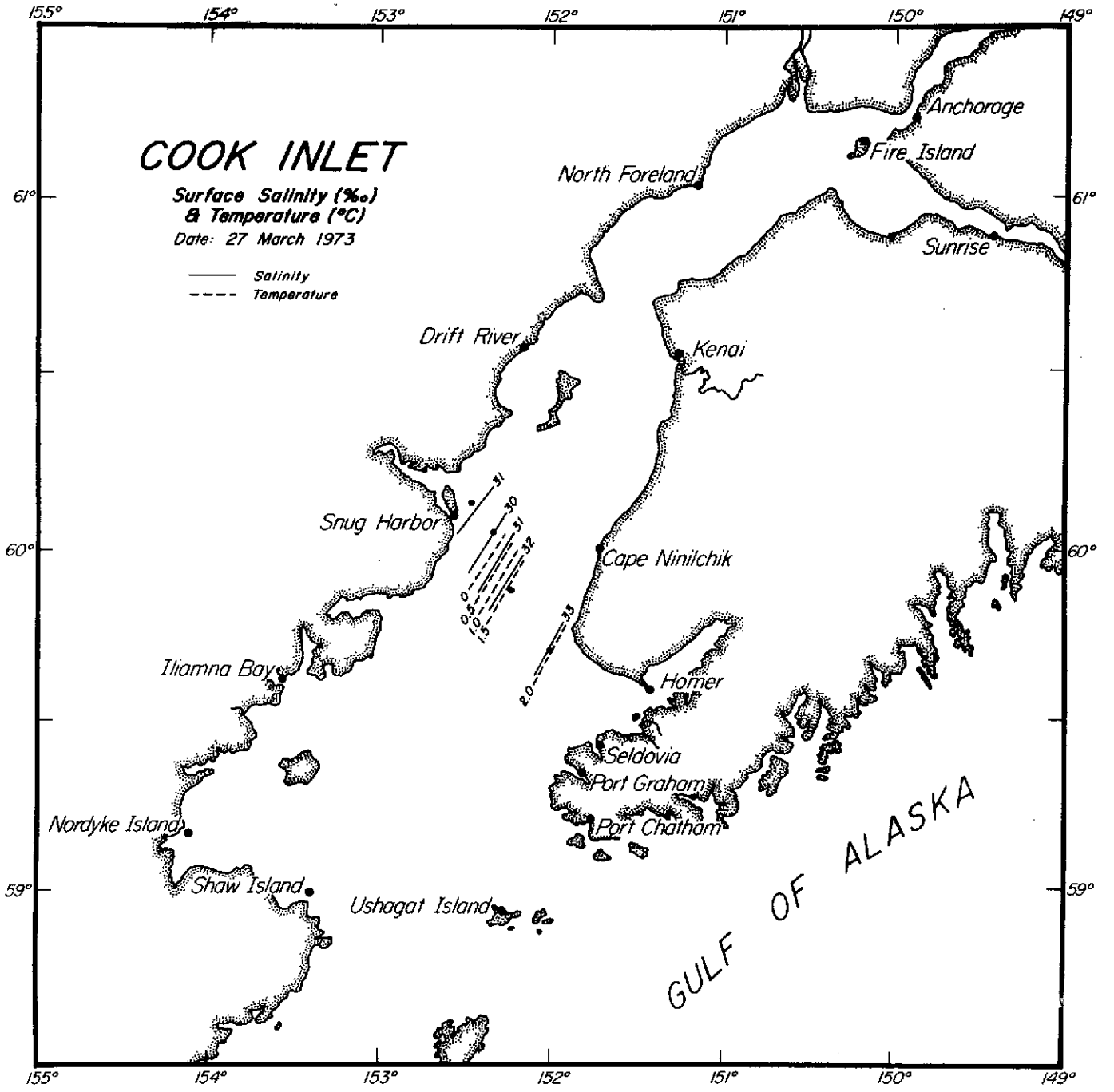

FIGURE 29. Surface water isohalines ($^{o}/_{oo}$) and isotherms (^{o}C.) in Cook Inlet, Alaska; 27 March 1973.

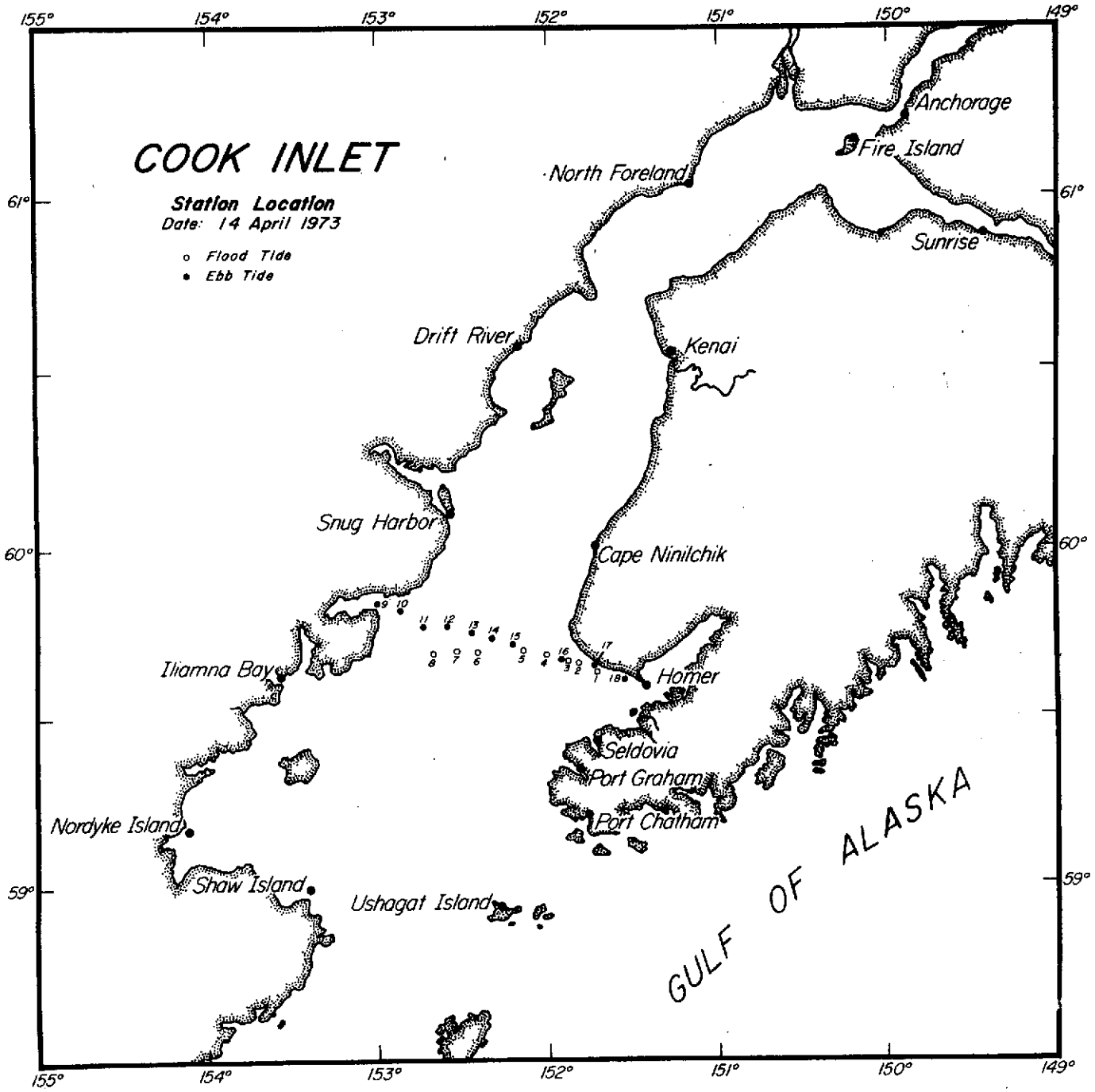

FIGURE 30. Station locations for sampling in Cook Inlet, Alaska; 14 April 1973.

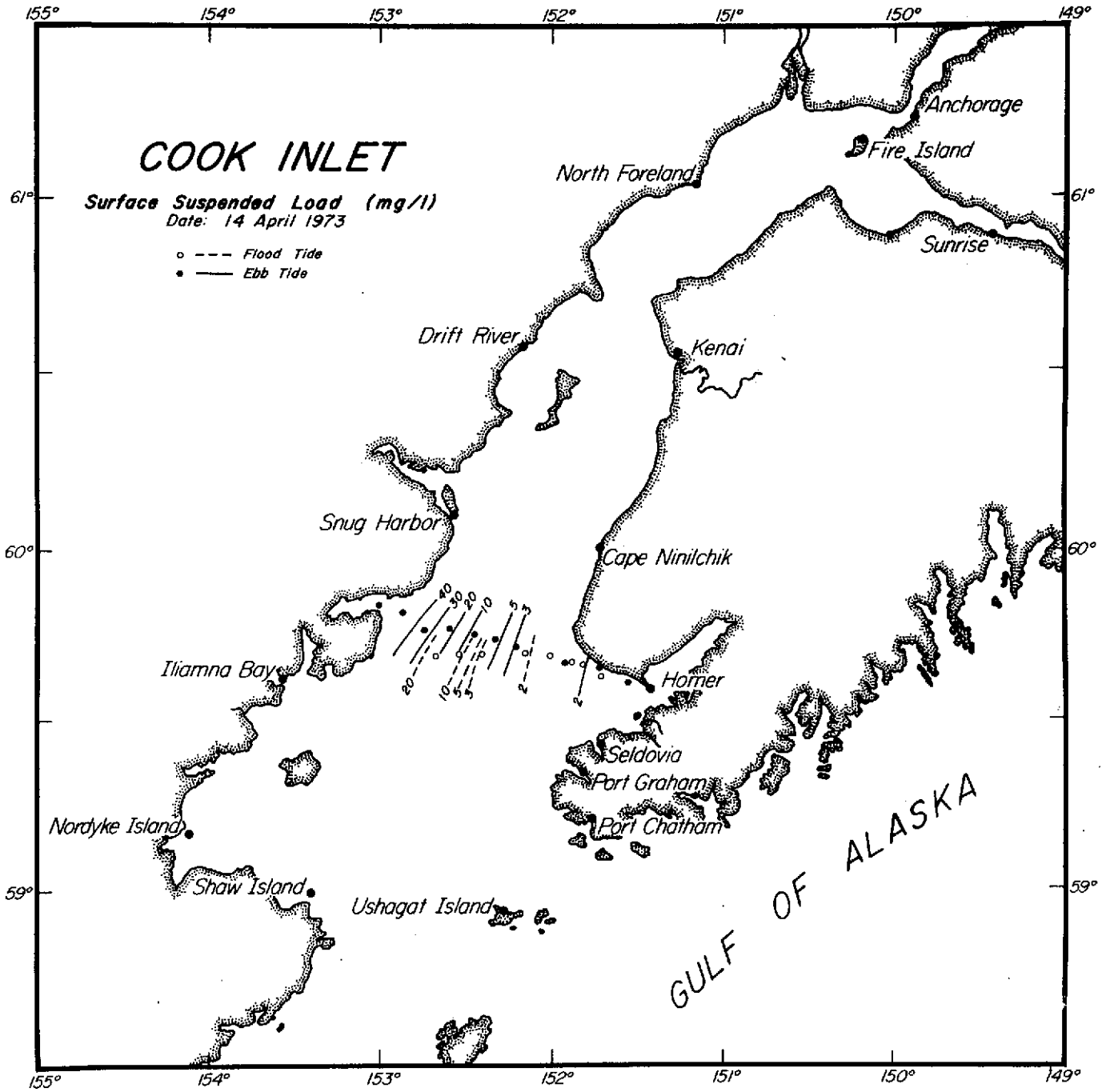

FIGURE 31. Suspended load distribution (mg/1) in surface waters of Cook Inlet, Alaska; 14 April 1973.

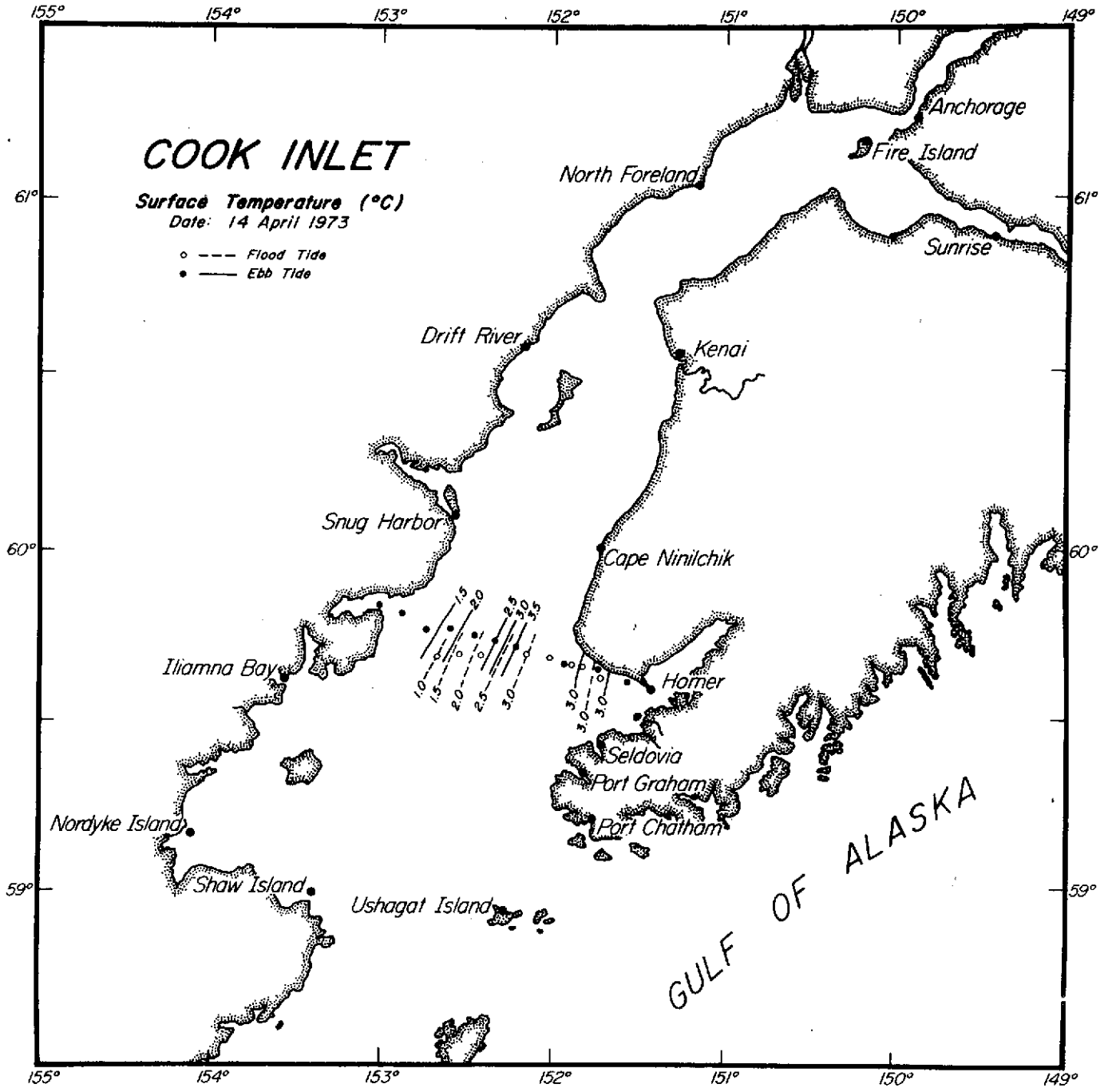

FIGURE 32. Surface water isotherms (°C.) in Cook Inlet, Alaska; 14 April 1973.

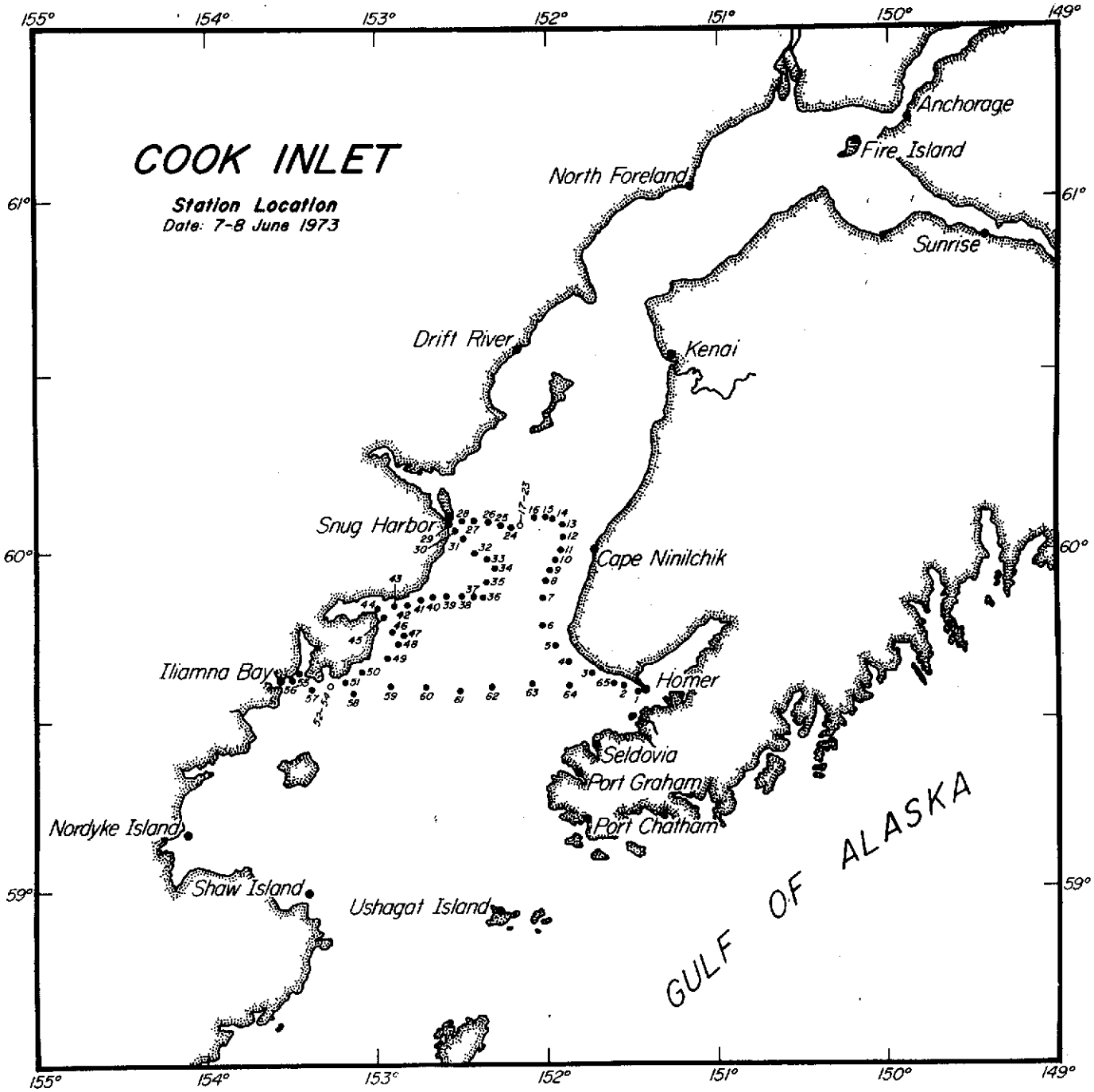

FIGURE 33. Station locations for sampling in Cook Inlet, Alaska; 7-8 June 1973.

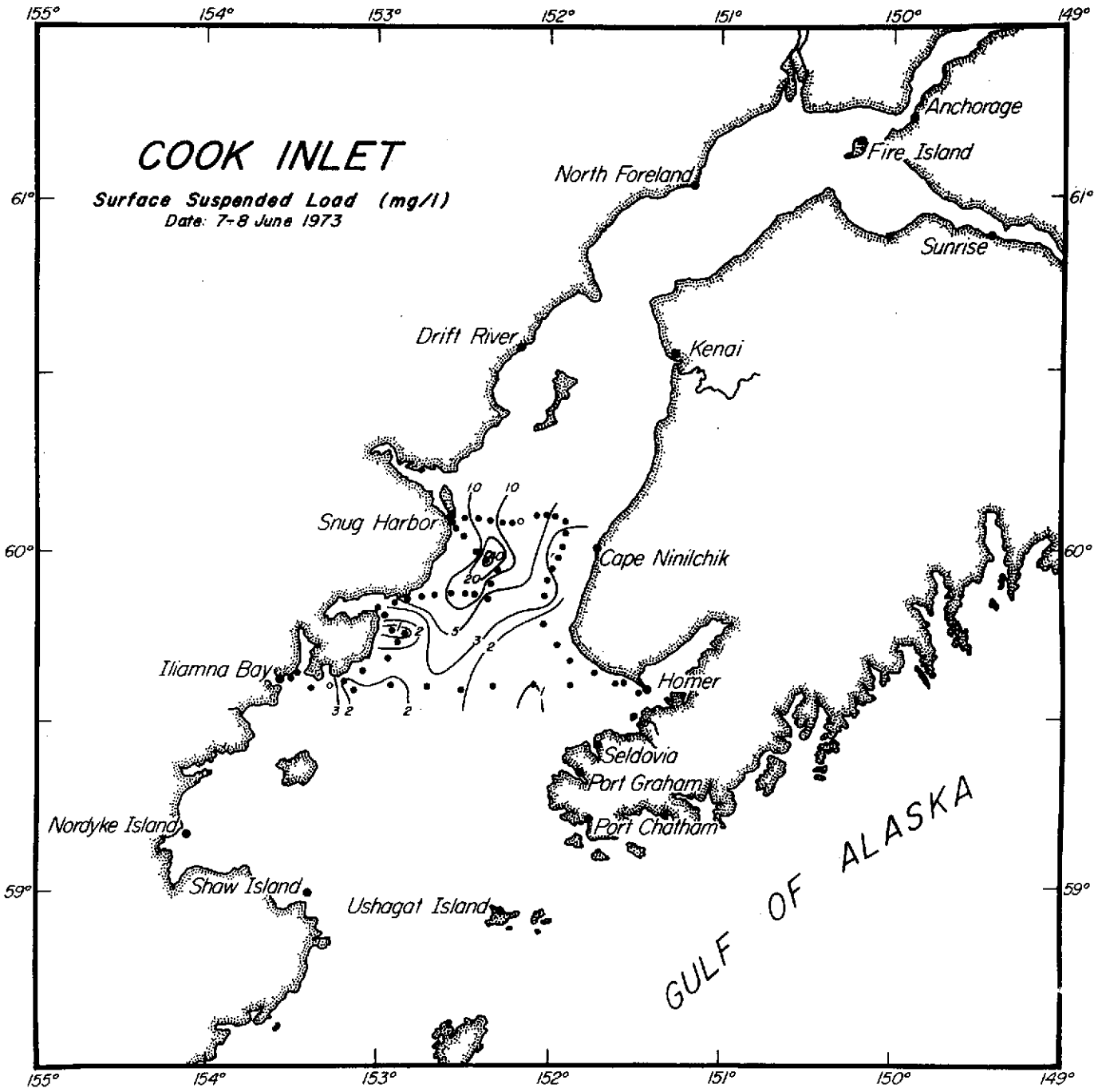

FIGURE 34. Suspended load distribution (mg/1) in surface waters of Cook Inlet, Alaska; 7-8 June 1973.

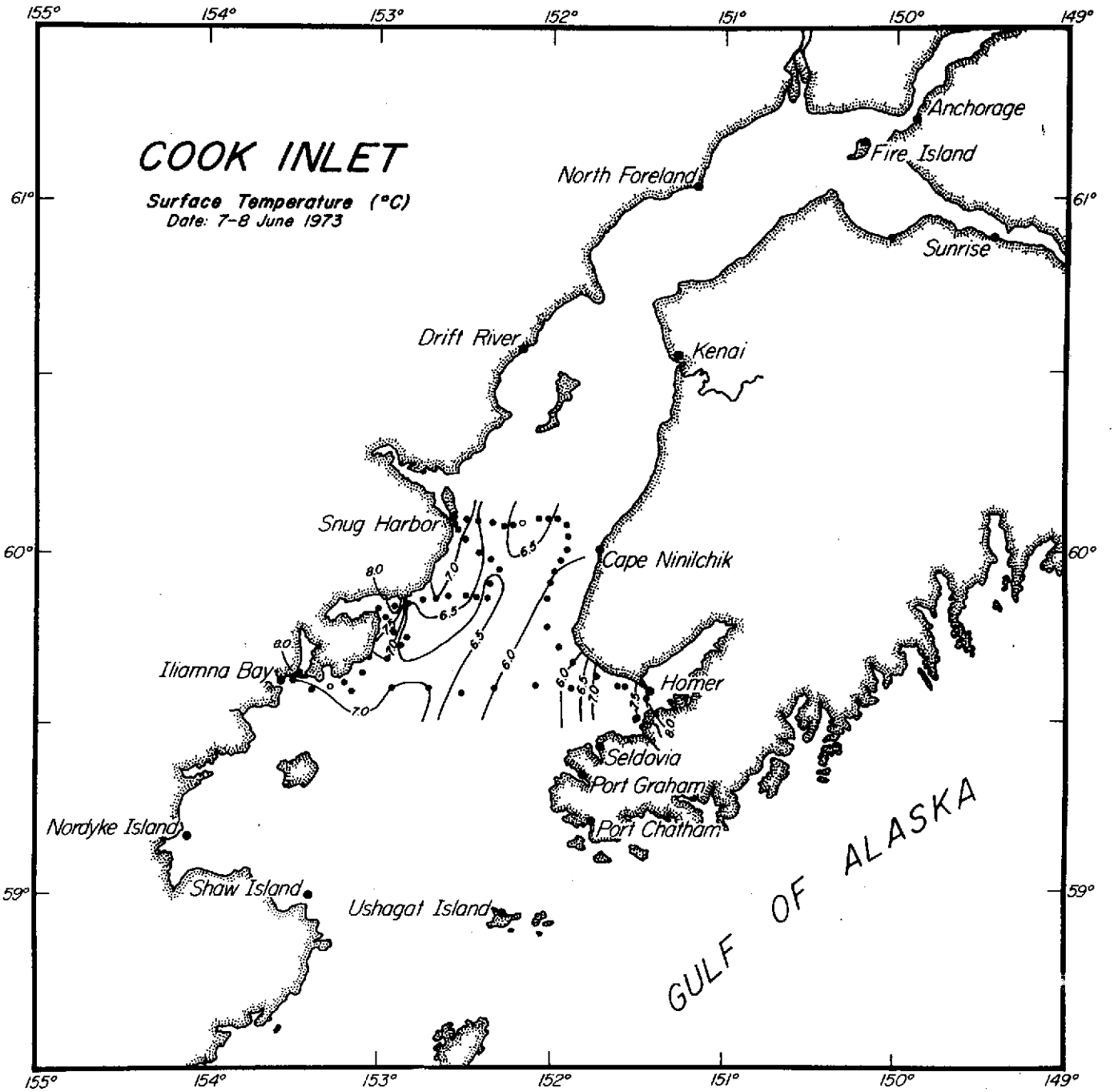

FIGURE 35. Surface water isotherms (°C.) in Cook Inlet, Alaska; 7-8 June 1973.

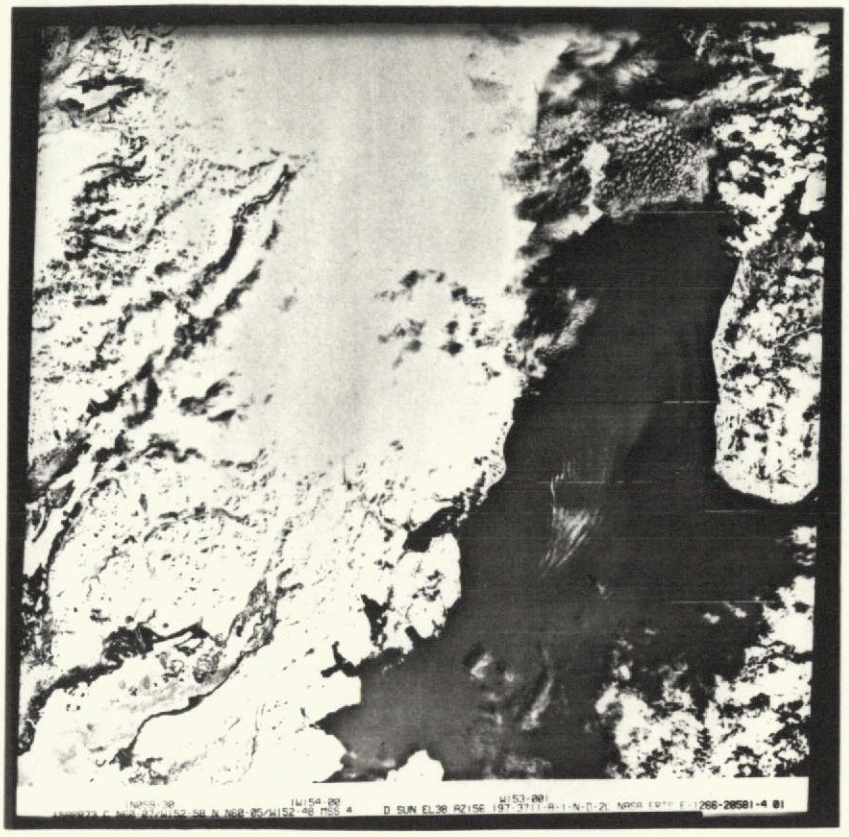

FIGURE 36. ERTS-1 image I.D. 1266-30581-4.

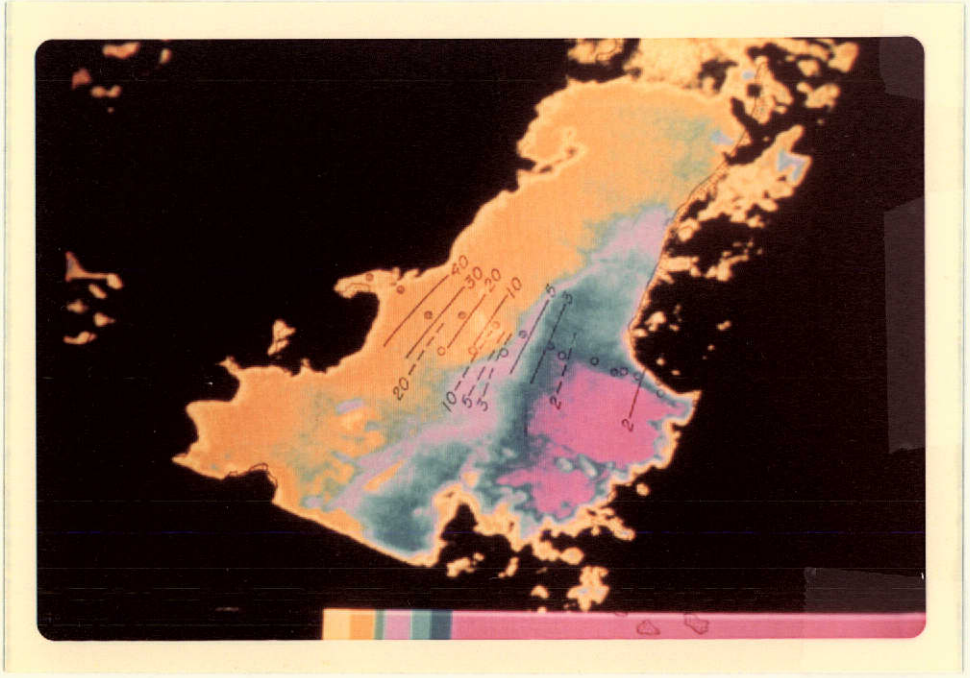

FIGURE 37. Color density slice of image I.D. 1266-20581-4.

inlet and along the west shore of almost the entire inlet. Clear sea water with approximately 1-2 mg/1 of suspended load intrudes near the mouth of the inlet and sometimes (during flood tide) extends along the eastern shore as far north as Kenai.

Basically the hydrography of Cook Inlet entails the mixing of these two distinct water masses, controlled by basin geometry and tides. The tidal amplification (approximately 10 meters near Anchorage) and extreme differences in tidal phase in various parts of the inlet produce complex circulation patterns in Cook Inlet which can be studied only through the use of ERTS imagery which provides truly synoptic data over the entirety of the unusually large estuary (over 250 km. in length).

The relative distribution of sediment in suspension interpreted from ERTS-1 composite image I.D. 1104-20574 and -20581-4 of 4 November 1972 is shown in Figure 38. Clear (suspended load approximately 1-2 mg/1) marine water is seen intruding near the mouth and, due to Coriolis force, moves northeastward along the east shore of Cook Inlet. Turbid sediment laden water is observed along the western shore, ultimately passing out of Cook Inlet via Shelikof Strait. This water originates in upper Cook Inlet and is extensively mixed in the Forelands area as seen in ERTS-1 composite image I.D. 1428-20554 and -20560-6 (Figures 39A and 39B) of 24 September 1973. The sediment sources near the head of the inlet are clearly shown by the turbid water originating from Knik Arm. The suspended load concentration of water discharged by the Susitna River is less than that from Knik Arm (Figure 40). Note that the clean water influence is evident in the September image (Figure 39) but not in the November image (Figure 41). This is apparently due to the greatly reduced river discharge in November (Figure 40). Turnagain Arm has no significant sediment sources within the Arm itself but instead receives sediments from Knik Arm which are washed into Turnagain Arm on the flood tide. The nearshore waters of upper Cook Inlet appear to contain rather large concentrations of sediments. This is primarily due to the amplified tides which generate strong tidal currents on the shallow tidal flats, thereby maintaining the fine sediments in suspension. The heaviest concentrations of suspended load along the northwest and southeast shores of the upper inlet (Figure 39A) conform closely with nearshore shoal areas with depths shallower than about 6 meters.

It should be noted that near the southern limit of Figure 39A, the suspended load concentration appears uniform across the entire inlet. However, this results because MSS Band 6 (used to produce Figure 39A) is incapable of accurately differentiating suspended load concentrations of $<$ 20 mg/1. MSS Band 5 (Figure 42) provides a more accurate density slice for this area.

Circulation in upper Cook Inlet, as interpreted from both ERTS-1 imagery (Figures 39A and 41) and ground truth data, appears to be a clockwise gyre. Apparently the jet effect of the East-West Forelands area, where during flood tide the configuration of the Forelands jets the flooding water to the west side of the inlet, is sufficient to overcome Coriolis force which would normally maintain northward flow up the east side of the inlet and result in a net counterclockwise gyre as in the lower inlet. Consequently sediments from Knik Arm move south down the east side of the inlet and the clearer flooding water from the lower inlet moves north on the west side of the inlet. The clockwise gyre appears to break down near the upper reaches of the upper inlet and water movement in this area is probably a northeast-southwest pulsation due to the flood and ebb of the tides.

The water circulation south of the East and West Forelands in the region of Kalgin Island appears to be much more complex and very dependent on the stage of tide. As seen in Figures 39A, B, 41 and 42, there appears to be a bifurcation of the relatively clear intruding sea water as this water reaches the vicinity of Kalgin Island. At the time of the 24 September 1973 imagery the tidal stage at Anchorage is approximately one hour before low tide and at Seldovia approximately two hours before high tide and for the 3 November 1972 imagery it is almost exactly low tide at Anchorage and high tide at Seldovia. Therefore in the several hours preceding this imagery the tide has been ebbing in the upper inlet and flooding in the lower inlet. The opposing ebb and flood, at this particular stage of the tide, will meet in the vicinity of the East and West Forelands. A schematic representation of the resultant circulation is shown in Figure 43. The box shows the area covered by Figure 44 which is a portion of density sliced image I.D. 1103-20513-6 of 3 November 1972 and exemplifies the Forelands area circulation at this tidal stage. Apparently the ebbing waters in the upper inlet are jetted through the Forelands, primarily in a southeasterly direction. This water meets and opposes the relatively clear sea water carried up the east side of the inlet by the flood tide. The path of least resistance for the intruding sea water will be to the west and north around the west side of Kalgin Island, producing the suspended load distribution as seen in Figures 39A, B, 41-42 and 44. It is emphasized that this particular circulation pattern is characteristic of this particular stage of tide, and may vary considerably at other tidal stages. Unfortunately all available clear imagery of this area of Cook Inlet (3 and 4 November 1972 and 24 September 1973) was obtained at about the same tidal stage (low tide at Anchorage and high tide at Seldovia).

It is also important to remember that, in an area such as Cook Inlet, the suspended load distribution represents a circulation which is superimposed upon the overall pulsating nature of water movement in the inlet. How-

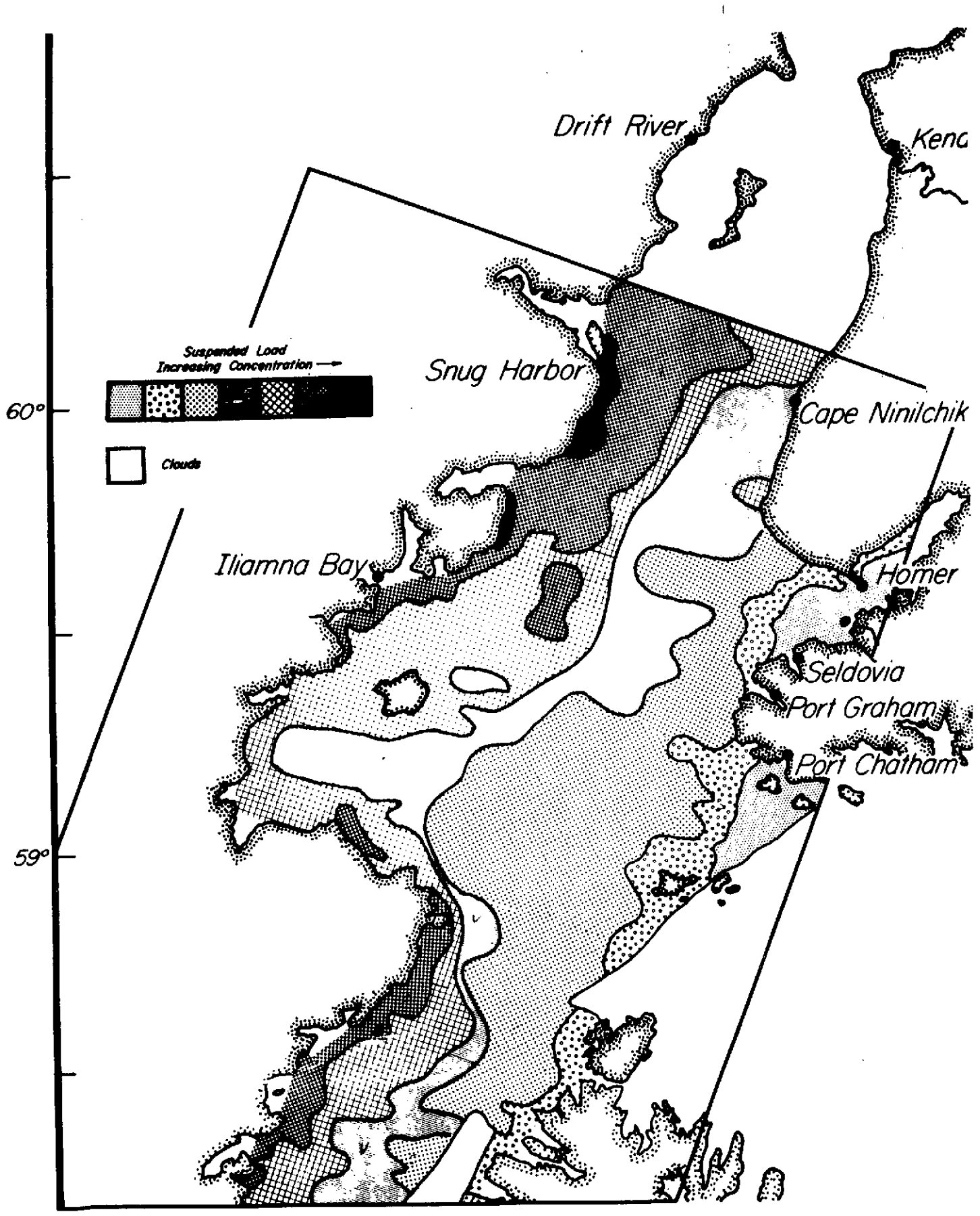

FIGURE 38. Relative suspended load distribution in lower Cook Inlet on 4 Nov 1972, based on color density slice of image I.D.'s 1104-20574 and -20581-4. Refer to area 12 of Figure 1.

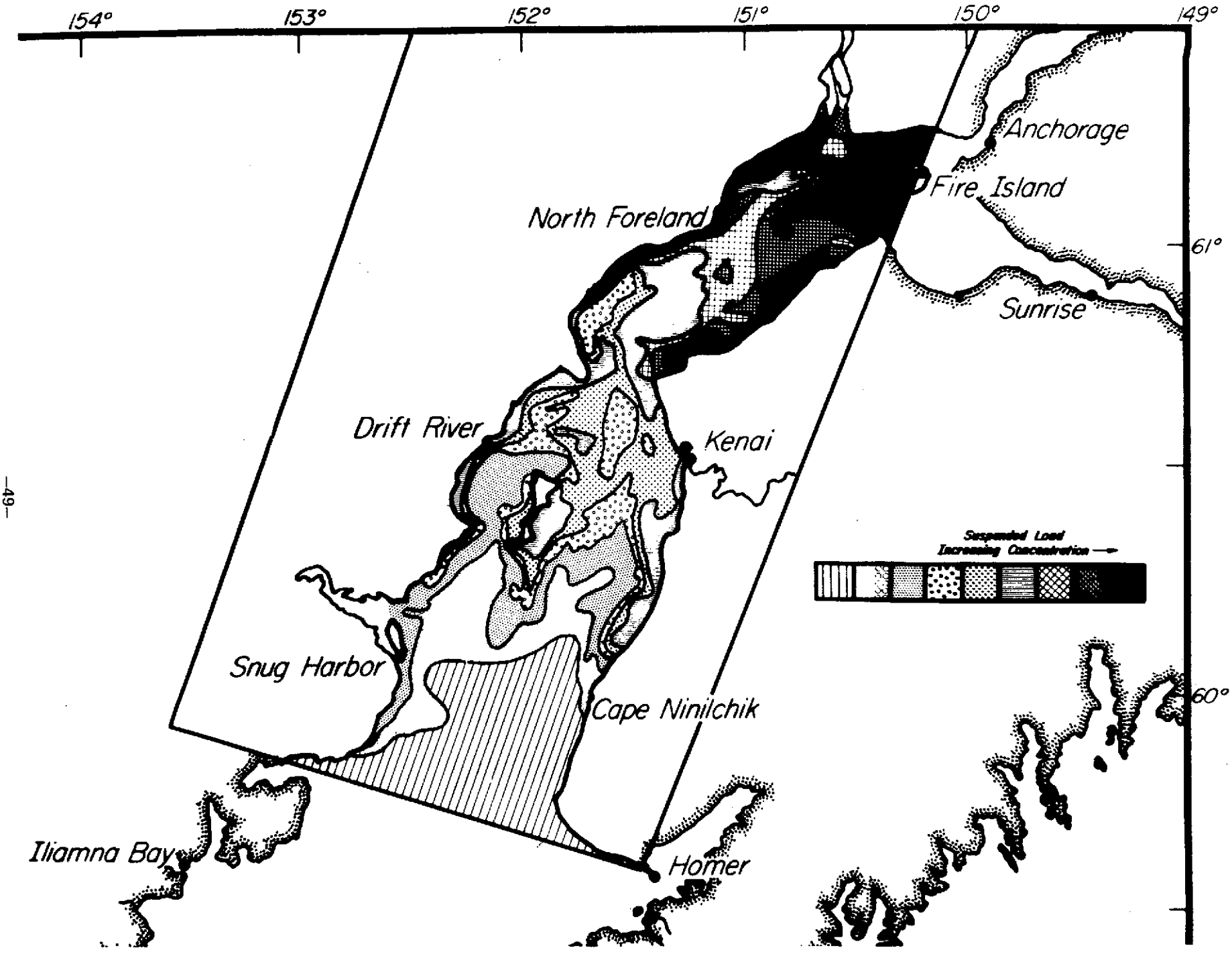

FIGURE 39A. Relative suspended load distribution in Cook Inlet on 24 Sep 1973, based on color density slice of image I.D.'s 1428-20554 and -20560-6. Refer to area 10 of Figure 1.

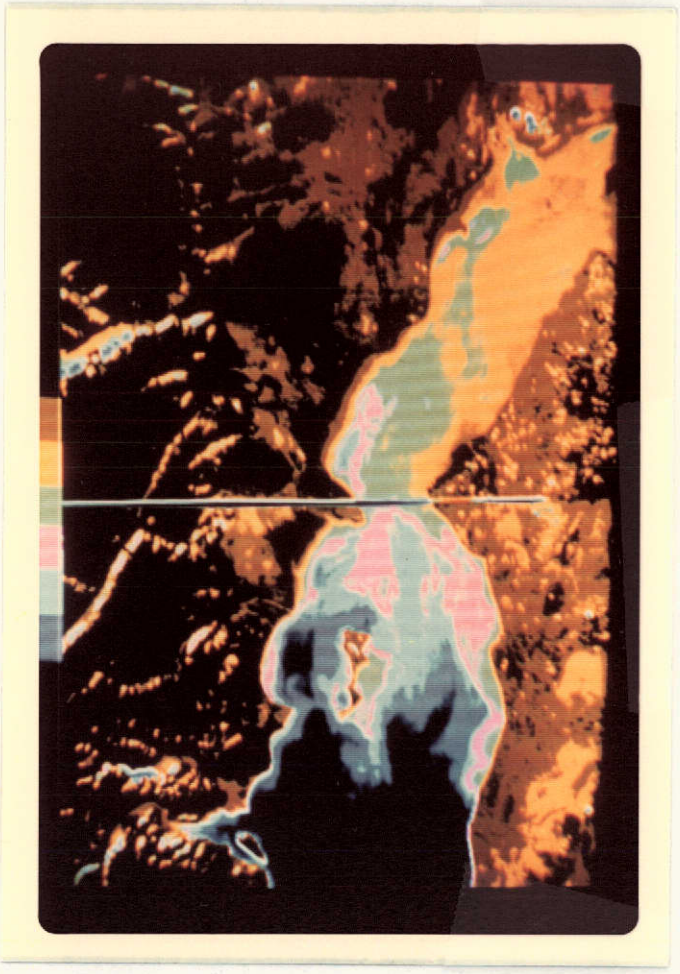

FIGURE 39B. Color density slice of Cook Inlet (image I.D.'s 1428-20554 and -20560-6, 24 Sep 1973). The two transparencies were spliced together prior to density slicing and, since the VP-8 is limited to 8 bands, is somewhat more general than Figure 39A. There is some distortion in the region just above the splice due to a dark band at the bottom of the upper transparency. This has been corrected in Figure 39A, which has been compiled from two separate density slices.

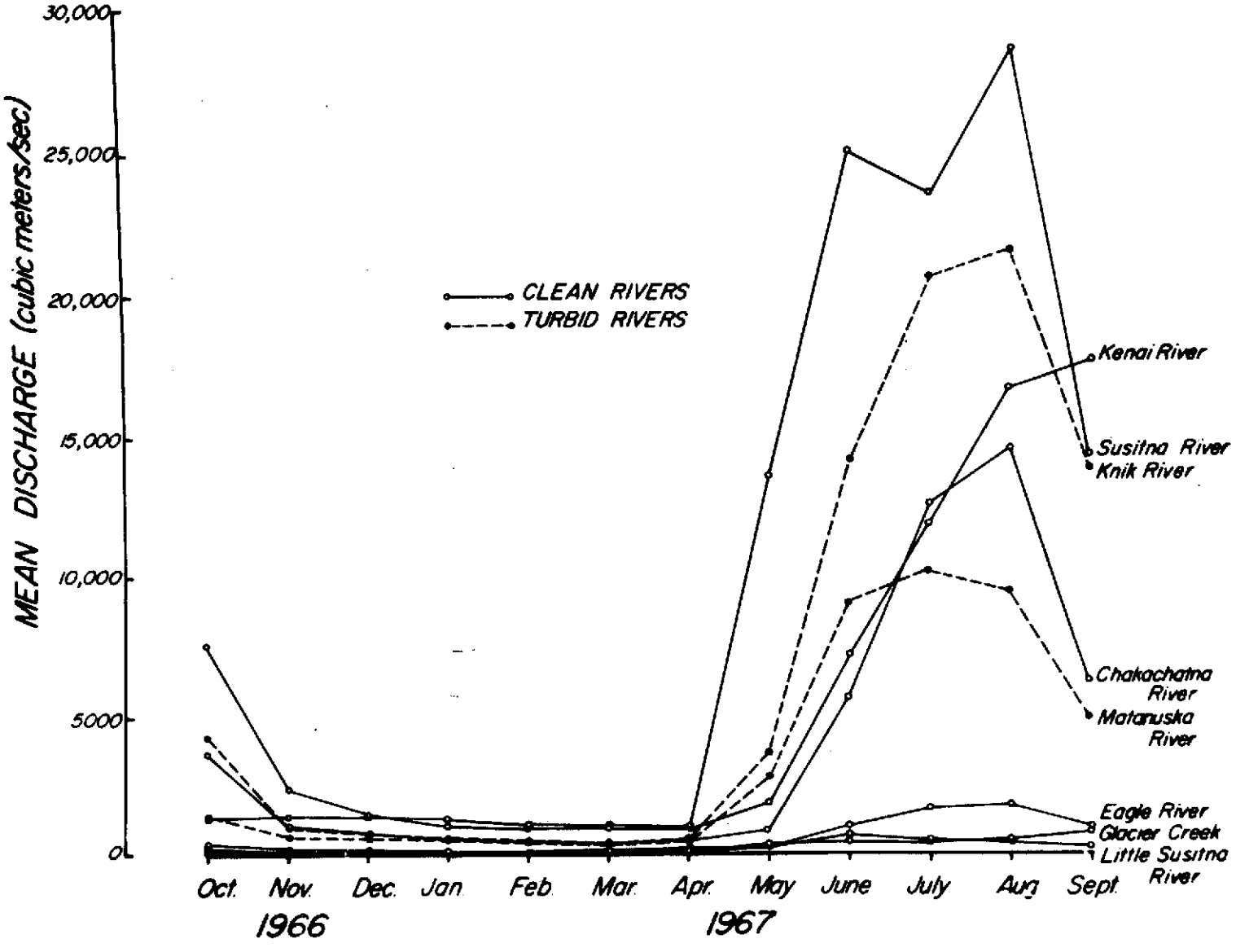

FIGURE 40. Mean water discharge (m^3/sec) during 1967 for clean and turbid rivers emptying into Cook Inlet, Alaska

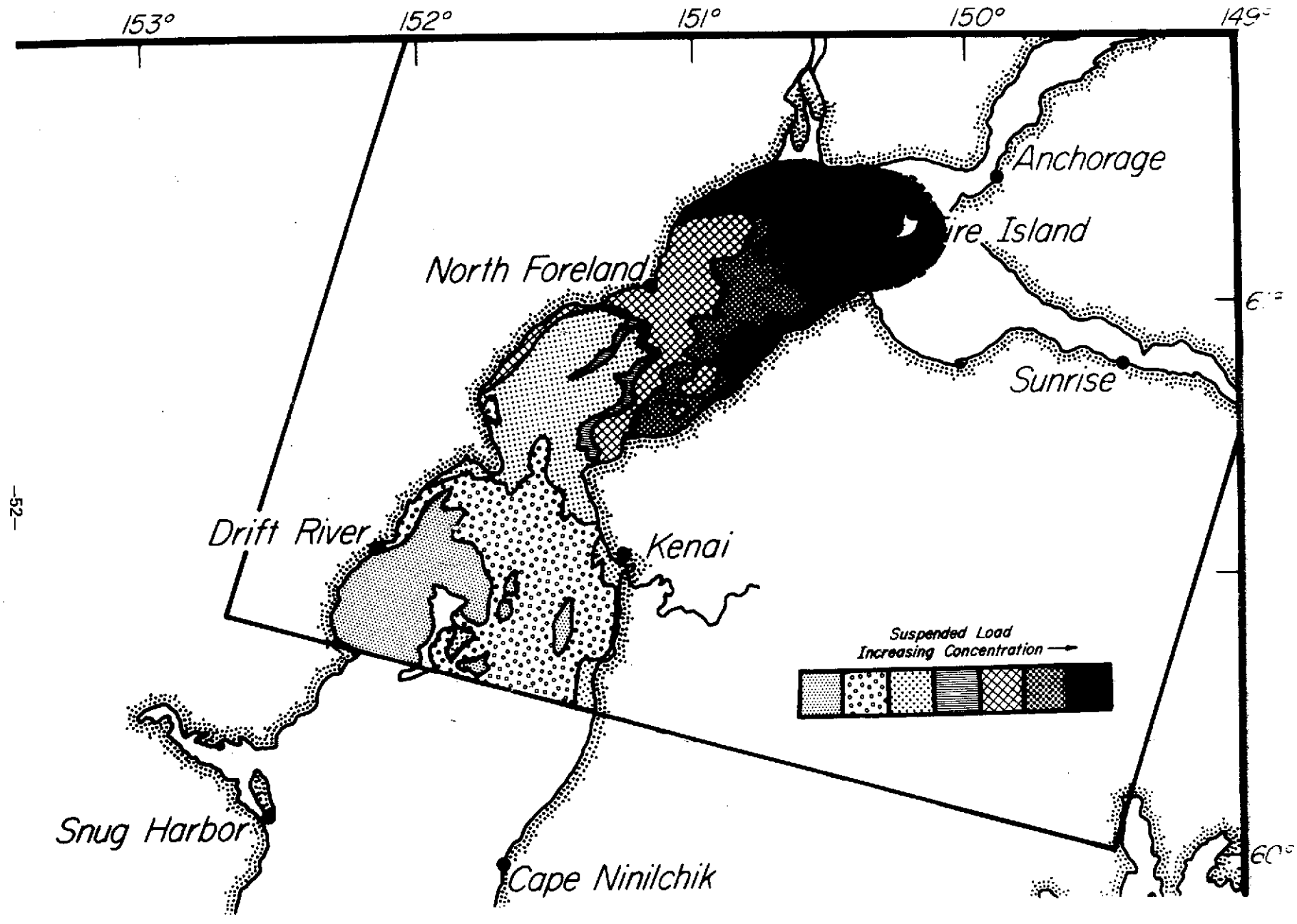

FIGURE 41. Relative suspended load distribution in upper Cook Inlet on 3 Nov 1972, based on color density slice of image I.D. 1103-20513-6. Refer to area 10 of Figure 1.

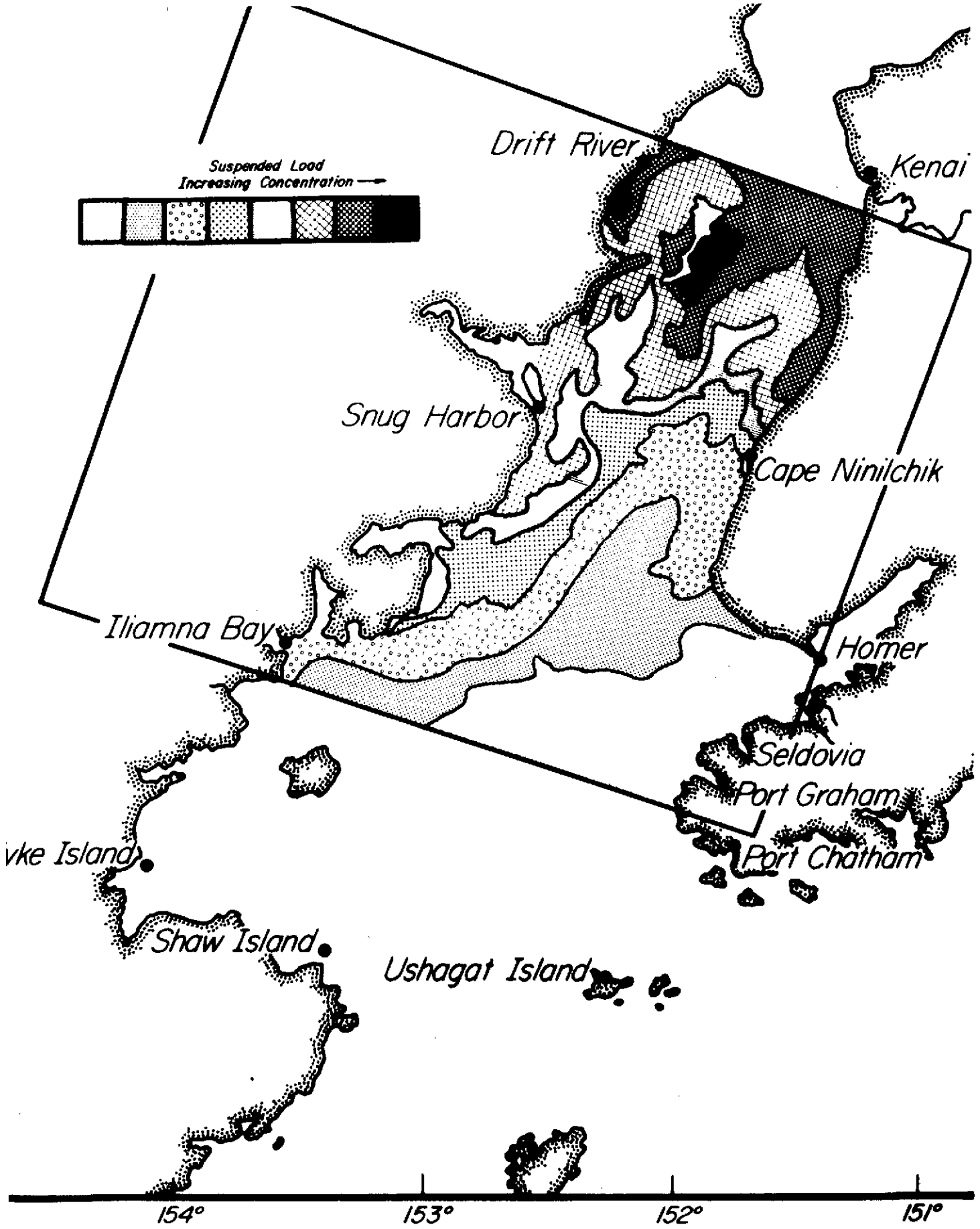

FIGURE 42. Relative suspended load distribution in lower Cook Inlet on 24 Sep 1973, based on color density slice of image I.D. 1428-20560-5. Refer to area 11 of Figure 1.

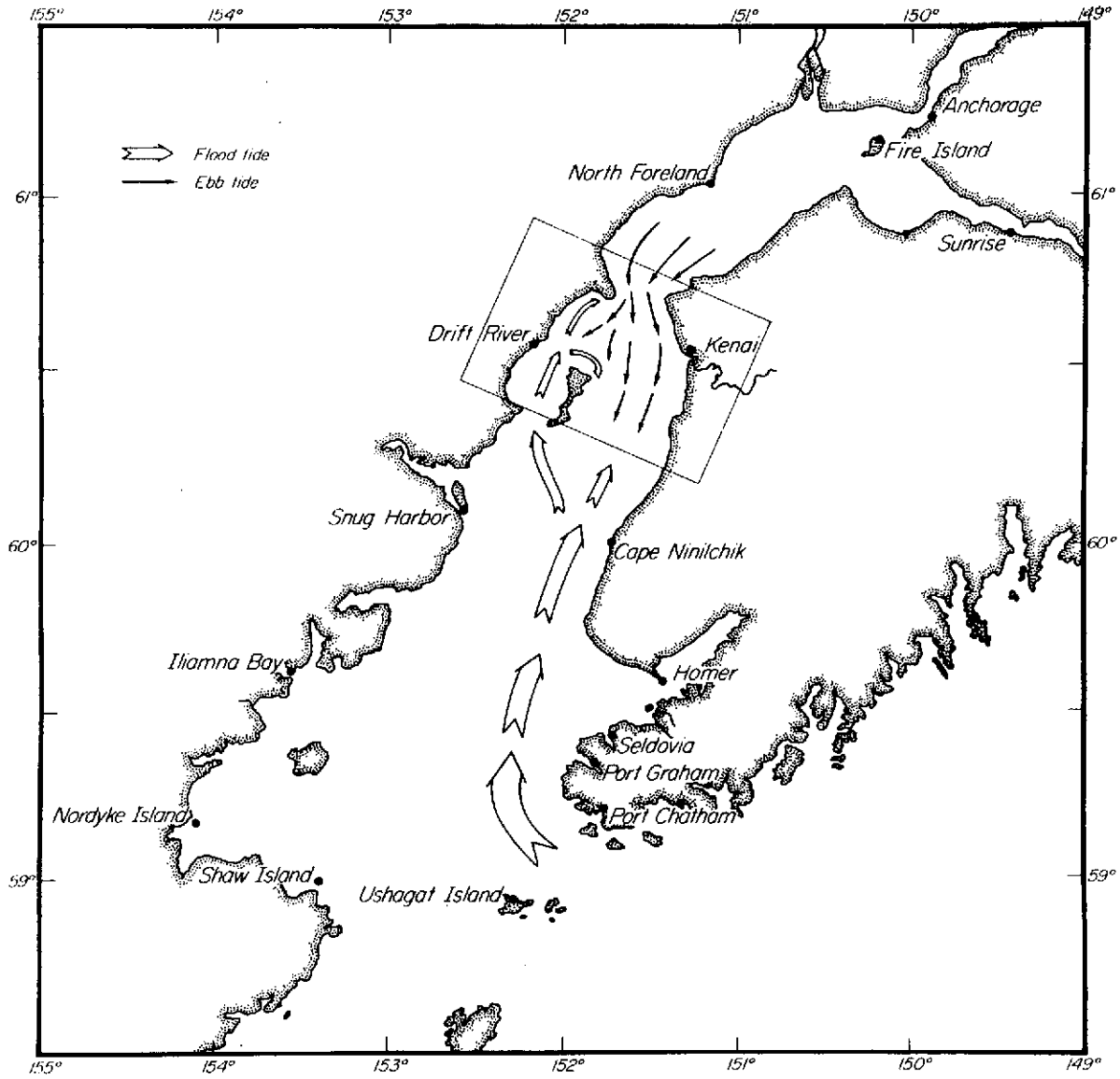

FIGURE 43. Surface water circulation in Cook Inlet when the tidal stage is near low at Anchorage and high at Seldovia. The area indexed refers to Figure 44.

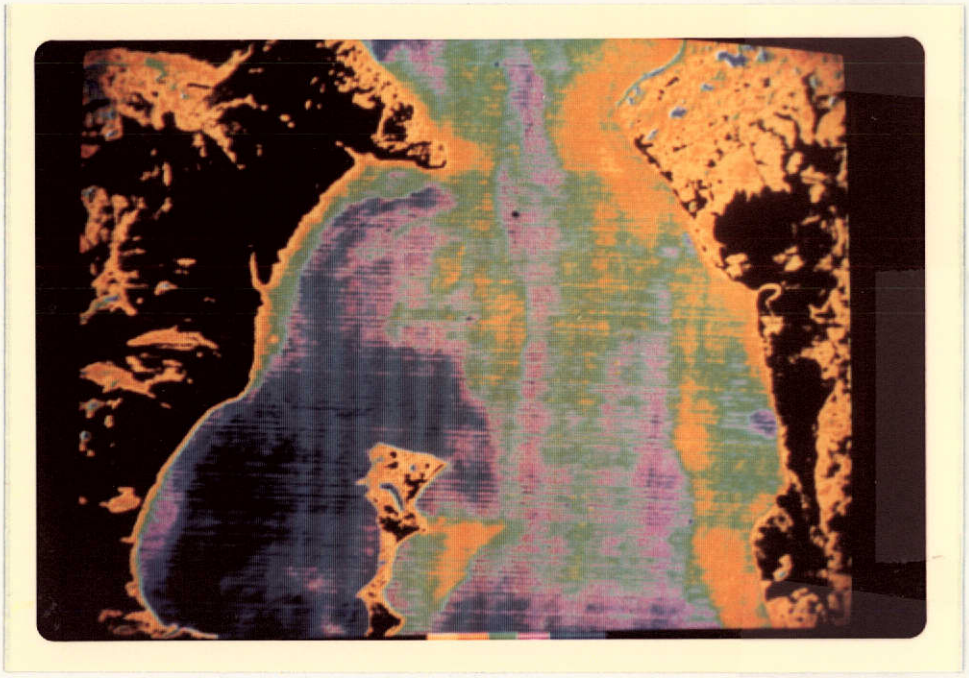

FIGURE 44. Color density slice of a portion of image I.D. 1103-20513-6 showing the region indexed i Figure 43.

ever, this superimposed circulation pattern is extremely important because it represents the ultimate trajectory of sediments and pollutants in estuarine waters.

Central Gulf of Alaska – Prince William Sound

A) General

Large deposits of oil have been recently discovered in Alaska. Oil from these deposits will be transported by pipeline from the North Slope oil fields to Port Valdez for transfer to large tankers. The resultant marine transfer and transport of Alaskan oil through the restricted waters of Prince William Sound increases possibilities of hydrocarbon contamination in the subarctic environment. The coast of the central Gulf of Alaska is a site of very high sedimentation. Suspended sediments produced by glacial and periglacial regimes of the hinterland are major sources for sediments. Turbid water plumes containing glacial flour extend offshore over marine waters and can often be seen quite clearly off the coast over areas of tens or hundreds of square kilometers (Figure 45). This turbid water plume may persist as discrete layers on or in the water column for a considerable time. The plume consists largely of silt and clay-size sediments which absorb oil and carry hydrocarbons to their depositional site. The study of sources and migratory paths of sediment in suspension in this area through ERTS-1 imagery therefore could provide information useful for proper navigational channels and abating possible hydrocarbon pollution.

B) Copper River and the adjacent shelf

An oceanographic cruise aboard R/V Acona was conducted in the central Gulf of Alaska and Prince William Sound during 21-24 February 1973. The cruise was conducted at no expense to the ERTS-1 Project 110-7 and was financed by the Institute of Marine Science.

The temperature, salinity and suspended load distribution for 21-24 February 1973 are shown in Figures 46-49. The sediments introduced into the Gulf of Alaska by the Copper River are carried westward along the shore as a distinct plume. Part of the plume is drawn into Prince William Sound where it disperses.

Since the cruise was conducted very early in the runoff season, the suspended load input from the Copper River is quite low in terms of both volume and sediment concentration. Moreover, the normally large suspended load input from the Bering Glacier (east of Kayak Island) is not present at this time of year, although some indication of the Bering Glacier plume is seen southwest of Kayak Island.

The water circulation in the Gulf of Alaska is primarily controlled by the permanent counterclockwise gyre (the Alaska current) formed in the northern Pacific (Figure 2) and seasonal large scale meteorological changes. During summer the large atmospheric high pressure cell over the northeastern Pacific gives rise to southwesterly winds with resultant Ekman drift of near surface waters to the east and southeast, accompanied by coastal divergence. Contrarily, in the winter a low pressure cell develops over the Gulf of Alaska, producing easterly and southeasterly winds with resultant Ekman drift to the north and coastal downwelling. Ekman drift may be responsible for transporting the suspended sediments observed (Figure 45) offshore over 150 km south of the Copper River.

The ERTS-1 images of 12 October 1972 (I.D. 1081-20284-4) and 14 August 1973 (I.D. 1387-20281-4, (Figures 50 and 51) show a circulation pattern similar to that indicated by the ground truth although with much greater detail and much higher suspended load concentrations. Two major sediment sources are observed in this area; the Copper River and Bering Glacier (east of Kayak Island). The Alaska current carries Bering Glacier suspended sediments westward until Kayak Island deflects the flow. The suspended sediments move south and then west around Kayak Island, and form a large clockwise gyre west of Kayak Island.

The Copper River plume is also carried westward by the Alaska current but the main body of the plume is retained fairly close to shore. Some sediments from the Copper River enter Prince William Sound through the passages northeast and southwest of Hinchinbrook Island. The remainder of the plume is carried southwest along the southeast shore of Montague Island and diffuses rapidly after passing the southwest tip of Montague Island.

The surface suspended load data, when superimposed on the textural characteristics of the bottom sediments from the Gulf of Alaska and Prince William Sound, imply that sediments from the Gulf are, in part, deposited in Prince William Sound.

The extensive navigation of tankers through Hinchinbrook Entrance (southwest of Hinchinbrook Island), which is also the major pathway of Gulf sediment into Prince William Sound, may pose a significant threat for hydrocarbon pollution in the case of oil spill. It is therefore recommended that baseline environmental data of sediments in this region be obtained prior to tanker navigation, and that this area be monitored for some time to

FIGURE 45. MSS Band 4 composite of the Prince William Sound/Copper River region of the Gulf of Alaska showing orientation and extension of surface plumes (includes image I.D.'s 1387-20275, 1387-20281, 1387-20284, 1389-20391, 1389-20394 and 1389-20400).

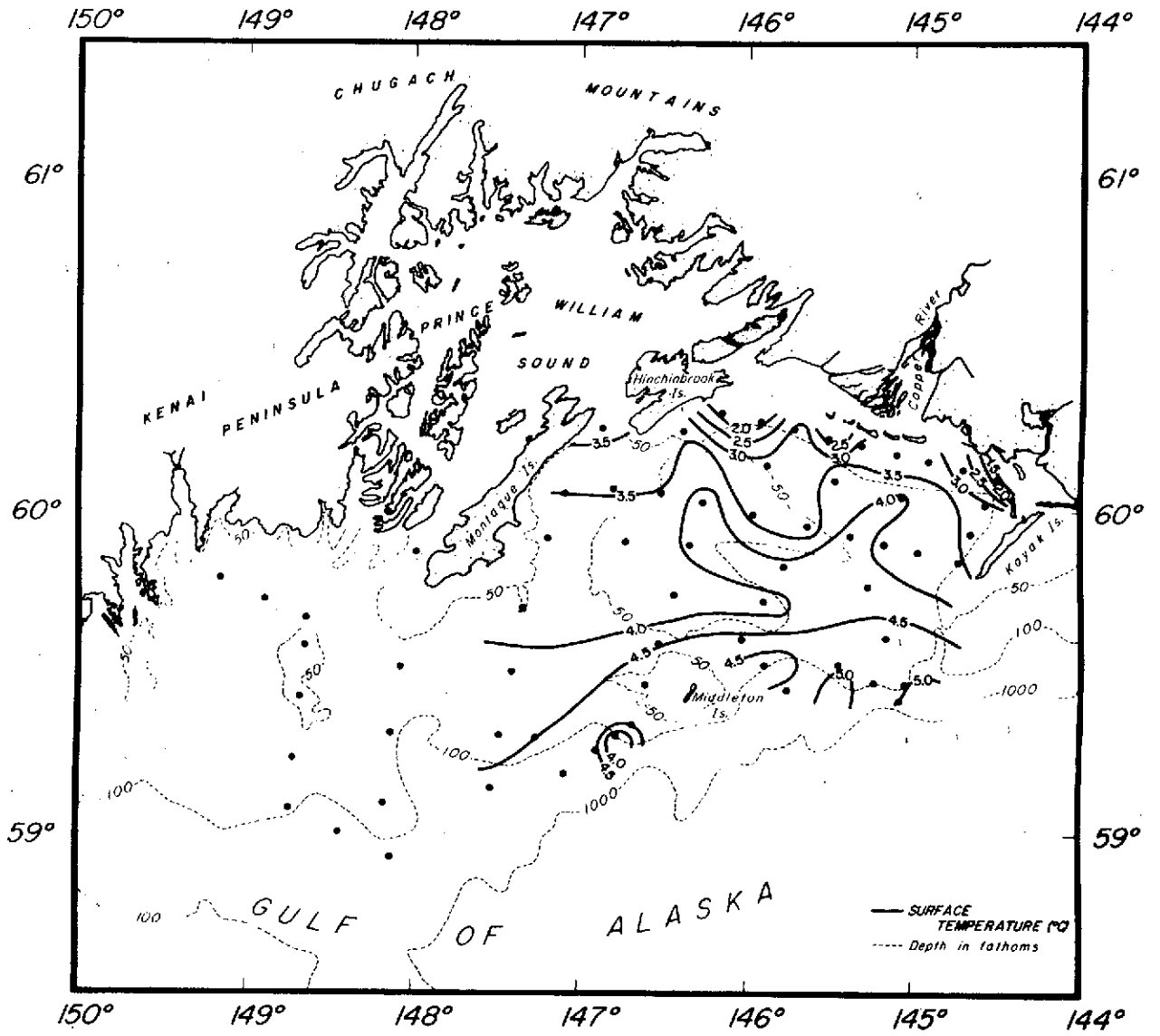

FIGURE 46. Surface water isotherms (°C.) in the Gulf of Alaska; 24-28 February 1973.

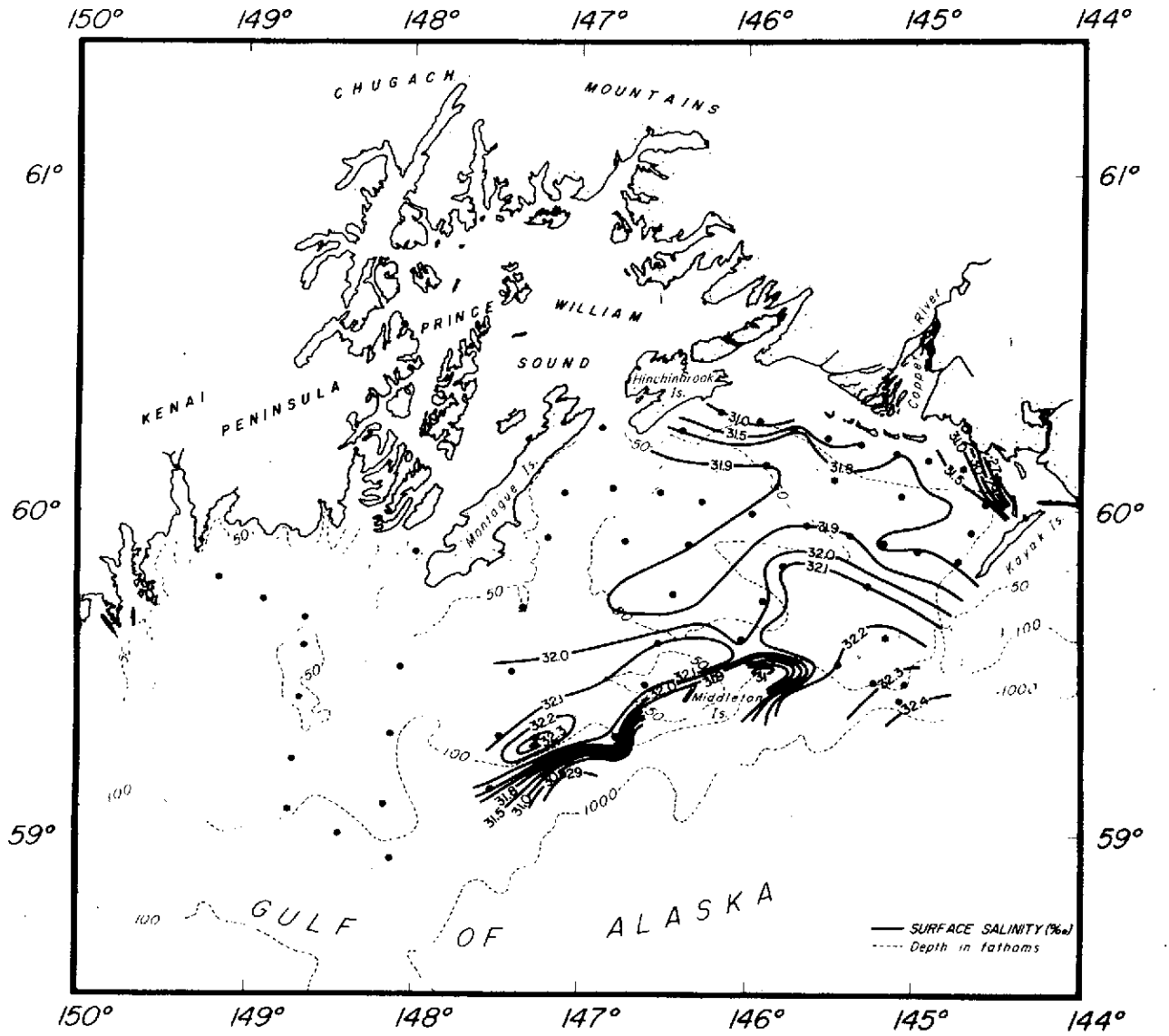

FIGURE 47. Surface water isohalines ($^{o}/_{oo}$) in the Gulf of Alaska; 24-28 February 1973.

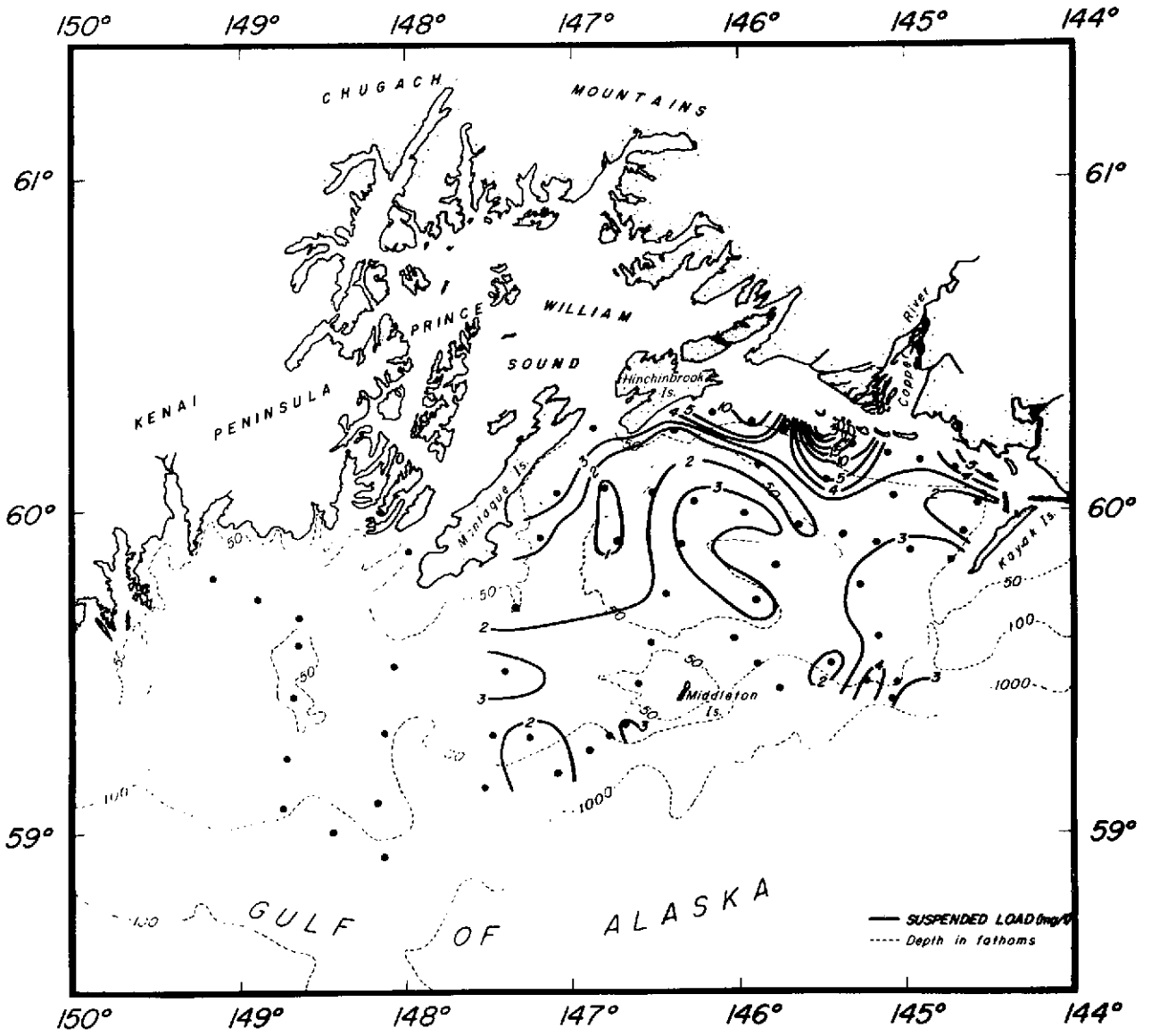

FIGURE 48. Surface suspended load distribution (mg/1) in the Gulf of Alaska; 24-28 February 1973.

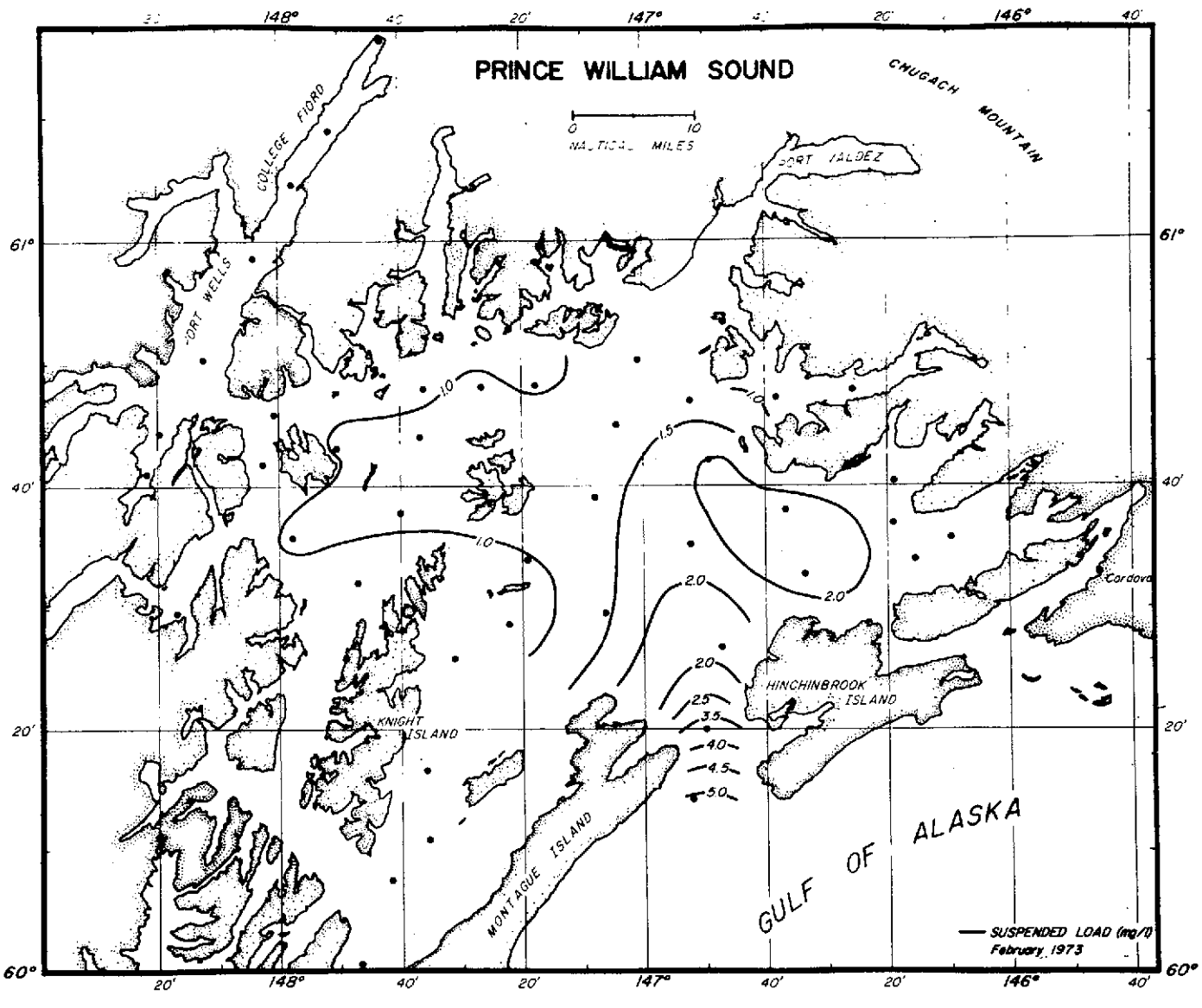

FIGURE 40 Surface suspended load distribution (mg/1) in Prince William Sound; February 1973.

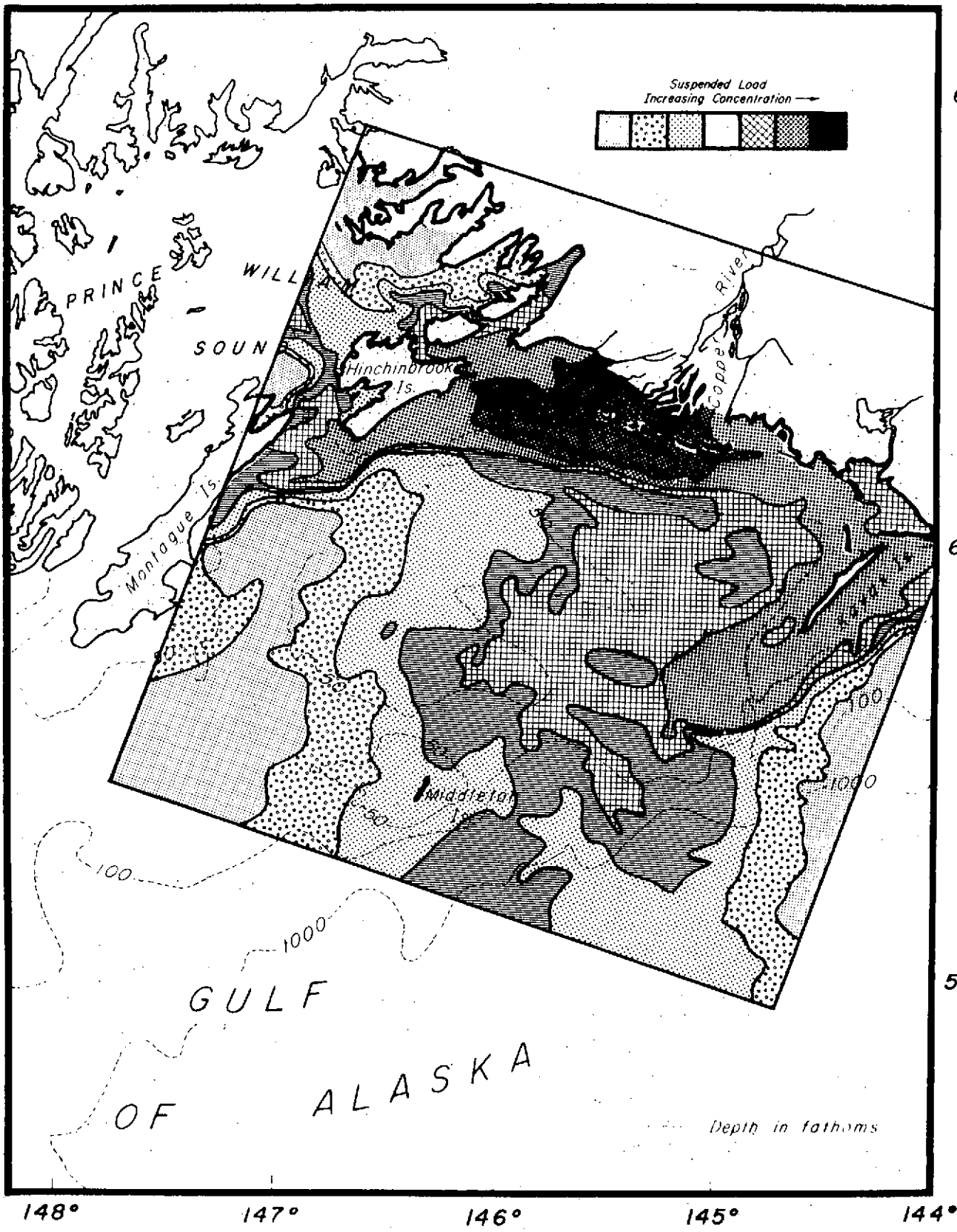

FIGURE 50. Relative suspended load distribution in the vicinity of the Copper River, Gulf of Alaska, on 12 Oct 1972, based on color density slice of image I.D. 1081-20284-4. Refer to area 13 of Figure 1.

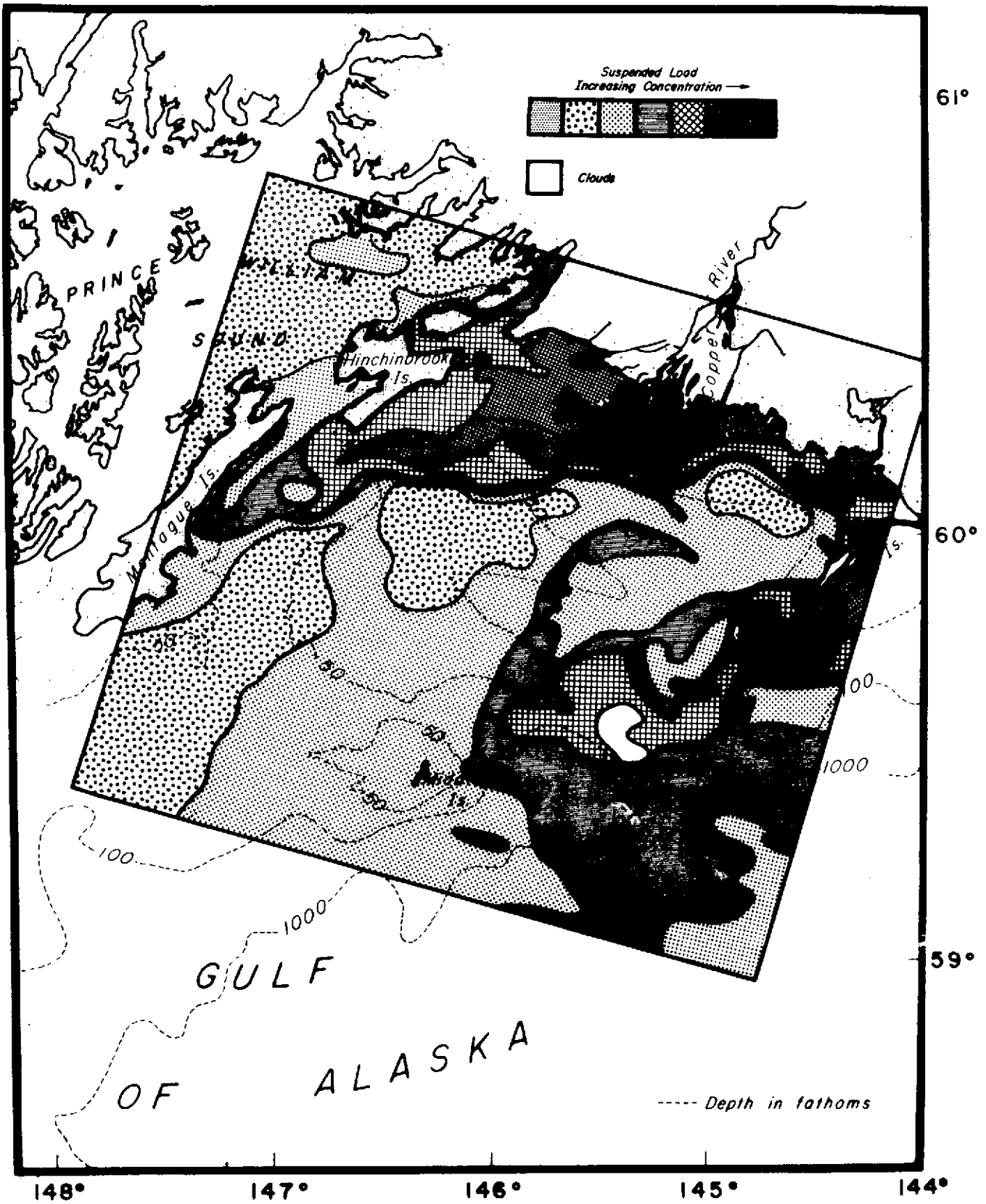

FIGURE 51. Relative suspended load distribution in the vicinity of the Copper River, Gulf of Alaska, on 14 Aug 1973, based on color density slice of image I.D. 1387-20281-4. Refer to area 14 of Figure 1.

evaluate the possible contamination due to future development.

C) Port Valdez

Port Valdez (Figure 52) was the subject of an intensive study during 1971-72 by the University of Alaska's Institute of Marine Science. During the course of the study an extensive and detailed examination of the water circulation and distribution of suspended load, temperature and salinity was accomplished. Unfortunately ERTS-1 was not launched until the study was essentially completed. Seven cruises in Port Valdez and Valdez Arm during the 1971-72 season were required to delineate the general suspended load distribution and circulation pattern. The field work ultimately clearly elucidated the general circulation pattern and suspended load distribution, (Sharma and Burbank, 1973) and subsequent ERTS-1 imagery has been analyzed here to compare our ERTS-1 interpretative techniques in an area with extensive ground truth.

ERTS-1 image I.D. 1388-20333-5 of 15 August 1973 was density sliced (Figure 53) using maximum enlargement on the VP-8 equipment. The general circulation pattern observed in Figure 53 conforms extremely closely with the general distribution of suspended sediment which was observed during the extensive field studies in Port Valdez. Moreover, Figure 53 brings out detail which required a considerable amount of field reconnaissance to determine.

Port Valdez is a relatively deep (average depth approximately 230 meters) fiord with a narrow constriction and shallow sill at its entrance. Surface water circulation in Port Valdez is controlled primarily by the relatively strong tides (tidal range 5.5 meters) and the fresh water runoff from various rivers. During flood tide (the imagery of Figure 53 was obtained at approximately maximum flood) relatively clear sea water from Valdez Arm intrudes through the Narrows. Coriolis force deflects the northeasterly moving surface water progressively to the right, forming a clockwise gyre in the western half of the port. The major influx of fresh sediment-laden water is from the Lowe River in the southeast corner of the port. This influx forms a prism of low salinity water, typically 2-10 meters thick, which flows to the northwest past the town of Valdez to form a counterclockwise gyre in the eastern half of the port. The coarser suspended sediments drop out rapidly, however, the plume is reinforced by suspended sediments from Mineral and Gold Creeks just west of Valdez.

Shoup Bay in the northwest area of the port is also a major source of sediments, however, it has been determined that most of its suspended load is deposited within the bay and only a minor amount is discharged into Port Valdez proper. This is clearly evident in Figure 53. The suspended load that does pass out of Shoup Bay is carried out of the port along the northwest shore. Some of the suspended sediments originating from the Lowe River normally extend along the entire northern shore of Port Valdez and join the plume from Shoup Bay. The plumes of several small streams can be observed along the southern shore of Port Valdez.

Although the net circulation pattern is a clockwise gyre in the west half of Port Valdez and a counterclockwise gyre in the east half, this circulation, as in Cook Inlet, is superimposed on the overall east-west pulsation of the surface waters due to the flood and ebb of the tides. However, the net circulation, as in Cook Inlet, describes the ultimate trajectory of suspended sediments and pollutants, and the value of this knowledge in the planning of harbor and industrial sites is self-evident.

The distribution of the surface suspended load in Port Valdez, as in many other areas, is closely related to the bottom sediment distribution, and in turn both the surface suspended load and the bottom sediment distributions have been found to be related to the benthic fauna distribution in Port Valdez. The surface suspended load also exerts significant control over the biological productivity in the near surface waters of Port Valdez. Detailed results of the Port Valdez studies are contained in *Environmental Studies of Port Valdez* (Hood, *et al.*, 1973).

SEA ICE STUDY AND SEA MAMMAL DISTRIBUTION IN THE BERING AND CHUKCHI SEAS

A) General

The marine mammals are important renewable resources of the Bering and Chukchi Seas, and are harvested by the United States, the Soviet Union, Japan and Canada. In its determination to conserve marine mammals the U.S. Government passed the Marine Mammal Act of 1972. Much of the knowledge required to implement the Marine Mammal Act is not yet available. Furthermore, marine mammals have been an integral part of the Alaskan Native's culture and have provided an important source of food, clothing and income. It is therefore important that all aspects of marine mammal ecology be investigated for proper management and preservation as well as to ensure continued ecological balance.

A large variety of marine mammals is associated with pack ice in the Bering and Chukchi Seas. Two species

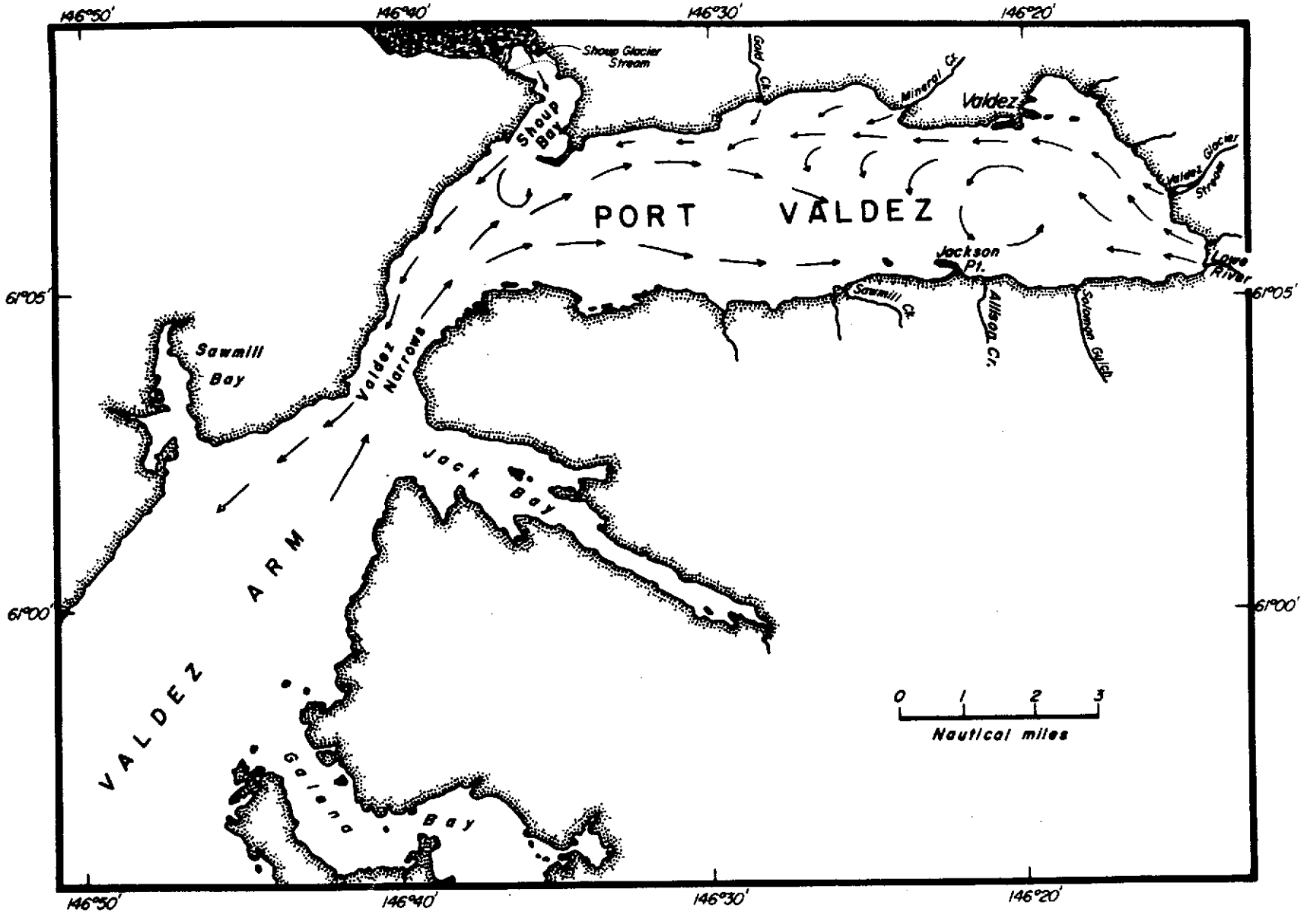

FIGURE 52. Generalized surface water circulation in Port Valdez, Alaska.

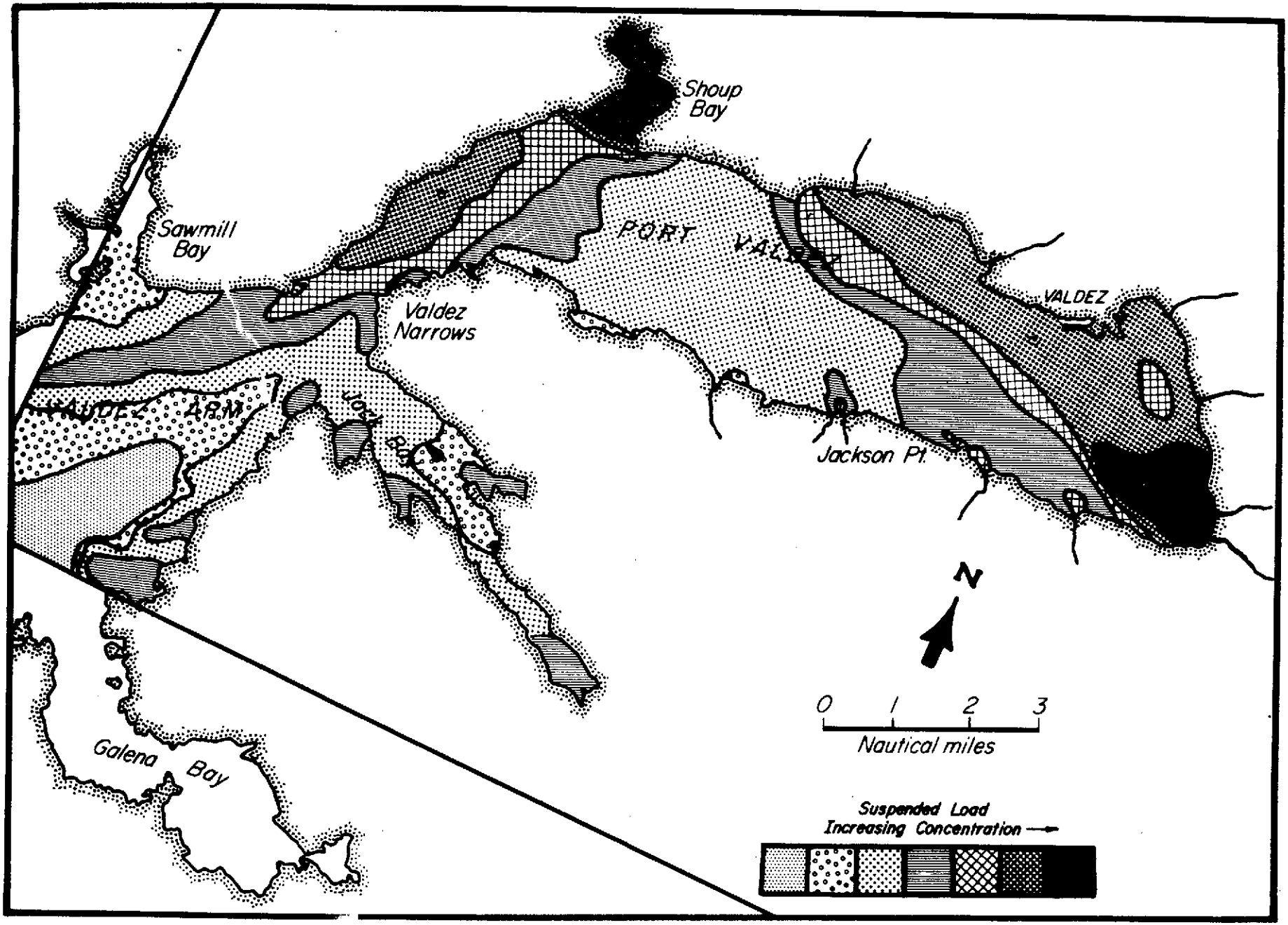

FIGURE 53. Relative suspended load distribution in Port Valdez on 15 Aug 1973, based on color density slice of image I.D. 1388-20333-5. Refer to area 15 of Figure 1.

(ribbon seal and largha seal) are indigenous only to the North Pacific region, including the Bering Sea, and the Pacific Walrus is found only in the Bering Sea and the western Arctic Ocean. Sea ice in the Bering and Chukchi Seas plays a major role in the marine mammal ecology. The nature of sea ice and its gross morphology (size of floes, their thickness and surface texture, and the open water between them) and dynamics (direction and rate of movement) apparently exert significant influence on the distribution and welfare of marine mammals. The knowledge of the distribution of sea ice is a prerequisite for the determination of the related distribution of various species.

In winter the sea ice extends to the south of Nunivak Island (Bering Sea) whereas in summer it recedes to high latitudes in the Chukchi Sea. The seasonal changes of sea-ice cover effects the distribution of marine mammals. Migration of the bowhead whales, for example, depends on the progressive deterioration of the winter sea ice. Large assemblages of marine mammals and their migration with the ice edge is perhaps due to the intense productivity observed in this region. In fact the production cycle in the Bering Sea begins in late winter with the development of a dense population of algae, mostly diatoms, on the subsurface of the sea ice. The bloom of ice algae appears to develop in the ice front zone and move northward as spring advances. Such an abundant food supply near the receding sea ice undoubtedly influences the biomass of prey species utilized by marine mammals.

The seasonal movement of sea ice is known to diversify the marine mammals. During the maximum extent of sea ice a large number of species of marine mammals are found to be associated with it. These species include bearded, largha, ribbon and ring seals, walrus, polar bear, bowhead whale and others. The movement of the sea ice during the year has a filter effect on marine mammals. For example the distributions of bearded and ring seals, walrus, and polar bears are generally closely related to the presence of sea ice. On the other hand the seasonal activity pattern of other mammals is governed by the dynamics of the sea ice, and their distribution is directly related to seasonal changes in sea ice. These marine mammals depend on the seasonal ice during periods of reproduction, rearing of young, and molting. During the ice free season, for example, largha seals migrate to coastal regions and ribbon seals become pelagic.

The importance of sea ice in marine mammal ecology is apparent. In the past some data concerning the distribution and migration of these species has been sporadically obtained. However, the significance of the data obtained could not be determined because of the lack of information on the nature and dynamics of ice in the Bering and Chukchi Seas. High resolution mustispectral data available now from ERTS-1 can be used to map the sea ice distribution. These two sets of data eventually will bring out a better understanding of the marine mammal ecology in the Bering and Chukchi Seas.

B) Sea Ice Distribution

The ERTS-1 image I.D. 1010-22135-5 covers the area along the northwest coast of Alaska and shows the prominent landmarks of Icy Cape, Wainwright and Point Franklin. The analysis shows (Figure 54) the southern edge of seasonal sea ice, which is undergoing both rapid deterioration and northward movement in the northwestern corner of the image. Different characteristics of the sea ice are quite discernible and have been delineated in Figure 54. Measurements of aerial extent of the different ice types were not made, however, the task can be achieved without difficulty. The image shows clearly that most of the snow cover has already melted except on the larger, irregular and rough ice floes. These floes (indicated by the number 5, Figure 54) appear to be remnants of what was formerly heavy, shore-fast ice. It is doubtful that they are floes of multi-year ice, because of thei presence in the ice edge, their rough surface sculpture and several other characteristics. Surface water currents, based on the orientation of ice tongues, appear to parallel the coast in near shore areas and trend in a northerly direction away from the coast.

The ERTS-1 image I.D. 1010-22133 MSS-6 covers the area northwest of Point Franklin which lies adjacent to the image described earlier. Total area covered by drifting ice is much more extensive and provides excellent examples of seasonal ice in the late stages of disintegration (Figure 55).

Although large irregular polynya are obvious, there are no leads characteristic of sea ice during winter and spring. The loose and fragmented nature of the ice pack precludes formation of distinct leads, as it is driven by the forces of winds and surface water currents. The almost complete loss of snow cover is especially evident in this image, due to the greater extent of ice cover and therefore the increased opportunity for comparison.

Tonal differences in ice zones are particularly evident as is the actual structure of ice within the zones. This is especially useful in delineating the various zones. Orientation of ice features again indicate currents parallel to the coast in the near shore areas and more northerly farther off-shore.

ERTS-1 image I.D. 1087-20595 MSS-5 covers the northern coast of Alaska, Barter Island being the prominent land-head (Figure 56). The image shows the process of ice formation during early fall, and is an excellent example of the detail and fine resolution which can be obtained from ERTS-1 imagery.

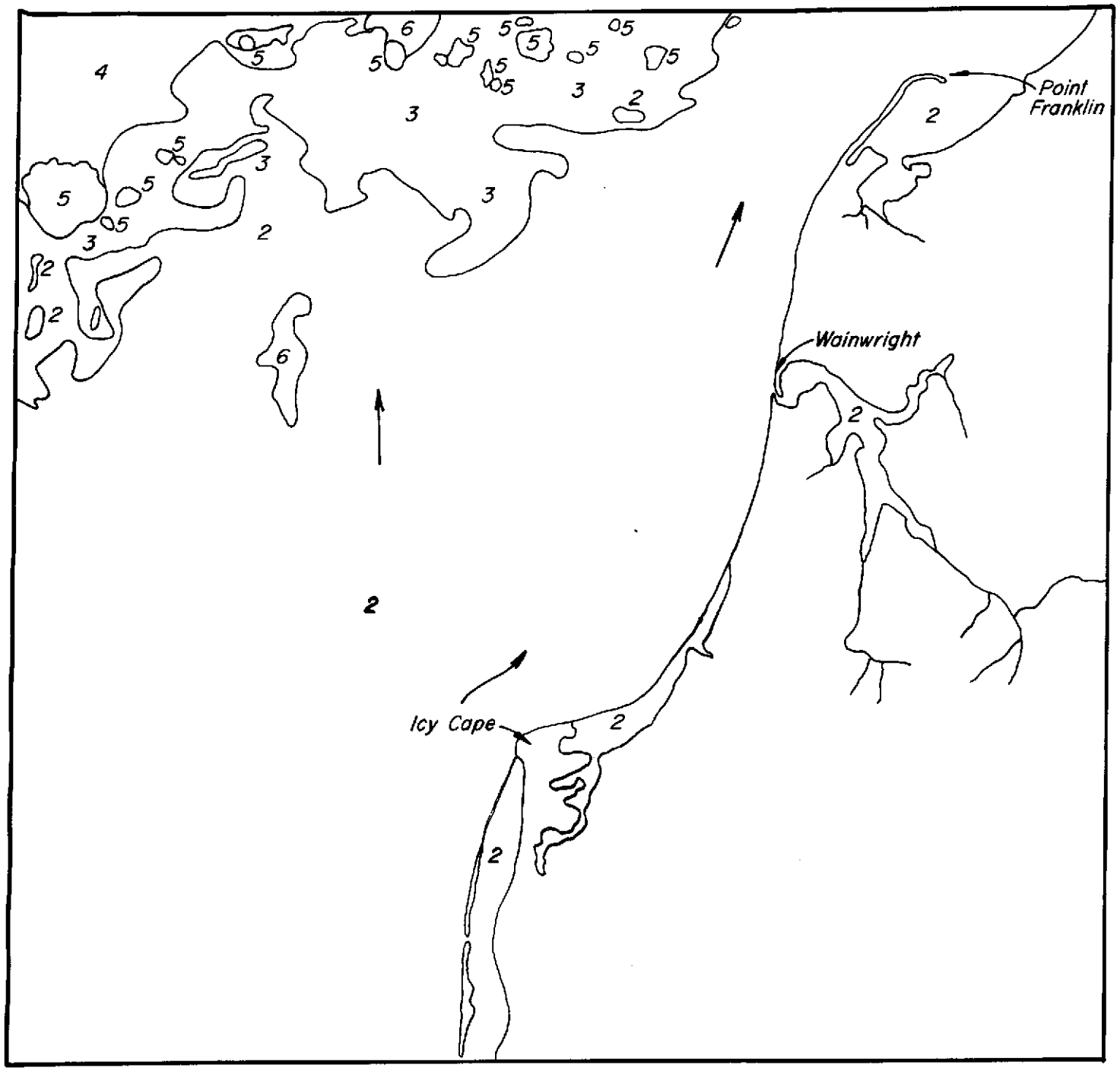

FIGURE 54. ERTS-1 image I.D. 1010-22135 MSS-5 with overlay showing characteristics and distributions of various sea ice types in the region of Wainwright, Alaska

1 – Land
2 – Open water (both fresh and salt)
3 – Disintegrating and weathered "ice edge zone"
4 – Disintegrating and weathered "pack ice zone"
5 – Individual and relatively heavy floes
6 – Clouds
7 – Loose and widely scattered floes

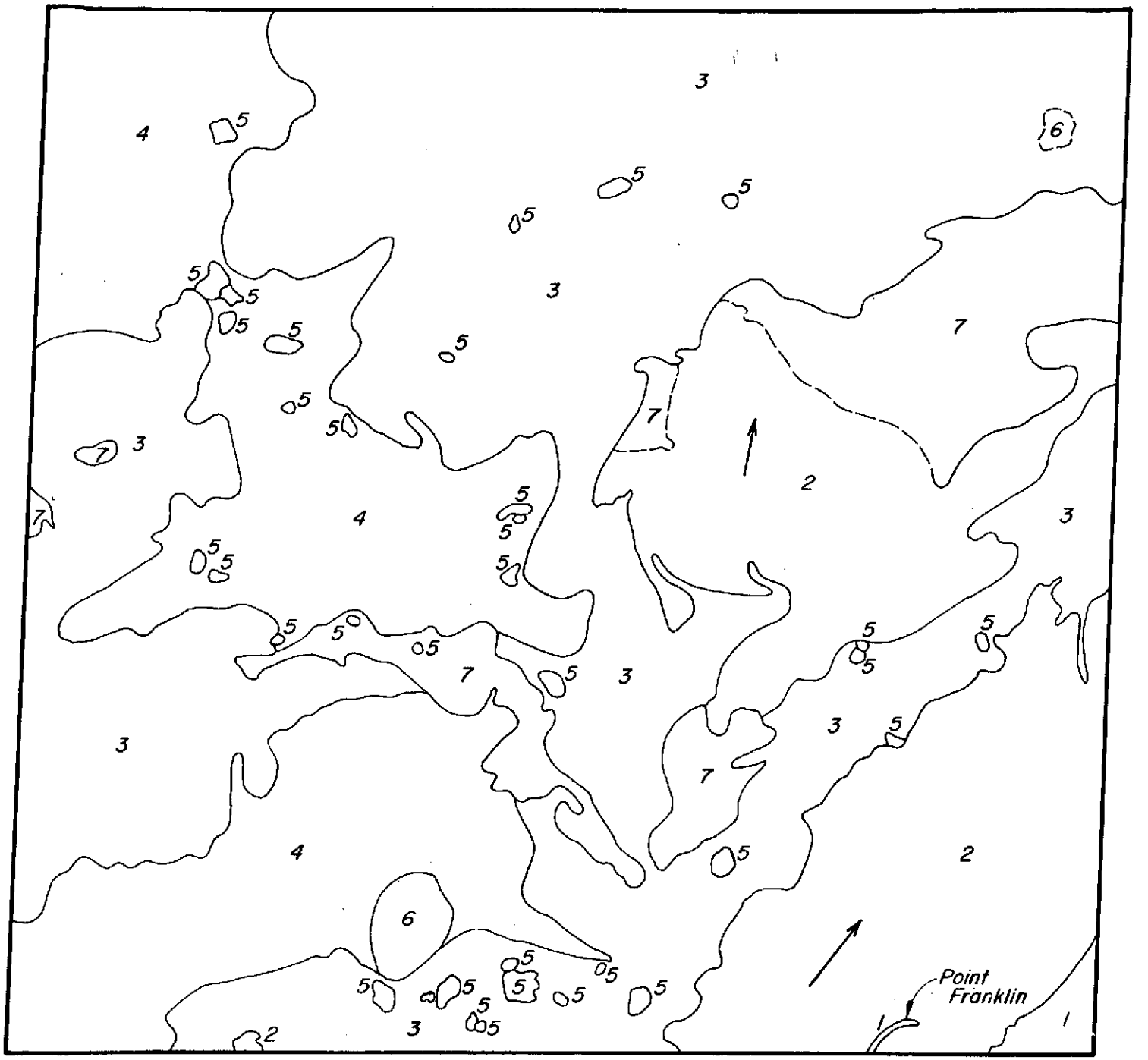

FIGURE 55. ERTS-1 image I.D. 1010-22133 MSS-6 with overlay showing characteristics and distributions of various sea ice types in the region of Point Franklin, Alaska

1 – Land
2 – Open water (both fresh and salt)
3 – Disintegrating and weathered "ice edge zone"
4 – Disintegrating and weathered "pack ice zone"
5 – Individual and relatively heavy floes
6 – Clouds
7 – Loose and widely scattered floes

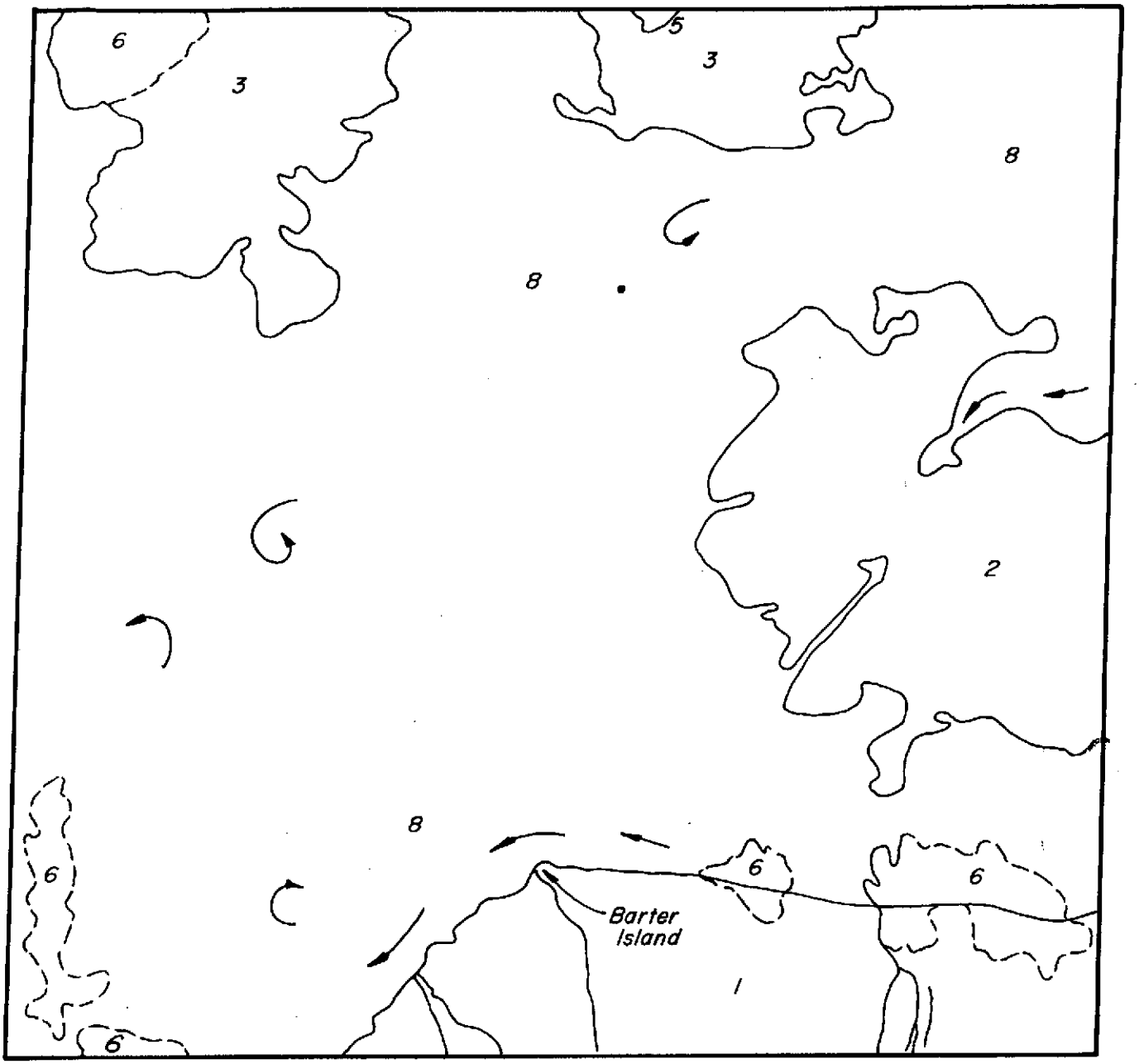

FIGURE 56. ERTS-1 image I.D. 1087-20595 MSS-5 with overlay showing characteristics and distributions of various sea ice types in the region of Barter Island, Alaska

1 – Land covered with snow
2 – Open water
3 – Edge zone of the pack ice, also covered with snow
5 – Individual and relatively heavy floes
6 – Clouds
8 – Actively forming, unconsolidate "slush" and "grease" ice

At the time this image was taken, the pack ice was approximately 65 to 70 miles north of Barter Island. Active ice formation was occurring in the open ocean and is evident as thin "grease" ice and slightly thicker but unconsolidated "slush" ice. The pattern of surface currents is particularly evident, paralleling the coast in the near shore and consisting of many eddies and gyres further offshore. The general direction of currents (and ice movement) is toward the west.

Ice cover in the Bering, Chukchi and Beaufort Seas results from two major processes which are evident in this image. These are the formation of new ice, more or less *in situ*, and the movement of previously formed ice into the area.

ERTS-1 imagery obtained during 6, 7 and 8 March 1973 which passes over the regions of eastern Chukchi and Bering Seas, was analysed in detail. The individual ice masses on these prints can be easily delineated and thus their movement can be traced during subsequent imagery. The sequence of three images provides the distribution of various ice types and their movements in the Bering Strait during this period (Figure 57).

The boundaries of land fast ice, distribution of pack ice and major polynya were studied in the vicinity of Bering Strait. Movement of pack ice during 24 hours was determined by plotting the distinctly identifiable ice floes on ERTS-1 imagery obtained from two consecutive passes.

A considerably large shallow area along the western Seward Peninsula just north of Bering Strait is covered by land fast ice. This ice hinders the movement of ice formed in eastern Chukchi Sea southward through the Bering Strait. The movement of ice along the Russian coast is relatively faster. Plotting of some of the ice floes indicated movement of ice in excess of 30 km in and south of Bering Strait between 6 and 7 March, 1973. North of Bering Strait the movement of ice approached 18 km. The movement of individual ice floes varied considerably both in southern Chukchi and northern Bering Sea.

The movement of ice observed during March 6 and 7 considerably altered the distribution and extent of polynya. These features when continually plotted should be of considerable aid in navigation for ice breakers. The movement of ice when correlated with distribution of sea mammals should reveal the seasonal migratory habits and routes of these mammals.

NEW TECHNOLOGY

None.

CONCLUSION

Along the Alaskan coastline, where large remote and relatively inaccessible areas are difficult to study by direct observations and classical oceanographic techniques are often impossible, ERTS-1 imagery provided synoptic data for a number of sea water parameters. Distinct water masses interfacing in nearshore waters are clearly discernable on ERTS-1 imagery. The light reflectance of water registered on ERTS-1 imagery showed a strong correlation with suspended load in water. The isodensity analysis of the positive and negative transparencies obtained using the "VP-8 Image Analyzer" provided the relative distribution of sediments in suspension. The distribution of the suspended load as seen on ERTS-1 imagery, therefore, can delineate sediment source and movement. Because sediments are retained in suspension over a period of days, concentrations of suspended matter can be used as tags on water masses for investigating physical oceanographic problems.

For sea ice studies in the Chukchi and Bering Seas ERTS-1 imagery provided multispectral data at a resolution previously not available. On the basis of variations in reflectance and the shape and size of the patterns various ice types and ice surface features can be identified. Differences in relectance between the shorter wavelength bands (MSS-4 and MSS-5) and the near-infrared band (MSS-7) have been useful for differentiating ice types. Repetitive and sequential imagery can provide quantitative data on ice accretion, degeneration and movement patterns over large areas. The information obtained is extremely useful for the study of the behavior and ecology of marine mammals, and the high primary productivity observed near the ice-edge in the Bering and Chukchi Seas.

The analyses of limited imagery from the eastern Chukchi Sea along the Alaskan Coast identified various sediment sources, and the movement and deposition of these sediments in the nearshore regions. The dominant influence of the general northward moving Bering Strait waters and the intermittent effect of wind is evident on sediment flow in this area.

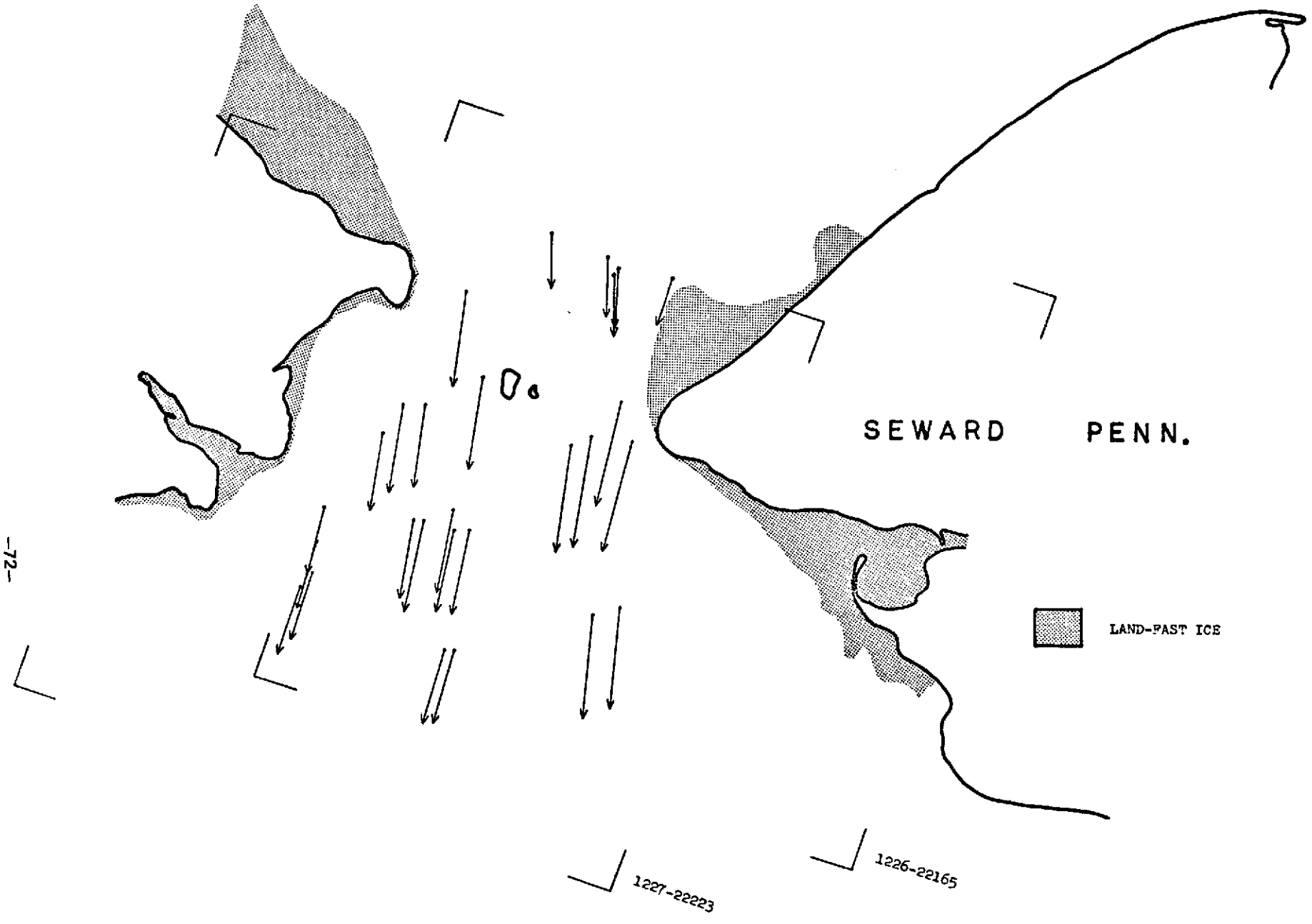

FIGURE 57. Movements and directions of ice floes in the Bering Strait and Bering Sea during 6-7 March 1973.

The Yukon River sediment plume, covering an extensive area near its mouth, provided information concerning the pathways for these sediments. The large influx of sediment brought by the river is mainly carried northwards towards the Bering Strait and only partly diverted eastwards into Norton Sound. The salinity, temperature and suspended load measurements in this region support the general movement of sediment interpreted from the analyses of ERTS-1 imagery. The general orientation of the plume and the northwestward movement of sediment also explain the lack of offshore deltaic deposits and the deposition of Yukon River sediments in the Chukchi Sea.

Water and sediment movement in the Norton Sound and Bristol Bay regions were also delineated from the analyses of various ERTS-1 imagery.

The water parameters from Cook Inlet, selected as a test area, were obtained during spring, summer and fall seasons. The ground truth data and the ERTS-1 imagery analysis demonstrated the feasibility for the use of imagery in delineating the complex water circulation and sedimentary pathways in such a large estuary. The need for the synoptic data obtained by ERTS-1 is displayed by the regional eddies and complex circulation developed in Cook Inlet during various stages of ebb and flood tide. These microcirculations within the inlet were not detected by oceanographic data obtained by classical techniques.

The analyses of ERTS-1 imagery from the Gulf of Alaska region showed the westward movement of coastal sediments under the influence of the Alaska Current. Sediments in suspension are also carried offshore by Ekman drift. Water circulation in Port Valdez and Prince William Sound, both semi-enclosed water bodies, as interpreted from the analyses of ERTS-1 imagery shows excellent correlation with the distribution of water parameters.

As more imagery becomes available we hope to cover the entire shelf of Alaska to prepare an Atlas showing sediment sources, migration and other measured parameters of water from this region. The Atlas will provide baseline data for environmental studies and will provide guidance on how to respond to, modify and accommodate the economic impact on the coastal waters of Alaska.

RECOMMENDATIONS

ERTS imagery provides a rapid and large scale method for studying and cataloging the various environmental parameters. Most of the oceanographic phenomena observed are relatively static, in at least seasonal equilibrium, however, the amount of variability of these features, both temporally and geographically, is critical and must be adequately assessed over a significant time span. Moreover, further ERTS imagery is needed to cover the entire shelf of Alaska to prepare an environmental "Atlas". The two years of ERTS observations have certainly proven the feasibility of using such imagery in high latitude circulation studies; additional observations are necessary to confirm and extend the utility of the system.

ACKNOWLEDGEMENTS

Logistic and financial support from the Institute of Marine Science, University of Alaska during the study is very much appreciated. We are grateful for the sampling opportunity provided aboard R/V OSHORU MARU, R/V ALPHA HELIZ, and R/V ACONA. We wish to thank Amoco Production Company, Marathon Oil Company, and Mobil Oil Company for collecting water samples in Cook Inlet during satellite passes. Special thanks are due Prof. A. E. Belon and his staff at the Geophysical Institute, University of Alaska for coordinating the project and for his generous advice during the entire study.

LIST OF PUBLICATIONS

Wright, F. F., G. D. Sharma and D. C. Burbank, 1973. ERTS-1 observations of sea surface circulation and sediment transport, Cook Inlet, Alaska. Symposium On Significant Results Obtained From The Earth Resources Technology Satellite-1, Vol. I: Technical Presentations Section B, p. 1315-1322, NASA Goddard Space Flight Center, New Carrollton, Maryland.

Sharma, G. D., J. J. Burns, F. F. Wright, and D. C. Burbank, 1973. Surface currents, suspended sediments and ice cover in the Bering Sea and their possible influence on the regional climate. 24th Alaskan Science Conf., Aug. 15-17, 1973, University of Alaska, Fairbanks, Alaska (Abst.).

Shapiro, L. H., and J. J. Burns, 1973, Satellite observations of sea ice movement in the Bering Strait region. 24th Alaska Science Conf. Aug. 15-17, 1973, University of Alaska, Fairbanks, Alaska (In press).

Wright, F. F., and G. D. Sharma, 1973. Satellite observations of high latitude estuarine circulation. Port and Ocean Engineering Under Arctic Conditions, Univ. of Iceland, Reykjavik, Iceland, Aug. 27-29, 1973 (Text in press).

Wright, F. F., and G. D. Sharma, 1973. ERTS studies of Alaskan coastal circulation. Am. Soc. of Photogrammetry and Am. Cong. on Surveying and Mapping. Fall convention Oct. 2-5, 1973, Orlando, Florida (Text in press).

Wright, F. F., G. D. Sharma, D. C. Burbank, and J. J. Burns, 1973. ERTS imagery applied to Alaskan coastal problems. Symposium on the Earth Resources Technology Satellite-1. Greenbelt, Maryland, Dec. 1973 (Text in press).

Sharma, G. D. F. F. Wright, and J. J. Burns, 1974. Sea-surface circulation, sediment transport, and marine mammals distribution, Alaskan continental shelf. Selected Water Resources Abstracts, Vol. 7, No. 1, pp. 18-19.

LIST OF REFERENCES

Colovocoresses, A. P. and R. B. McEwen, 1973. Progress in cartography, EROS program. Symposium on Significant Results Obtained from ERTS-1, NASA/FSFC, March 5-9, 1973.

Creager, J. S., and D. A. McManus, 1966. Geology of the southeastern Chukchi Sea, in Wilimovsky, N. J. Ed., Environment of the Cape Thompson region, Alaska. U.S. Atomic Energy Commission, Clearinghouse for Fed. Scientific and Tech. Information, Springfield, Virginia, p. 755-786.

Fleming, R. H., and D. Heggarty, 1966. Oceanography of the southeastern Chukchi Sea, in Wilimovsky, N. J. Ed., Environment of the Cape Thompson region, Alaska. U.S. Atomic Energy Commission, Clearinghouse for Fed. Scientific and Tech. Information, Springfield, Virginia, p. 697-754.

Environmental Studies of Port Valdez. Hood, D. W., W. E. Shiels, and E. J. Kelley Eds. Institute of Marine Science, University of Alaska, Fairbanks, Occasional Publication 3. July 1973.

McManus, D. A., J. C. Kelley, and J. S. Creager, 1969. Continental shelf sedimentation in an arctic environment. Geol. Soc. Am. Bull. V.80,p. 1961-1984.

Sharma, G. D., and D. C. Burbank, 1973. Geological oceanography, in Hood, D. W., W. E. Shiels, and E. J. Kelley, Eds. Environmental Studies of Port Valdez. Institute of Marine Science, University of Alaska, Fairbanks, Occasional Publication No. 3.

Sharma, G. D., and D. C. Burrell, 1970. Sedimentary environment and sediments of Cook Inlet, Alaska. Am. Assoc. Petroleum Geologists Bull., V.54, p. 647-654.